This is to certify that the

dissertation entitled

GELATION OF CHICKEN BREAST MUSCLE MYOSIN : INFLUENCE OF HEATING TEMPERATURE AND ACTIN-TO-MYOSIN WEIGHT RATIO

presented by

Shuefung Wang

has been accepted towards fulfillment
of the requirements for

Ph. D. degree in Dept. Food Sci. & Human Nutrition

Denise M. Smith
Major professor

Date Sept. 17, 1993

GELATION OF CHICKEN BREAST MUSCLE MYOSIN : INFLUENCE OF HEATING TEMPERATURE AND ACTIN-TO-MYOSIN WEIGHT RATIO

BY

Shuefung Wang

A DISSERTATION

Submitted to
Michigan State University
in partial fulfillment of the requirements
for the degree of

DOCTOR OF PHILOSOPHY

Department of Food Science and Human Nutrition

1993

ABSTRACT

GELATION OF CHICKEN BREAST MUSCLE MYOSIN : INFLUENCE OF HEATING TEMPERATURE AND ACTIN-TO-MYOSIN WEIGHT RATIO

BY

Shuefung Wang

Heat-induced gelation of chicken breast myosin in 0.6 M NaCl, pD or pH 6.5 as influenced by heating temperature and actin (A) to myosin (M) weight ratios (A:M of 1:0, 1:1.3, 1:15, and 0:1) were studied. Changes in rheological properties, thermal stability, and secondary structure were monitored using dynamic testing, differential scanning calorimetry (DSC), and Fourier transform infrared spectroscopy (FTIR), respectively. Sol-to-gel transition of myosin was observed at 55°C. Myosin heated at 75°C for 30 min had more viscous character, while myosin at 55 and 65°C formed more elastic gels. After 40 min cooling to 30°C, loss tangent, storage and loss moduli of myosin increased at 65 and 75°C, while cooling had little effect on myosin at 55°C. Second-derivative infrared spectra of myosin showed absorption bands for α-helix (1652 cm^{-1}) and ß-sheet (1636 cm^{-1} paired with 1676 cm^{-1}) decreased with an increase in temperature above 45°C, indicating myosin unfolding during the sol-to-gel transition. The bands at 1683 cm^{-1} and 1613 cm^{-1} (intermolecularly

hydrogen-bonded ß-structure) became significant at 55°C and above, but band intensity did not correlate with dynamic moduli after cooling from the three heating temperatures.

The DSC endotherm, scanned at 1°C/min, of myosin had four transitions at 49, 50, 57 and 67°C with a calorimetric enthalpy (ΔH_{cal}) of 2215.8 ± 89.3 kcal/mol. Addition of 5 mM sodium pyrophosphate (PPi) to myosin resulted in a similar heat capacity profile but reduced the ΔH_{cal} to 1727.9 ± 45.4 kcal/mol. Both endotherms had a cooperative ratio (CR) below unity and were deconvoluted into 10 two-state transitions. The endotherm of F-actin showed a single peak at 75.5 ± 0.4°C, with a ΔH_{cal} of 143.4 ± 9.6 kcal/mol. The CR of F-actin was higher than unity, indicating intermonomer interaction. Addition of PPi to F-actin resulted in a major peak at 75.6 ± 0.5°C and a minor peak at 53.3 ± 0.1°C (attributed to G-actin). Myosin with and without PPi showed similar rheograms in dynamic testing. The G' of F-actin increased at a higher temperature than actin with PPi.

Addition of actin delayed the initial unfolding temperature of myosin and significantly changed the enthalpy profile. This stabilizing effect was decreased with addition of PPi. Storage and loss moduli of A:M 1:1.3 sol at 30°C were greater than those of myosin and A:M 1:15 sols, while A:M 1:1.3 had a higher loss tangent (more viscous) at 80°C. Addition of PPi increased viscous character after heating to 80°C. Actin affected the denaturation of structural domains of myosin and possibly altered the gelation mechanism.

ACKNOWLEDGMENTS

The author expresses sincere appreciation to the major professor, Dr. D. M. Smith for her inspiration, counsel and encouragement during this study.

Appreciation is also extended to Drs. J. F. Steffe, G. Strasburg and J. Wilson for their assistance and advice given as members of the guidance committee. Special thanks are expressed to Dr. J. L. Gill for his assistance in statistics.

Lastly, I would like to thank my parents and my husband for their love, encouragement and support throughout this graduate study.

TABLE OF CONTENTS

LIST OF TABLES

LIST OF FIGURES

Figure | Page

CHAPTER ONE : INTRODUCTION

Skeletal meat products generally supply not only a major portion of daily protein intake, but provide high quality protein. Consumption of saturated fat and cholesterol have been implicated as contributing factors in cardiovascular disease. In meat fat, the most abundant fatty acid is mono-unsaturated oleic acid. Subcutaneous fat from chicken, pork, beef, and lamb contains about 33, 45, 54, and 58 percent saturated fat, respectively (Judge et al., 1989a). Recent trends in meat consumption are toward poultry because of its lower saturated fat content (Bruhn et al., 1992).

In the skeletal muscle system, proteins constitute 16 to 22 percent of the muscle mass (Judge et al., 1989b), and are categorized as sarcoplasmic, myofibrillar or stromal based on their solubility. Myofibrillar proteins require intermediate or high ionic strength buffer for their extraction, so are referred to as salt-soluble proteins. Of the myofibrillar proteins, myosin and actin are two major proteins responsible for muscle contraction. Myosin has been found to be prerequisite for developing desired gel strength in model systems (Samejima et al., 1969) and contributes to the binding properties and waterholding capacity in comminuted meat

products (Fukazawa et al., 1961).

Due to the complexity of muscle systems, simplified models are used to provide information on functionalities of individual components and optimum processing parameters. Fundamental research on physical-chemical properties of myosin is of great interest. Additionally, models for protein thermal gelation have been proposed and generalized by several researchers (Ferry, 1948; Hermansson, 1978; Clark et al., 1981; Ashgar et al., 1985; Foegeding and Hamman, 1992). By understanding the relationship between the mechanism of thermal gelation and myosin molecular properties, it is possible to improve gel properties by influencing protein unfolding or rate of aggregation. This information can be used to develop new meat products to meet consumer demands. Furthermore, nonmeat proteins, such as soy proteins (McMindes, 1991), or hydrocolloids (Foegeding and Ramsey, 1986; Egbert et al., 1991) used in low-fat meat products as fat replacers, as well as other ingredients, can be more successfully utilized in formulations when their interactions with myosin during processing are better understood.

The molecular properties of myosin and its interaction with other components greatly determine its functionalities in meat products. The present research was divided into three studies, focusing on thermal effects on rheological behavior and structure of myosin (Study I), the relation between thermal unfolding and viscoelasticity development of the two

most abundant myofibrillar proteins -- myosin and F-actin (Study II), and the interactions between myosin and F-actin (Study III), which affect gel network development and properties. The objectives of these three studies were:

Study I -- (a) to characterize the dynamic rheological properties of myosin in 0.6 M NaCl, pH 6.5 during and after isothermal heating, and (b) to observe secondary structural changes of myosin after heating;

Study II -- (a) to monitor the denaturation temperature and enthalpy changes of myosin and F-actin during heating, (b) to monitor the changes in dynamic rheological properties of myosin and F-actin during gel development, and (c) to examine the effect of pyrophosphate on myosin and F-actin;

Study III -- (a) to monitor the changes in enthalpic profile and dynamic rheological properties of actomyosin solutions of different actin-to-myosin weight ratios, and (b) to examine the effect of pyrophosphate on enthalpic profile and rheological properties as a function of actin-to-myosin weight ratios during heating.

CHAPTER TWO : LITERATURE REVIEW

2.1 Myosin Molecule

The myosin molecule is made of two heavy chains (Young et al., 1968; Lowey et al., 1969), and two pairs of light chains (Gershman et al., 1969; Gazith et al., 1970). With limited digestion by trypsin, the myosin molecule is split into two fragments: heavy meromyosin (HMM) and light meromyosin (LMM) (Lowey, et al., 1969). The HMM fragment can be further split by papain into two subfragments: S-1, which corresponds to the globular head of myosin, and S-2, which is the rod-like part of HMM (Fig. 2.1) (Balint et al., 1968). The region at the LMM/S2 junction is very susceptible to proteolysis and is known as the "hinge region" (Burke et al., 1973). This hinge region of myosin rod was postulated to be the primary flexible site of force generation and shortening in a contracting muscle (Burke et al., 1973; Harrington, 1979b; Rodgers and Harrington, 1987). At a salt concentration approximating physiological conditions, myosin aggregates to form bi-polar filaments; the central region of the filament where no S-1 heads project from the surface is known as the "bare zone" (Huxley, 1963). The insolubility of myosin at ionic strength

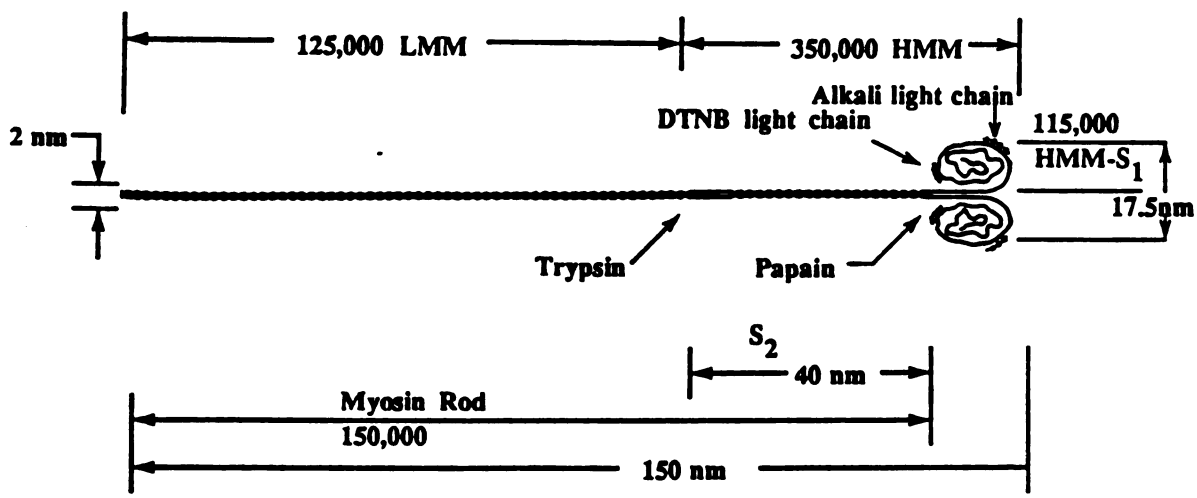

Figure 2.1. Schematic representation of the myosin molecule: HMM, heavy meromyosin; LMM, light meromyosin; S_1, myosin subfragment-1; S_2, myosin subfragment-2; DTNB, 5,5-dithiobis-(2-nitrobenzoate) (adapted from Smith et al., 1983).

below 0.3 derives from the rod region, which is insoluble in low salt (Harrington, 1979a). In vitro, these pure myosin molecules aggregate to form synthetic myosin filaments at low ionic strength, like native thick filaments but of variable length (Huxley, 1963).

A. Topography of the Myosin Head

The myosin head is irregularly folded as a typical globular protein (McLachlan, 1984), and contains the actin binding site and catalytic site for ATPase activity. Tonomura and his colleagues have shown evidence that two heads in one myosin molecule are not identical (Arata et al., 1977; Inoue et al., 1977, 1979). Each heavy chain in the myosin head is composed of three major proteolytic segments, described as the 25-kDa, 50-kDa, and 22-kDa segments starting from the N-terminal end of the heavy chain. The precise molecular mass of these segments is still uncertain (Balint et al., 1978; Muhlrad and Morales, 1984). Three fragments of 23, 50, and 22 kDa were obtained from adult chicken pectoralis myosin, containing a total of 837 residues. Four post-translationally methylated amino acids were found in the myosin head region: ϵ-N-monomethyllysine at position 35, ϵ-N-trimethyllysine at 130 and 551, and 3-N-methylhistidine at 757. None was found in the myosin rod region (Hayashida et al., 1991; Komine et al., 1991; Maita et al., 1991a). Sequence homologies (percentage of identical amino acids) of these S-1 fragments

were higher in chicken embryonic pectoralis and rabbit skeletal myosin than in chicken cardiac and chicken gizzard myosin. This suggested the amino acid substitutions in myosin reflects the type of muscle (e.g. skeletal vs. smooth muscle) rather than species differences (Hayashida et al., 1991; Komine et al., 1991; Maita et al., 1991a).

The three segments are probably domains within the myosin head, and each has its own function (Mornet et al., 1979; Muhlrad and Hozumi, 1982; Setton and Muhlrad, 1984; Burke et al., 1987). It has been demonstrated that both the 22- and 50-KDa segments contain binding sites for actin (Yamamoto and Sekine, 1979a, b, c; Mornet et al., 1979, 1981a, b; Sutoh, 1983; Muhlrad and Morales, 1984; Muhlrad et al., 1986). Each S-1 binds to two adjacent actin monomers; when actin and S-1 are mixed in a ratio of 1:1, each actin monomer is in contact with two S-1s (Mornet et al., 1981a). The 25- and 50-kDa regions appear to contain nucleotide binding sites (Mahmood and Yount, 1984; Nakamaye et al., 1985). The 22-kDa domain contained two thiol groups, SH_1 and SH_2 separated by nine residues, which have a structural and functional role in the ATPase activity of myosin (Burke and Reisler, 1977; Wells and Yount, 1979; Wells et al., 1980). Blocking of SH_1 group leads to an increase in Ca^{2+}-ATPase and a loss of K^+-ATPase activity in the presence of ethylenediaminetetraacetic acid (EDTA). Modification of SH_2 group resulted in the loss of both Ca^{2+} and K^+ ATPase activities (Reisler et al., 1974; Schaub et al.,

1975). Binding of nucleotides reduced the distance between these two thiol groups from > 1.2 to 0.2 nm (Wells and Yount, 1979; Wells et al., 1980). It was suggested that these thiol groups at the C-terminal end of S-1 (22-kDa domain) are in close proximity to the ATP binding site in the 25-kDa domain at the N-terminal, indicating that the myosin head is highly folded (Takashi et al., 1982).

Rayment et al. (1993a) reported the three-dimensional structure of chicken pectoralis myosin S-1 with two light chains (essential or Alkali light chain, and regulatory or DTNB light chain) using single crystal X-ray diffraction. The secondary structure of the myosin head is dominated by α-helices with approximately 48% of the amino acid residues in this conformation. The α-helix extending from the major part of the head constitutes the light chain binding region (Fig. 2.2). The actin and nucleotide binding sites are located on opposite side of the protein. The entire thick portion of the myosin head contains a central seven-stranded ß sheet motif, mostly parallel, surrounded by α-helices, loops or turns. These seven ß strands are formed from all three major proteolytic fragments (25, 50, and 20-kDa). The 50-kDa fragment contains two major domains, referred to as the upper and lower domains, which are separated by a long narrow cleft. The helix connecting two reactive thiol groups (Cys^{707} and Cys^{697}) lies at the base of a cleft at the junction between the lower domain of the 50-kDa and the N-terminal 25-kDa

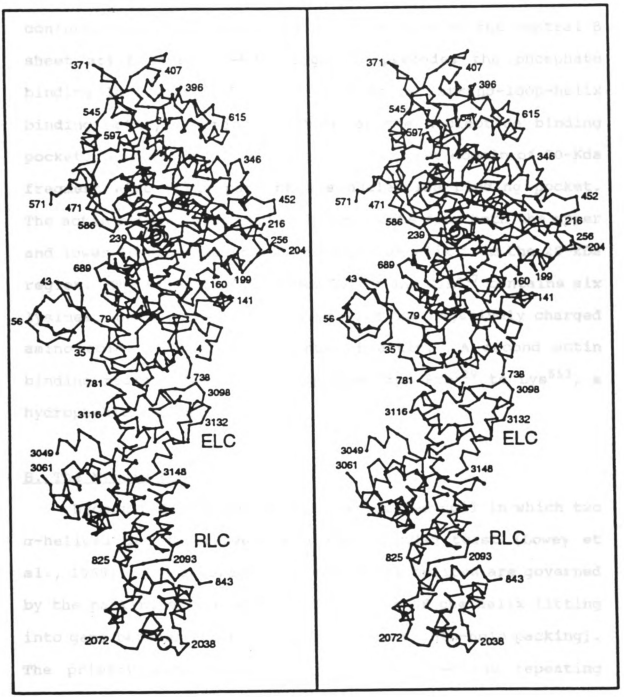

Figure 2.2. A stereo α-carbon plot of the entire myosin head (adapted from Rayment et al., 1993a).

fragments. The nucleotide binding pocket is in an open conformation (Fig. 2.2). The fourth strand of the central ß sheet motif (from 25-kDa fragment) precedes the phosphate binding loop and is followed by a helix (strand-loop-helix binding motif), forming the base of the nucleotide binding pocket. Another helix belonging to the upper domain of 50-Kda fragment also forms part of the nucleotide binding pocket. The actin binding site contains components from both the upper and lower 50-kDa domains and the first α-helix from the 20-kDa region. The segment of residues Tyr^{626} and Gln^{647} contains six lysines, and can readily interact with the negatively charged amino acids at the NH_2-terminus of actin. A second actin binding region lies in the sequence from Pro^{529} to Lys^{553}, a hydrophobic region.

B. The Myosin Rod

Myosin rod is a double-stranded coiled coil in which two α-helices are interwoven in a right-handed twist (Lowey et al., 1969). The interactions between the helices are governed by the packing of the side chains, those of one helix fitting into gaps between those of the other (knob-into-hole packing). The primary sequence of rod has a heptapeptide repeating pattern (*a-b-c-d-e-f-g*) of coiled-coil structures where residues *a* and *d* are hydrophobic and form the interface between the α-helices in the folded protein (McLachlan and Stewart, 1975; Parry, 1981). The helix surface is highly

charged, with acidic and basic residues clustered mainly in the outer positions *b*, *c* and *f* (McLachlan and Karn, 1982). The amino acid sequence of the hinge region in myosin S-2 also has a coiled-coil helical structure, but with fewer hydrophobic interactions. A significant number of charged residues were reported in the hydrophobic core of the hinge region which suggested reduced stability (Lu and Wong, 1985; Watanabe, 1989). Maita et al. (1991b) predicted an α-helical structure (residues 1292-1304) sandwiched between coil/turn structures (residues 1283-1287 and 1305-1310) at the S-2/LMM junction based on the amino acid sequence of chicken pectoralis myosin, while S-1/rod junction contained α-helical structure with a proline breakdown (position 840). Coil/turn structures were found between residue 819-825.

C. Myosin Light Chains

Myosin molecules contain four light chains, two to each head. Vertebrate skeletal muscles with a fast-twitch response contain three different light chain types, referred to as Alkali or A-light chains (two types A1 and A2) and DTNB light chains according to the method used to separate them. DTNB is 5,5-dithiobis-(2-nitrobenzoate). The A1, DTNB and A2 light chains are sometimes referred to as LC1, LC2 and LC3, in the order of molecular mass (22, 18 and 16 kDa, respectively). Slow-twitch muscle contains only two types of light chains that are similar to fast muscle LC1 and LC2 (Squire, 1986).

Neither type is required for ATPase activity of the head (Wagner and Giniger, 1981). The LC1 and LC3 have common amino acid sequences over their C-terminal 142 residues. The size difference is caused by an additional 41 amino acids present at the NH_2-terminus of LC1 (Frank and Weeds, 1974). Residues 1-41 of LC1 were found to interact with actin (Sutoh, 1982a, b, 1983). The DTNB light chain, also named as regulatory or P-light chain, has a single divalent cation binding site, and can be reversibly phosphorylated to modulate muscle contraction (Adelstein and Eisenberg, 1980). Electron microscopic studies done by Vibert and Craig (1982) showed that part of this light chain lies very close to the junction between myosin heads and the rod. Binding of divalent cation to the regulatory light chain was found to protect the S-1/rod junction from digestion (Weeds and Pope, 1977).

2.2 Actin Molecule

Based on amino acid sequence, globular actin (G-actin) has a molecular mass of ca. 42,000 daltons (Elzinga et al., 1973) with a diameter of 4-5 nm (Hanson and Lowy, 1983). Based on comparisons of primary structures, Pollard and Cooper (1986) suggested that actin has been highly conserved throughout evolution. At physiological salt concentration, G-actin polymerizes into a double-stranded filamentous form

(F-actin) with highly polar structure (Huxley, 1963). The usual polymerization is accompanied by the liberation of inorganic phosphate with 1 mole of ATP cleaved per G-actin monomer polymerized (Harrington, 1979a), the binding of Mg-ATP and its hydrolysis to Mg-ADP which remains firmly bound in F-actin. Actin gradually loses its ability to undergo self-assembly if bound nucleotide and tightly bound divalent cation are removed (Harrington, 1979a).

From X-ray diffraction analysis of crystals of 1:1 complexes of actin with either DNase (Suck et al., 1981) or profilin (Carlsson et al., 1976), it became evident that actin monomer is highly asymmetric and bi-lobed, consisting of a two-domain structure separated by a pronounced cleft. By limited proteolysis, actin is split into a 33-kDa C-terminal fragment and a small 9-kD a N-terminal fragment (Mornet and Ue, 1984). Actin has a single high-affinity and multiple low-affinity binding sites for divalent cations, and also a nucleotide binding site. It was suggested by Mornet and Ue (1984) that the small domain probably contained the high-affinity binding site for divalent cations; while the 33-kDa domain contains the nucleotide binding site. In contrast, based on the atomic structure of actin:DNase I.complex, Kabsch et al. (1990) proposed actin is composed of two domains of about the same size. The "small" domain (the historical term) contains both the amino- and carboxy-terminus of actin. Both domains can be further subdivided into two subdomains: the

"large" domain consists of subdomain 1 and subdomain 2; while the "small" domain contains subdomain 3 and subdomain 4. Subdomains 1 and 3 form a five-stranded ß-sheet consisting of a ß-meander and a right-handed ßαß unit flanked by several α-helices (Fig. 2.3). The nucleotide is bound in the cleft between the two domains. Only one calcium ion was found within the actin molecule, sitting in a deep hydrophilic pocket formed by the phosphate moiety of nucleotide and actin residues (Fig. 2.3). According to the atomic structure, this ion is shielded from the bulk solvent, which probably explains its high binding affinity (Kabsch and Vandekerckhove, 1992).

The structure of F-actin can be described as a single left-handed helix with a rise per monomer of 2.75 nm (13 actin molecules per 6 turns). Because the rotation angle per molecule is -166.2° around the filament axis, the structure has an appearance of two right-handed long-pitch helices intertwined with each other (Kabsch and Vandekerckhove, 1992). Holmes et al. (1990) reported an atomic model of the actin filament by assuming that the structure of G-actin in F-actin and in DNase I complex are the same. The large domain (comprising the subdomains 3 and 4) is located near the central axis of the filament, and the small domain (comprising the subdomains 1 and 2) is located at large radius from the filament axis (Fig. 2.4).

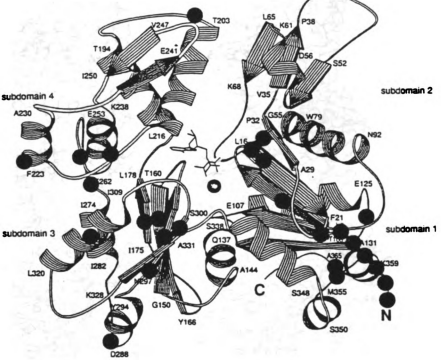

Figure 2.3. Schematic representation of the structure of actin. ATP and Ca^{2+} are located between the small (right) and large (left) domain (adapted from Kabsch et al. 1990).

Figure 2.4. Atomic model of F-actin as a stereo pair (adapted from Holmes et al., 1990)

2.3 Interaction between Myosin and Actin

The binding between myosin HMM region and actin has long been considered as the element responsible for the generation of contractile force in muscle. In the absence of ATP, myosin heads bind to the adjacent actin filaments, and remain firmly attached to each other until ATP is added to the system (Eisenberg and Moos, 1968). As a result, the muscle becomes stiff and is in the rigor state. In a meat system, this interaction greatly influences meat tenderness and product quality. Upon depletion of ATP after slaughter, the interaction between myosin and actin filaments results in "rigor mortis", an irreversible muscle contraction. Rigor shortening is more severe than normal contraction because more crossbridges are formed. Softening of rigor mortis is probably due to enzymatic degradation of muscle ultrastructure (Judge et al., 1989c).

It has long been accepted that contraction involves an active sliding process developed between filaments of actin and myosin (Huxley and Hanson, 1954; Huxley and Niedergerke, 1954; Huxley, 1969; Huxley and Simmons, 1971; Eisenberg and Greene, 1980). This sliding-filament model comprises a cyclic interaction accompanied by ATP hydrolysis without permanent changes in conformation of myosin and actin. Binding of Mg^{2+}-ATP to myosin rapidly dissociates the actomyosin complex; free myosin then hydrolyzes ATP and forms a stable myosin-product

complex; actin recombines with this complex, and the products dissociate, forming the original actomyosin complex (Lymn and Taylor, 1971). Transduction of energy of ATP hydrolysis into mechanical forces occurs during product release, and the site of force generation was placed in the region of actin-myosin interaction. Further elaboration of this cyclic model incorporates the weakly and strongly bound states for the actin-myosin interaction. The crossbridge first binds in a weak binding conformation, then undergoes isomerization to a strong binding form. The power stroke occurs within the tightly bound states so that the energy of hydrolysis can be transduced as movement (Eisenberg and Greene, 1980). Current theories favor a force-generating mechanism based on the structural changes within the myosin molecule, converting chemical energy into mechanical work in muscle. However, the region generating force within the myosin molecule is still under investigation. A number of observations favor the existence of a hinge within the rod portion of myosin, probably close to the junction between HMM and LMM. The helix-to-coil transition within the hinge is conjectured to be the possible origin of tension generation in muscle (Huxley and Simmons, 1971; Harrington, 1971, 1979b; Tsong et al., 1979; Swenson and Ritchie, 1980; Lu and Wong, 1985; Rodgers and Harrington, 1987). However, other results failed to support this hypothesis, showing no evidence for a hinge (Rosser et al., 1978; Hvidt et al., 1982, 1984). Skolnick

(1987) argued the necessity of the hinge in Harrington's model (1979b), and proposed a coil-to-helix transition model of tension generation located in the swivel (random conformation) at the junction of S-1 and myosin rod. The existence of the flexible swivel is supported by other researchers (Mendelson, et al., 1973; Thomas, 1978). Moreover, there is an evidence that a proline residue is present at the S-1/S-2 junction (Karn et al., 1983) that acts as a "stop" to α-helix propagation, and therefore separates the coiled-coil region from the globular portion of myosin (Skolnick, 1987).

By establishing the three dimensional structure of myosin, Rayment et al. (1993b) proposed a model of actomyosin complex that explains the conformational changes of myosin during muscle contraction. The major portion of S-1 binds actin filament at an angle of about 45° to the filament axis. The long helices consisting of the light chain binding region projects away from the filament axis at an angle of about 90°. Rayment et al. (1993b) suggested that binding of F-actin to myosin is a sequential, multistep process that forms weakly bound and tightly bound states. The actomyosin interaction involves the opening and closure of the cleft that splits the 50-kDa fragment into the lower and upper domains (Rayment et al., 1993a). This interaction begins with a weak binding of the myosin loop Tyr^{626} to Gln^{647} in the 50/20-kDa junction (five lysines in the loop) with the six negatively charged residues on actin. This interaction is expected to be

sensitive to ionic strength, and allows the next stereospecific interaction to occur which involves the closure of the narrow cleft of 50-kDa fragment on forming the rigor complex. An additional loop (Arg^{405} to Lys^{415}) from the upper 50-kDa fragment strengthens this interaction. Binding of ATP allows the narrow cleft in 50-kDa fragment to open, disrupting the strong binding interaction between actin and myosin. In the second stage of ATP binding, the release of myosin from actin occurs when the γ phosphate of the nucleotide binds the active site pocket and disrupts the actin binding site on myosin. Closure of the nucleotide binding pocket due to binding results in a movement of the COOH-terminus of the heavy chain toward actin. The proposed crossbridge cycle is shown on (Fig. 2.5).

In the cyclic model of muscle contraction, myosin, actin and nucleotide are three major elements. Research has been done to study the conformational changes in myosin structure induced by nucleotides or actin, as well as the domain structure of S-1 using ATP and/or nonhydrolyzable analogues, such as ADP and inorganic pyrophosphate (PPi). Nauss et al. (1969) reported myosin and HMM bound approximately 2 moles of PPi per mole of protein, while actomyosin bound only 1 mole of PPi in 50 mM Tris, pH 7.5, 1 mM $MgCl_2$, 0.5 M KCl. Addition of actin to myosin reduced both the PPi binding ratio and the association constant. It is possible that actin and PPi have a common binding site; however, actin can stimulate myosin

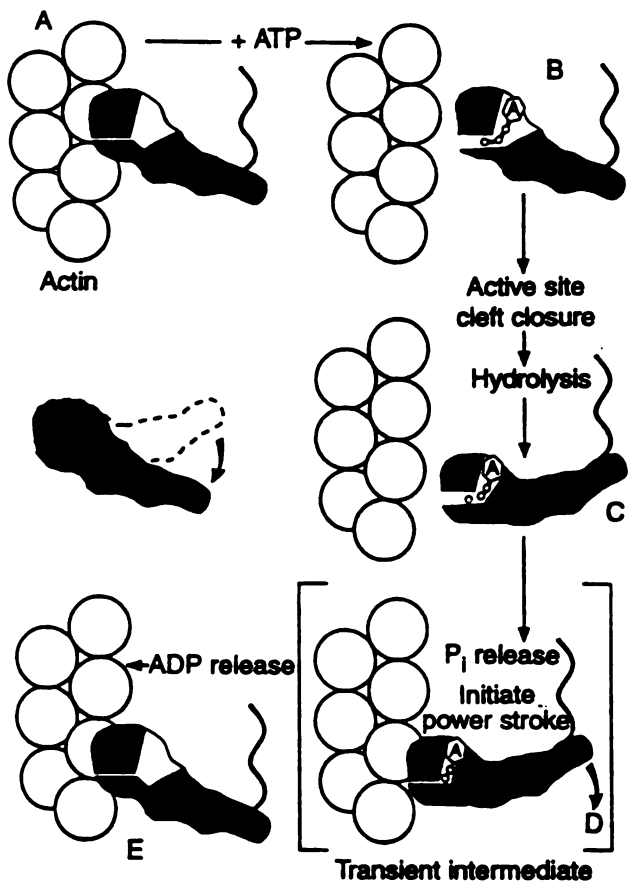

Figure 2.5. The contractile cycle incorporating structural features of the myosin head and their proposed involvement in the cycle. Actin is represented as a sphere. The narrow cleft splitting the 50-kDa fragment of the myosin head is represented as a horizontal gap perpendicular to the actin filament axis (adapted from Rayment et al., 1993b).

ATPase in the presence of Mg^{2+} which indicates separate sites for actin and ATP. Therefore, the authors suggested local structural changes in S-1 induced by binding of ATP or other nucleotides. Later, Shriver and Sykes (1981) suggested two conformers of S-1 existed in equilibrium with each other. This equilibrium depended on ambient factors such as temperature or pH, and was perturbed by the binding of nucleotides or actin. This two-conformer hypothesis was supported by other researchers (Yamada et al., 1981; Shriver and Sykes, 1982; Redowicz et al., 1987; Kamath and Shriver, 1989; Muhlrad and Chaussepied, 1990).

Hamai and Konno (1989) reported that ADP- and PPi-binding protected the 50kDa fragments and decreased the inactivation rate of S-1 ATPase activity by incubation at 40°C; however, the turbidity of the solution increased significantly in the presence of ADP and PPi. By SDS-PAGE characterization of components in both supernatant and pellet, it was found that S-1 pellet contained very few light chains. The rate of degradation of light chain by thermal treatment was the same as for 20- and 27-kDa domains, fast for nucleotide-bound S-1 and slow for nucleotide-free S-1. The authors suggested that binding of PPi or ADP destabilized the light chains-heavy chain binding, resulting in turbidity due to formation of aggregates of the light chain-deficient heavy chains. This detachment of light chain upon heating was proposed due to structural change around light chain binding site, probably on

the 20- or/and 27-kDa domains. Addition of these nucleotide analogues were also found to result in a change in both muscle fiber tension and fiber stiffness. These changes could be due to cross-bridge detachment (Thomas and Cooke, 1980; Chen and Reisler, 1984; Brenner et al., 1986) or changes in cross-bridge structure upon ligand binding (Goody et al., 1976; Padron and Huxley, 1984). It was also found that this ligand-induced dissociation of actomyosin is enhanced by high ionic strength and by low temperatures (Konrad and Goody, 1982; Biosca, et al., 1986; Pate and Cooke, 1988).

2.4 Differential Scanning Calorimetry (DSC)

A. Instrumentation

Calorimetry is the only method for direct determination of enthalpy associated with changes in protein state (Privalov and Potekhin, 1986). It measures changes in heat capacity (C_p) when macromolecules are heated or cooled at constant pressure. The heat capacity measured is not absolute but rather the difference between sample and reference. The heat capacity profile is characterized using melting temperature (T_m), the temperature of 50% denaturation (designated as the peak temperature in the curve), calorimetric enthalpy (ΔH_{cal}), van't Hoff enthalpy (ΔH_{vH}), and cooperative ratio (CR). These parameters are explained below according to literature.

Heat capacity (C_p, cal*mol^{-1}*K^{-1}) is a temperature (T) derivative of the enthalpy (H) function,

$$C_p = (dH/dT)_p \qquad (2\text{-}1)$$

The enthalpy function can be estimated by integration of the heat capacity:

$$H(T) = \int_{T_0}^{T} C_p(T)\, d(T) + H(T_o) \qquad (2\text{-}2)$$

A two-state process of protein denaturation represents the transition between two thermodynamically stable states, the native (N) and denatured (D) states, where the concentrations of intermediate states between these two states are very low at equilibrium. The equilibrium thermodynamic expression is valid:

$$\left(\frac{d\ln K}{dT}\right)_P = \frac{\Delta H_{vH}}{RT^2} \qquad (2\text{-}3)$$

where K is the equilibrium constant of the process, T is the absolute temperature, ΔH_{vH} is van't Hoff enthalpy, R gas constant and P denotes constant pressure(s) (Chowdhry and Cole, 1989). Calorimetric data can be used to obtain an estimate of the corresponding van't Hoff enthalpy by integrating the experimental heat capacity data and plotting the average enthalpy, $\overline{H}$ vs. T (Fig. 2.6B). The extrapolated base lines for obtaining the enthalpy of native (H_N) and denatured states (H_D) in the transition region is made from

Figure 2.6. Schematic illustration of the heat capacity and variation in the enthalpy for a two-state thermal transition. (A) temperature dependence of the heat capacity in the temperature region where the thermal transition occurs. T_L and T_H are reference temperatures located below and above the transition region, respectively. The extrapolation of low- and high-temperature base lines is necessary to estimate the heat capacity of the native and the denatured state over transition temperature range. It is indicated by the segments BQ and CP, respectively.
(B) Representative variation in the enthalpy with temperature in the region of the two-state thermal transition, obtained by integration of the curve in part A. The extrapolated base line (dashed lines) is obtained from the extrapolated heat capacities shown in part A.
(adapted from Jackson and Brandts, 1970).

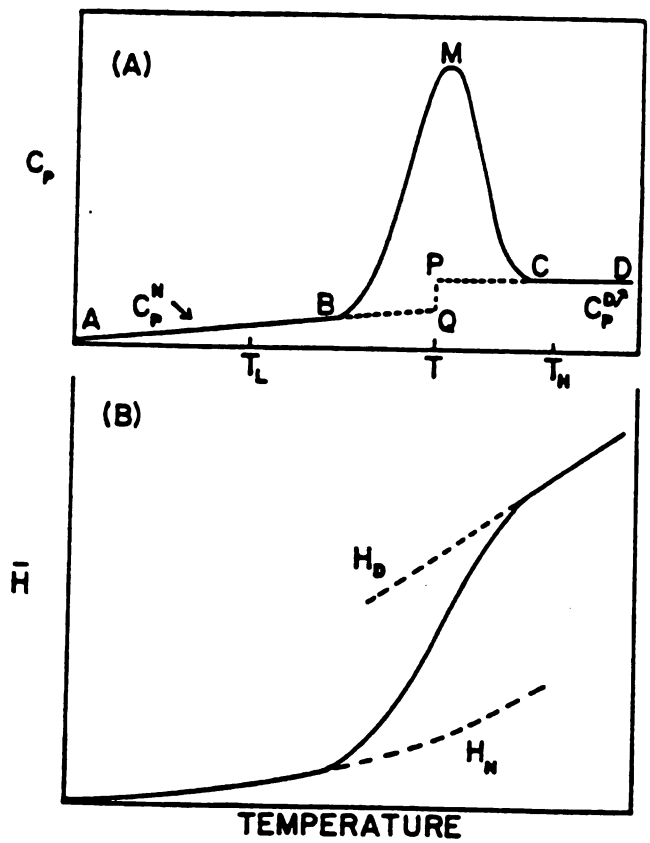
(A)
M
C_p
P
C
D
A
C_p^N
B
Q
$C_p^{D?}$
T_L
T
T_N
(B)
$\bar{H}$
H_D
H_N
TEMPERATURE

the extrapolated heat capacities shown in Figure 2.6A (Jacksonand Brandts, 1970). Assuming a two-state equilibrium process between D and N, then the "equilibrium constant" is

$$K = (H_D - \overline{H}) / (\overline{H} - H_N) \qquad (2\text{-}4)$$

The ΔH_{vH} can be obtained by plotting the logarithm of the above equilibrium constant against reciprocal temperature (Krishnan and Brandts, 1978). Therefore, for a two-state process carried out under equilibrium conditions:

$$\Delta H_{vH} = \Delta H_{cal} = \Delta h_{cal} M \qquad (2\text{-}5)$$

where ΔH_{cal} is the calorimetric enthalpy (cal x mol^{-1}) and M is the molecular mass of the molecule (Chowdhry and Cole, 1989). The cooperative ratio ($CR = \Delta H_{vH} / \Delta H_{cal}$) allows one to determine whether or not a two-state assumption is valid. If $\Delta H_{vH} < \Delta H_{cal}$ (CR below unity), it indicates that one or more domains exist in the overall process. If $\Delta H_{vH} > \Delta H_{cal}$ (CR greater than 1), then intermolecular interaction/aggregation is indicated (Tsong, et al., 1970).

For macromolecules with multistate transitions, deconvolution of the melting profile into population subfractions or domains can be performed according to Freire and Biltonen (1978a). Consider a macromolecule undergoes a thermal unfolding from its native state (I_0) to an unfolded state (I_n) through (n-1) intermediate states, the partition function, Q, is defined as followed:

$$Q = 1+\sum_{i=1}^{n} \omega_i \exp(-\Delta G_i/RT) \qquad (2\text{-}6)$$

The fraction of molecules in the ith state, F_i is defined as

$$F_i=[I_i]/\sum_{i=0}^{n} [I_i] =\omega_i \exp(-\Delta G_i/RT)/Q \qquad (2\text{-}7)$$

Using the excess enthalpy relative to the initial state, $\langle\Delta H\rangle$, as the observable, then we obtain:

$$\langle\Delta H\rangle=\sum_{i=0}^{n} \Delta H_i F_i \qquad (2\text{-}8)$$

where each ΔH_i is the enthalpy difference between the ith state and the initial state, i.e. $\Delta H_i = (H_i - H_o)$. Once the temperature dependence of $\langle\Delta H\rangle$ is known, the partition function, Q, of the system can be obtained:

$$d(\ln Q) = \frac{\langle\Delta H\rangle}{RT^2} dT \qquad (2\text{-}9)$$

Direct integration of the above equation yields

$$\ln Q = \int_{T_0}^{T} \frac{\langle\Delta H\rangle}{RT^2} dT \qquad (2\text{-}10)$$

where T_0 is a temperature at which all molecules exist in the initial state. Having Q as a function of temperature, the fraction of molecules in the initial state, F_0, can be obtained:

$$F_0 = \frac{1}{Q} = \exp\left(-\int_{T_0}^{T} \frac{\langle \Delta H \rangle}{RT^2} dT\right) \qquad (2\text{-}11)$$

By definition, $(1-F_0)$ represents the fraction of molecules in all but initial states. If the excess apparent molar enthalpy, $\langle \Delta H \rangle$, is divided by $(1-F_0)$, a new enthalpy averaged over states 1 to n is defined. For a two-state transition, $\langle \Delta H \rangle/(1-F_0)$ is equal to the enthalpy change for the transition. For a multistate transition, $\langle \Delta H \rangle/(1-F_0)$ is an S-shaped curve whose lower limit is equal to the enthalpy difference (Δh_1) between the first intermediate and the initial state (Fig. 2.7). A new average excess enthalpy $\langle \Delta H_1 \rangle$ can be defined:

$$\langle \Delta H_1 \rangle = \frac{\langle \Delta H \rangle}{(1-F_0)} - \Delta h_1 \qquad (2\text{-}12)$$

and used to calculate the second partition function, Q_1

$$Q_1 = \exp\left(\int_{T_0}^{T} \frac{\langle \Delta H_1 \rangle}{RT^2} dT\right) \qquad (2\text{-}13)$$

Here, Q_1 is the summation over all the energy states except the first. Sucessive applications of these relations are used to calculate Δh_i, Q_i, $\langle \Delta H_i \rangle$ for each transition state of the unfolding reaction.

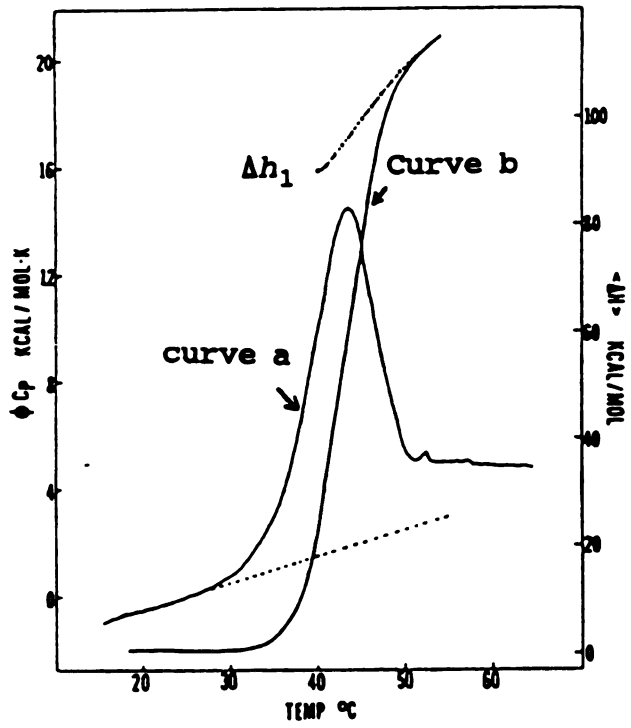

Figure 2.7. Experimental ϕC_p (curve a) and $\langle \Delta H \rangle$ (Curve b) vs. temperature profiles of a multistate transition of ribonuclease A. The upper dotted line is the $\langle \Delta H \rangle / (1-F_Q)$ function whose lower limit is equal to the enthalpy difference, Δh_1, between the first intermediate and the initial state. The bottom dotted line (calorimetric baseline) was calculated by a least-squares fit of the heat capacity function up to 25°C (adapted from Freire and Biltonen, 1978a).

B. Denaturation of Myosin & Subfragments

Thermal denaturation of myosin is influenced by various factors. Single or multiple transitions monitored by DSC have been ascribed to myosin and vary with pH, salt concentration, heating rate, muscle type and species (Stabursvik and Martens, 1980; Wright and Wilding, 1984; Akahane et al., 1985; Rodgers et al., 1987; Xiong et al., 1987; Davies et al., 1988; Kijowski and Mast, 1988; Bertazzon and Tsong, 1990a, b). Wright and Wilding (1984) found two major transitions for rabbit myosin in low salt solutions (0.012 M and 0.212 M KCl), 50 mM potassium phosphate, 0.5 mM DTT at pH 5.5 to 8.0. Increasing KCl to 0.962 M (μ=1.0) separated the endotherm into three processes. Kijowski and Mast (1988) observed a single peak at 57.9°C for chicken breast myosin, and 80.8°C for F-actin at pH 6.9 at an ionic strength near zero. Under similar solvent conditions, Park and Lanier (1989) reported a broad peak at 52°C for fish myosin and 61°C for actin. An endotherm of rabbit myosin in 0.5 M KCl, 20 mM potassium phosphate, 1 mM EDTA, pH 7.0 exhibited a peak at 46°C and three shoulders at 43, 49 and 54°C, with an ΔH_{cal} of 1715 kcal/mol (Bertazzon and Tsong, 1989). Little change in enthalpy profile was detected when myosin was soluble (i.e. KCl concentrations $\geq$ 0.3 M). Reducing the salt concentration (myosin aggregates) caused the domain transitions to converge, with little effect on the ΔH_{cal} of denaturation. The results suggested that filament formation is mainly an entropic process (Bertazzon and Tsong,

1989), which was in agreement with Josephs and Harrington (1968).

Thermal transitions during denaturation were thought to be associated with discrete regions of the myosin molecule. Wright and Wilding (1984) assigned a single transition at 52°C in 0.012 M KCl and 46.8°C in 0.962 M KCl to S-1 subfragment. Bertazzon and Tsong (1989) observed a melting temperature of 46.3°C for S-1 with a ΔH_{cal} of 255 kcal/mol, in 20 mM KP_i, 0.5 M KCl and 1 mM EDTA, pH 7.0. Shriver and Kamath (1990) observed the unfolding of myosin S-1 was irreversible in 50 mM TRIS, 0.6 M KCl, 5 mM $MgCl_2$, 1 mM dithioerythritol (DTE), pH 8.0. The thermal melting of S-1 showed a single transition at a T_m of 45°C followed by an aggregation exotherm. The T_m was stabilized by nucleotide binding.

Studies on the denaturation of myosin rod demonstrated the unfolding of myosin rod was remarkably sensitive to salt and pH changes. Cross et al. (1984) reported two major transitions for skeletal muscle myosin rod at 43 and 52°C in 0.6 M KCl, 10 mM Na-phosphate, pH 7.0 using DSC. The first component was attributed to LMM, and the second to S-2. Under physiological ionic conditions (0.12 M KCl), LMM was stabilized approximately 10°C and superimposed on the transition of S-2. In contrast, Akahane et al. (1985) found only a broad, single peak at 60°C which reflected the denaturation of LMM in low ionic strength solutions. Bertazzon and Tsong (1989) reported two peaks at 43 and 54°C

for the unfolding of a double-stranded rod, with a ΔH_{cal} of 1058 kcal/mol at 0.5 M KCl, pH 7.0. The enthalpy profile was sensitive to pH changes between 6-8 (Bertazzon and Tsong, 1990b). King and Lehrer (1989) reported that myosin rod unfolded at 43, 47, and 53°C in 0.6 M NaCl, pH 7.0 using circular dichroism and tryptophan fluorescence measurement. The transitions at 43 and 53°C were mainly attributed to LMM and the 47°C transition to the S-2 region.

Depending on the conditions of protease digestion, a shorter and longer form of S-2 can be obtained. It has been shown that myosin long S-2 from rabbit skeletal muscle is 20-25% unfolded (structural changes) at 37°C whereas short S-2 is essentially native (Sutoh, et al. 1978). The COOH-terminal part of long S-2 has been identified as the hinge region (Lu, 1980). Swenson and Ritchie (1980) assigned an endotherm at 41°C only found in long S-2 to the hinge region and the 55°C endotherm to the remainder of S-2 in 0.6 M KCl, 20 mM sodium phosphate, pH 6.6. Shriver and Kamath (1990) suggested long S-2 existed as a single domain in HMM with a T_m of 41°C in 50 mM TRIS, 0.1 M KCl, 1 mM $MgCl_2$ and 1 mM DTE, pH 7.9. The unfolding of S-2 was reversible, and characterized by a large ΔC_p of about 30 kcal/(deg mol).

C. Deconvolution of myosin endotherm

From heat capacity profiles, it was evident that rabbit myosin rod unfolds in a multi-stage process consisting of

several quasi-independent cooperative zones (Fig. 2.8). The T_m of these six transitions of myosin rod in 0.5 M KCl, 25 mM K-phosphate buffer, pH 6.5 are 43, 48, 50, 51, 56, and 61°C with enthalpies of 820, 440, 710, 760, 680, and 490 kJ/mol, respectively (Potekhin et al., 1979). In general aggrement with Potekhin and coworkers, Bertazzon and Tsong (1990b) also resolved the endotherm of myosin rod into six independent domains with T_m of 41.7, 45.4, 48.2, 51.6, 56.2, and 56.3°C in 0.5 M KCl, 20 mM potassium phosphate and 1 mM EDTA (pH 6.45). The corresponding enthalpies were 193, 191, 255, 142, 186 and 147 kcal/mol, respectively. At least two of six domains showed less than full cooperativity in melting ($\Delta H_{vH}/\Delta H_{cal} < 1$) which suggested the domains could be further resolved into subdomains. The endotherms of LMM and S-2 were fitted, respectively, into five (T_m's of 41.4, 48.7, 49.8, 55.9, 57.6°C) and three (T_m's of 47, 48.4 and 53.8°C) two-state-like transitions at all pH's ($\Delta H_{vH}=\Delta H_{cal}$) (Bertazzon and Tsong, 1990b).

D. Denaturation of Actin

Calorimetric analysis of G-actin at pH 8.0 showed a broad peak at 57°C with a ΔH_{cal} of 142±5 kcal/mol and cooperative ratio of 0.7, suggesting the existence of domains in G-actin (Bertazzon et al., 1990). The endotherm was fitted into two quasi-independent two-state transitions. In contrast, transition of F-actin showed a sharp single peak at 67°C, with

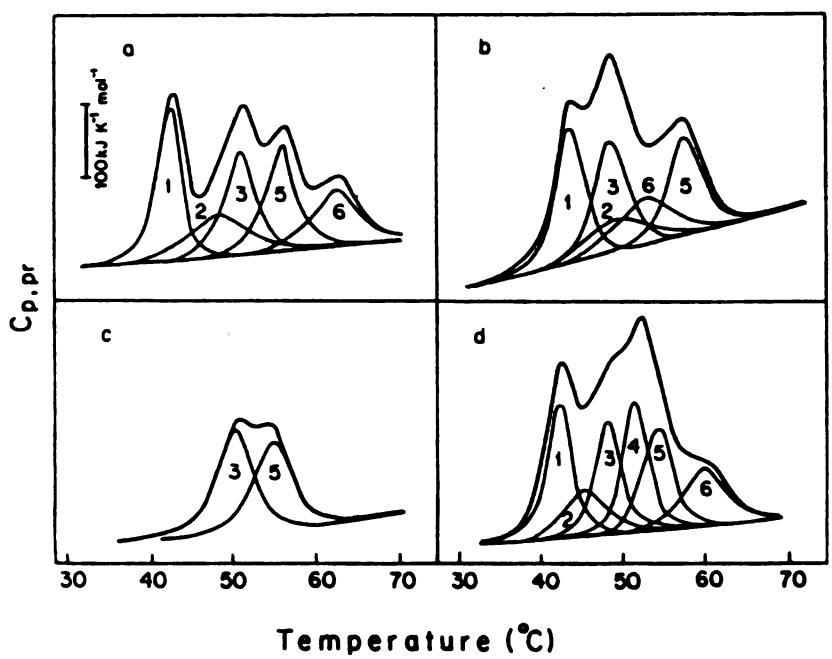

Figure 2.8. The heat capacity (Cp) profile of myosin fragments in 0.5 M KCl, 25 mM K-phosphate buffer, pH 6.5. (a) light meromyosin obtained from trypsin digestion (LMM_t); (b) light meromyosin obtained from pepsin digestion (LMM_p); (c) the small fragment of LMM, LF-3, by trypsin digestion; (d) TR (total rod) (adapted from Potekhin et al., 1979).

a ΔH_{cal} of 162±10 kcal/mol, and a CR of 1.4, suggesting intermonomer interaction (Bertazzon et al., 1990). Thermal stability of G-actin was sensitive to changes in Ca^{+2} concentration. Millimolar concentrations of Ca^{+2} facilitated the formation of polymers. When Ca^{+2} concentration increased from 0.2 to 0.8 mM, the stability of G-actin increased. The T_m (from 62.7°C to 67°C) and CR (from 0.82 to 1.25) increased along with a sharpening of the endotherm, even though the CR value did not reach that of fully polymerized protein (F-actin). On the contrary, the stability of F-actin was not affected by a range of calcium concentrations (Bertazzon and Tsong, 1990a). However, the endotherm of F-actin was sensitive to pH changes between 6 and 8. A decrease in pH was found to stabilize F-actin by a shift in T_m from 68.2°C at pH 7.9 to 74.3°C at pH 5.9 (Bertazzon and Tsong, 1990a).

2.5 Dynamic Rheological Testing

Rheology is a study of the deformation and flow of all matter, including the classical extremes of Newtonian viscous liquids and Hookean elastic solids. Most materials are viscoelastic which means they exhibit both viscous and elastic properties, depending on the time-scale of the experiment (Barnes et al., 1989). A liquid-like material does not maintain a constant deformation under constant stress, but

slowly deforms with time. Most energy input is dissipated as heat, manifesting itself as internal friction or mechanical damping. If such a material is constrained at constant deformation, the stress required to hold it gradually diminishes. On the other hand, a solid-like material stores some of the energy input as potential energy, instead of dissipating it all as heat; it may partially recover when the stress is removed. When a perfectly elastic solid is subjected to a sinusoidally oscillating stress, the strain is exactly in phase with the stress; for a perfectly viscous liquid, the strain is 90° out of phase. For a viscoelastic material, some energy input is stored and recovered in each cycle, while some is dissipated as heat. The strain is neither in phase nor 90° out of phase, but is somewhere in between (Ferry, 1980a).

Small-amplitude oscillatory shear or dynamic testing is a valuable technique for investigating viscoelastic behavior of food, including monitoring starch gelatinization, protein coagulation or denaturation, curd formation or melting in cheese, and texture development in meat products (Steffe, 1992). It refers to a situation in which the stress and strain vary harmonically with time, the rate usually being specified as frequency in radians/sec. An experiment is carried out by imposing a strain and measuring the output stress developed in the sample (Murayama, 1978). Let a harmonic strain of amplitude γ_o with frequency ω be applied to

the upper face of a thin block of material. Then the applied strain is:

$$\gamma = \gamma_0 \cos \omega t \qquad (2\text{-}14)$$

which results in a stress:

$$\sigma = \sigma_0 \sin (\omega t + \delta) \qquad (2\text{-}15)$$

The behavior of a material may be characterized by the phase lag, δ, and the amplitude ratio, γ_0/σ_0. For dynamic testing at a given frequency, it has been assumed that materials deform in a linear manner, i.e., the harmonic stress amplitude (output) is proportional to the applied strain amplitude (input) with a phase lag relative to the strain which is independent of amplitude. This is called linear viscoelasticity. Within linear viscoelastic behavior, the amplitude ratio, γ_0/σ_0 and phase lag, δ are not a function of input strain amplitude, but in general, both vary with frequency. Since the storage modulus (G') and loss modulus (G") are:

$$G' = (\sigma_0 \cos \delta)/\gamma_0 \qquad (2\text{-}16)$$

$$G'' = (\sigma_0 \sin \delta)/\gamma_0 \qquad (2\text{-}17)$$

therefore, G' and G" are also independent of input strain amplitude, but a function of frequency (Ferry, 1980a). If the amplitude of strain is large enough, then the stress varies

with the same frequency but is non-sinusoidal; it can have high harmonics, showing nonlinear viscoelastic behavior (Murayama, 1978).

Stress and strain amplitude and frequency are related to heat generation in materials during oscillation:

$$Q = \omega G'' \gamma_0^2/2 \qquad (2\text{-}18)$$

where Q is the energy dissipated per second, ω is frequency, G" is loss modulus, and γ_o is the maximum value of strain amplitude (Ferry, 1980b). The temperature of a material will increase when subjected to high frequency, high strain amplitude oscillation. The internal heat generated by oscillation will cause structural changes in heat-sensitive biopolymers, e.g., proteins. High strain amplitude and high frequency can also result in permanent changes in part of the structure due to breaking of bonds, fatigue and rupture. Therefore, low levels of strain amplitude within the linear viscoelastic range and low frequency are often selected (Murayama, 1978).

Small-amplitude oscillatory measurements can be performed usually using a parallel plate or cone and plate apparatus. Parallel plate works well within a wide range of viscosities and molecular sample sizes; high shear rate is possible with a small gap setting. However, strain and shear rate are a function of the radius--both are higher close to the rim of the plate, and lower close to the center. In this system, the

percent strain, which depends on the geometry, means the distance traveled at the rim of the plate (dl/H) instead of the angular displacement (Steffe, 1992):

$$\theta = \gamma\, H/R \qquad (2\text{-}19)$$

where θ is the sweep angle or strain amplitude in radians, γ is the strain selected, H is the gap width, and R is the radius of the plate. By varying gap width and/or plate radius, the actual angular displacement may be different at the same given percent strain.

Because the linear viscoelasticity is required in dynamic testing, it is necessary to determine the limits of linearity. However, the testing limits of the instrument are another concern which is based on transducer compliance. The transducer will be "deformed" along with the sample during oscillation. Instrument compliance can affect oscillatary measurements by changing gap separation due to normal compliance, and the set displacement due to finite torsional stiffness of the instrument (Gottlieb and Macosko, 1982). The magnitude of the actual sample displacement is calculated by subtracting the transducer displacement from the measured motor displacement:

$$\theta_{sample} = \theta_m - \theta_{td} \qquad (2\text{-}20)$$

Here θ_{sample} is the actual sample strain vector, θ_m is the measured strain vector (motor displacement), and θ_{td} is the

transducer compliance vector. Errors occur if transducer compliance is too large relative to motor displacement. According to Hooke's law,

$$\theta_{td} = K M \qquad (2\text{-}21)$$

where K is transducer compliance constant and M is the torque. Different compliance constants (K) can be applied depending on the sensitivity of the transducer (Gottlieb and Macosko 1982).

For example, the Rheometrics Fluid Spectrometer (RFS) contains a 100 gm-cm full scale transducer that has a 1,000 to 1 dynamic range and is a high sensitivity transducer. According to Gottlieb and Macosko (1982), and the information from the RFS manufacture:

compliance constant (K) = $2.2 * 10^{-6}$ rad/gm-cm,

which gives a transducer stiffness ($1/K$) value of $4.5 * 10^{5}$ gm-cm/rad. By multiplying the full-scale torque obtainable on the RFS (i.e. 100 gm-cm), the maximum compliance displacement is given by

$$\theta_{td} = KM = 2.2 * 10^{-4} \text{ rad.}$$

It was suggested by the RFS manual that the maximum sample stiffness is 10% of transducer stiffness, therefore the maximum sample stiffness is given as $4.5 * 10^{4}$ gm-cm/rad. Based on the following equation, the maximum allowed modulus can be calculated with a given geometry (Morris and Ross-Murphy, 1981):

$$G^* = \frac{2 H g M}{\pi R^4 \theta} \qquad (2\text{-}22)$$

where G^* is complex modulus, H is the gap width, g is the acceleration of gravity, R is the plate radius, and M/θ is sample stiffness. This is the major factor limiting instrument testing ranges.

Strain sweeps monitor the changes in G' and G" of samples within a range of strain, and are used to determine the limits of linear viscoelasticity at a given frequency. Within the linear range, G' and G" are independent of the strain amplitude, so the lower and upper limits of strain can be determined on the rheograms. Any strain within that linear range can be selected for further experiments. Strain-stress amplitude ratio and phase lag (or G' and G") are two frequency-dependent functions. Therefore, a fixed value of frequency is required. Different instruments will possess different working ranges of frequency; however, the natural (resonant) frequency puts an upper limit on the accessible frequency range of the instrumentation. For RFS-8400, the frequency range lies between 0.01 to 500 rad/sec with an accuracy of 0.1% of selected rate, but transducer resonance limits dynamic measurement to 100 rad/sec. Also high frequency and strain magnitude increase viscous heating. Therefore, a low strain within the linear range and a frequency below the highest accessible frequency is desirable. Torque is another factor to consider. The torque must be

within instrumental sensitivity to avoid both scattering data and force overload (0.01 to 100 gm-cm for RFS).

2.6 Fourier Transform Infrared Spectroscopy (FTIR)

A. Instrumentation

Vibrational spectroscopy is a technique for studying the structure of molecules. Raman and infrared spectroscopies measure molecular vibrational frequencies but differ in their sensitivity to different types of vibrations (Braiman and Rothschild, 1988). Infrared absorption spectroscopy is sensitive to vibrations that modulate a molecule's electric dipole moment, and has been recognized as a potential tool for estimating the secondary structure of polypeptides and proteins (Krimm, 1962; Braiman and Rothschild, 1988). Protein three-dimensional structure and its vibrational force field uniquely determine vibrational frequencies (Krimm and Bandekar, 1986). On the basis of Cartesian atomic coordinates obtained by X-ray crystallography, it becomes possible to establish an objective criteria (numerical values) to qualitatively and quantitatively evaluate the secondary structure of proteins (Byler and Susi, 1986). Because of band broadness and overlapping, the interpretation of infrared spectra of proteins is difficult. In principle, Fourier transform infrared spectroscopy (FTIR) improves the

signal-to-noise ratio and frequency accuracy (Gerasimowicz et al., 1986). Fourier self-deconvolution (FSD), second derivative, and band curve-fitting have been employed to enhance the resolution of overlapping bands and identify the peak maximum (Susi and Byler, 1983, 1986). Surewics and Mantsch (1988) have reviewed the resolution-enhancement procedures and band assignments for different secondary structures.

Frequency assignment

The spectral region most important for determining the secondary structure of proteins is the region between 1600 to 1700 cm^{-1} which contains the amide I bands (Krimm, 1962). The amide I band involves mostly C=O stretching vibrations arising from the peptide bond. This vibrational mode is very sensitive to changes in hydrogen bonds and thus leads to characteristic infrared bands from different conformations of the peptide backbone. Most protein conformations are determined in aqueous solution, but water has a strong absorption band at 1650 cm^{-1}, which is in the frequency range of the amide I region. Consequently, D_2O is frequently used as a solvent (Cantor and Timasheff, 1982). Due to improvements in FTIR sensitivity, it is now possible to measure amide I spectra for proteins in water when using a short path-length cell (6-10μm) (Arrondo et al., 1988; Gorga et al., 1989; Dong et al., 1990; Dousseau and Pezolet, 1990).

In the literature, the amide I' region is sometimes designated for the spectra of deuterated proteins (Prestrelski et al., 1991a, b). By using the spectra of synthetic polypeptide and proteins with known X-ray structure, certain band frequencies are assigned to a particular conformation (Table 2.1).

The α-helix has a maximum around 1654 cm^{-1}.; ß segments or extended chains exhibited several low-frequency components between 1620-1640 cm^{-1}, and a single high-frequency component near 1675 cm^{-1}. For highly helical proteins, Byler and Susi (1986) observed a strong helix band near 1650 cm^{-1}, and a weak pair around 1635 and 1675 cm^{-1} which could be short extended chains connecting helical cylinders. Both infrared spectra and theoretical research suggested antiparallel ß-strands showed a strong component in the 1637 cm^{-1}, paired with a

Table 2.1. Amide I' spectra-structure assignments for proteins[1]

Band frequency (cm^{-1})	Conformation
1625	extended strand[1], ß-sheet[2]
1635	extended strand[1], ß-sheet[2]
1639	3_{10}-helix
1645	irregular, disordered
1654	α-helix, loops
1664	turns
1674	extended strand, ß-sheet[2], possibly type II ß-turns
1683	turns, possibly type II ß-turns
1689	turns
1695	turns, possibly carboxyl C=O

[1] See Prestrelski et al. (1991a, b) and references cited therein.
[2] See Susi and Byler (1987).

weaker band in the 1670-1680 cm^{-1} region (Krimm, 1962; Susi et al., 1967; Timasheff et al., 1967; Byler and Susi, 1986; Casal et al., 1988). Another low-frequency component around 1624 cm^{-1} was assigned to exposed ß-strands or strands not part of the core of ß-sheet (Casal et al., 1988). Frequencies around 1626-1640 cm^{-1} were assigned by Bandekar and Krimm (1988a & b) to parallel ß-sheet based on known protein structures. However, Susi and Byler (1987) reported that proteins containing parallel (flavodoxin and triosephosphate isomerase), antiparallel ß-strands (concanavalin A), or mixed ß-chains (carboxypeptidase A) all exhibited a strong amide I band at 1626-1639 cm^{-1} and a weak band near 1675 cm^{-1}. The authors suggested that it was not possible to distinguish both conformations on the basis of amide I infrared frequencies, whereas, only proteins containing all-parallel and mixed ß-chains showed a strong band of helical segments (1652 cm^{-1}). These helical segments might connect parallel ß-strands.

The IR bands near 1663, 1670, 1683, 1688 and 1694 cm^{-1} were assigned to turns, which were in good agreement with theoretical calculations for peptides (Byler and Susi, 1986). Stein et al. (1991) assigned the band at 1684 cm^{-1} as a type III turn in ovalbumin; however, Prestrelski et al. (1991a) reported that type II ß-turns in bovine trypsin absorb in the region of 1672-1685 cm^{-1}. A band close to 1645 cm^{-1} was originally assigned to "unordered segments", or conformations without intrachain hydrogen bonds (Byler and Susi, 1986).

However, Prestrelski et al. (1991a) suggested using the term "irregular" instead, because such segments might still retain certain conformation. The same report also showed that certain loops in proteins might contribute to frequencies around 1655 cm^{-1}.

B. Thermal effect on the structure of proteins

The thermal unfolding of α-helix, accompanied by an introduction or increase of ß-structure has been reported by various researchers. Susi et al. (1967) reported an IR band at 1615 cm^{-1} dominated the amide I spectra during the thermally-induced helix-to-ß sheet transition of poly-L-lysine. Koenig and coworkers, using Raman spectroscopy, suggested that ß-structure was formed by intermolecular hydrogen bonding prior to intermolecular disulfide exchanges (Lin and Koenig, 1976; Painter and Koenig, 1976). In addition, the same authors reported that continuous unfolding of α-helices occurred during aggregation and gel formation. Clark et al. (1981), using IR and laser-Raman spectrocopy to study globular protein gels, also observed that formation of ß-sheet correlated with the aggregation process. This finding was later supported by Byler and Purcell (1989), as evidenced by the appearance of new peaks near 1614 and 1684 cm^{-1} in ß-lactoglobulin and bovine serum albumin prior to gelation. An amide I component below 1620 cm^{-1} has not been observed in the spectra of typical native proteins. In addition, the band

associated with α-helix was observed after thermal denaturation, suggesting not all of the α-helices had uncoiled. In contrast, α-lactalbumin heated at 90°C had no amide I peak below 1620 cm^{-1} and did not gel after heat treatment. Li-Chan and Nakai (1991), using Raman spectroscopy, suggested thermal gelation of lysozyme resulted in a decrease in α-helix, but an increase in ß-sheet structure and random coil, as well as an exposure of aromatic residues. Herald and Smith (1992) compared the changes in secondary structure with denaturation temperatures and rheological properties of S-ovalbumin. The authors observed few changes in secondary structure when S-ovalbumin was heated below the onset temperature determined by DSC; decreases in ß-sheet, α-helix, 3_{10}-helix and increases in peaks of 1614 and 1684 cm^{-1} were observed on FTIR spectra between onset and denaturation temperatures at pD's 3, 7 and 9. Increases in intensity of bands at 1614 and 1684 cm^{-1} also corresponded to increases in G' of S-ovalbumin gels during heating.

2.7 Thermally-induced Gelation of Myosin

A. Mechanism of Protein Gelation

Gelation is one of the important functional properties in foods. Clark (1992) classified gels into four categories based on microstructural characteristics: (1) Lamellar liquid

crystalline mesophases, (2) disordered covalently cross-linked polymeric networks, (3) polymeric networks cross-linked by physical aggregation, and (4) particulate networks. The author also summarized several gelation theories. The Flory-Stockmayer polycondensation model (Flory, 1941; Stockmayer, 1943, 1944) described that the sol fraction consisted of free monomers and small aggregates. As cross-linking proceeds, the sol fraction decreases and the solid character becomes greater. The gel point is a sudden event which occurs when a critical degree of cross-linking is reached. Eventually, most of the monomers become crosslinked into the gel network. The potential reversibility of cross-links and the presence of solvent was considered by Hermans (1965) based on Flory-Stockmayer theory. Hermans (1965) related the extent of cross-linking to polymer concentration to further define the critical gelling concentration. Several other models developed from the Flory-Stockmayer theory were listed in the same review paper. All of these models ignore the volume and the space-filling geometry of aggregates. An alternative theory that Clark described was the percolation theory (Stauffer et al., 1982). The approach is to place monomers on a lattice and randomly introduce a certain proportion of inter-monomer bonds. Clusters of monomers develop that at a critical threshold of bonding, cross-links are throughout the entire lattice. Modern approaches to describe gelation use computers to simulate aggregation processes, using

diffusion-limited aggregation (DLA) models. The details of the models were also described in Clark's paper (1992).

The mechanism of heat-induced protein gelation varies with different protein sources, pH and salt concentrations, as well as heating treatments. Generally thermal gelation of proteins is described as a two-step process involving unfolding of proteins followed by aggregation into a three-dimensional network (Ferry, 1948). The slower the protein aggregation relative to unfolding, the better the denatured chains orient themselves and thus the finer the gel network (Hermansson, 1978). A generalized scheme for thermal gelation based on current accepted gelation models is shown in Fig. 2.9 (Foegeding and Hamann, 1992). The gel point is defined as a branching point at which critical degree of aggregation is reached, the viscosity diverges rapidly to infinity, and the system's elastic modulus changes from an effectively zero value to a growing result. Before the gel point, aggregation proceeds and leads to a more viscous solution (Clark, 1992).

By monitoring the changes in Raman spectra of bovine serum albumin, Lin and Koenig (1976) proposed a gelation mechanism for globular protein systems (Fig. 2.10). Continuous unfolding of α-helices, which was reversible at low temperature, occurred throughout the gelation process. As temperature was increased, intermolecular disulfide exchanges resulted in an aggregation, and the irreversible unfolding of

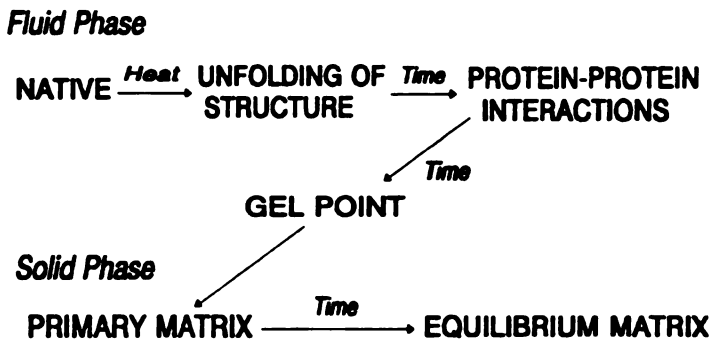

Figure 2.9. Generalized scheme for thermally induced gelation of proteins (adapted from Foegeding and Hamann, 1992).

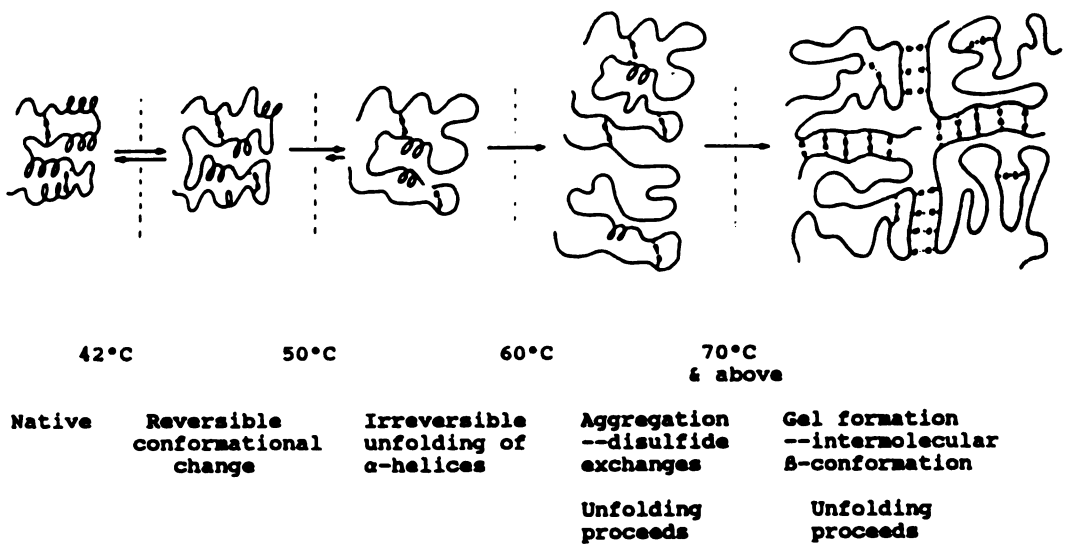

Figure 2.10. Mechanism for heat denaturation of bovine serum albumin (adapted from Lin and Koenig, 1976).

α-helices proceeded. Clark et al. (1981) suggested network formation arose through a competition between attractive forces generated between protein molecules after thermal unfolding, and repulsive forces existing because of protein charge. The authors challenged Lin and Koenig's theory (1976) regarding the formation of new, more ordered ß-conformation during gelation. Proteins with a high content of ß-sheet might undergo structural changes within existing sheets instead of forming new ß-structures. Additionally, the formation of ß-structure might be a feature of one particular type of gelation mechanism.

Several studies have reported an increase in surface hydrophobicity in the first stage (unfolding), and a decrease in the second stage (aggregation) of thermal gelation by measuring intrinsic fluorescence and/or using fluorescence probes (Nakai, 1983; Wicker et al., 1986; Nakai and Li-Chan, 1988; Wicker and Knopp, 1988; Wicker et al., 1989; Morita and Yasui, 1991). Greater hydrophobic surface exposed to polar environments was found to promote the formation of a network (Chan et al., 1992). Gelation was inhibited by urea or guanidine hydrochloride, which suggested the involvement of hydrophobic interactions (Samejima et al., 1976; 1981). These results concluded that hydrophobic groups play an important role in gel formation. Hydrophobic interactions are a consequence of strong interactions between water molecules, rather than of direct interactions between nonpolar residues

of proteins (Tanford, 1980; Nakai and Li-Chan, 1988; Creighton, 1993). When a nonpolar molecule is introduced into water, it decreases the entropy by increasing the ordering of water around the nonpolar molecule. To minimize this unfavorable entropic change, nonpolar residues of a protein are forced into the interior of protein globules. Therefore, hydrophobic interactions are considered the primary driving force for protein folding and stability (Creighton, 1993).

As temperature is increased, the water structure is randomized and the positive contribution from entropy is decreased, so proteins unfold. At high temperature, hydrophobic interactions become weaker than van der Waals interactions between nonpolar residues and hydrogen bonding in water, thus the enthalpy term dominates the stability of proteins (Nakai and Li-Chan, 1988; Creighton, 1993).

An increase in exposed sulfhydryl groups occurs during protein unfolding. The role of disulfide bonds in heat-induced gelation is not clear. Voutsinas et al. (1983) observed that thermal gelation of proteins was significantly correlated with hydrophobicity of unfolded protein and sulfhydryl content. Wicker et al. (1989) suggested gelation at high temperature more likely involves disulfide and electrostatic linkages, because naturing or denauring salts (used to perturb hydrophobic interaction) did not change the temperature at which rigidity increased in fish myosin (around 55°C). Li-Chan and Nakai (1991) found little change in

lysozyme SH content even though a strong gel was formed at 100°C, 12 min, for lysozyme containing four disulfide bonds but no free sulfhydryl groups. However, Raman spectra showed a change in disulfide stretching vibrations at 100°C, from all gauche to a gauche-gauche-trans conformation. The authors suggested that these intramolecular disulfide bond interchange reactions at high temperature resulted in destabilization of lysozyme structure, and thus proteins were easier to unfold. It was thought that intermolecular disulfide cross-links resulting from disulfide interchange were present due to the formation of gels which could not be solubilized by 8 M urea. The authors concluded that intermolecular disulfide cross-links were not necessary for gelation, but could lead to more stable gels.

B. Thermal Gelation of Myosin

Role of myosin subfragments in thermal gelation

Early investigations on the gelation of muscle proteins were done by Samejima, Yasui and coworkers. These authors indicated that rabbit skeletal myosin had a marked influence on development of high gel strength, showing two transitions at 43 and 55°C (Samejima et al., 1969; Yasui et al., 1980). Intact myosin and myosin rod were able to form firm gels, while S-1 exhibited poor gelling ability upon heating (Samejima et al., 1981). These authors suggested that oxidation of two sulfhydryl groups located in the myosin S-1

might be involved in the thermal aggregation of the head portion of rabbit muscle myosin. In the presence of F-actin, there were no changes in thermal gelling properties of myosin head and helical tail fragments. In contrast, addition of F-actomyosin had a significant effect on the gelation of the myosin rod, but no influence on gelation of the S-1 sub-fragment. Therefore, Yasui et al. (1982) concluded that even though the S-1 and HMM possess actin-binding sites, they lack the necessary tail portion for the production of a gel network. The cross-linking between free and bound myosin molecules was initiated only through interactions between the myosin rod. Samejima et al. (1984) reported that light chains contribute little to gelation of myosin in model systems, but possibly provide some stability to the gel if pH is increased above 6.0. Morita and Ogata (1991) observed alkali light chains (LC1 and LC3) of rabbit muscle myosin began to decrease in band intensity at about 35°C by SDS-gel electrophoresis, while regulatory light chains (LC2) did not dissociate from myosin even above 70°C. The LC2-deficient myosin showed lower rigidity than intact myosin at KCl concentrations below 0.3 M. The amount of F-actin required for maximum rigidity of LC2-deficient myosin gels was higher than that needed for intact myosin, suggesting myosin and F-actin interaction was affected by LC2 removal. The authors suggested LC2 might have a role in heat-induced gelation.

Mechanism of myosin gelation

Ziegler and Acton (1984) summarized the thermal denaturation process of natural actomyosin based on observations reported in literature. The changes of actomyosin begin with dissociation of tropomyosin from F-actin at 30-35°C. The super helical structure of F-actin dissociates into single chains at 38°C. The conformational changes in myosin head and hinge region occurs in the temperature range of 40-45°C, followed by actin-myosin complex dissociation (45-50°C). Helix-coil transitions in LMM and rapid aggregation are induced at 50-55°C. Actin undergoes major conformational changes above 70°C.

With the introduction of dynamic rheological testing in food systems, the transition temperatures and gelation progress can be monitored during heating. Egelandsdal et al. (1986) studied the viscoelasticity of myosin isolated from beef loin (*Longissimus dorsi*), and suggested interfilamental self-association of HMM (ionic strength < 0.34) contributed to the rheological properties of myosin filaments at low temperature (<40°C). Denaturation of myosin HMM occurred between 40 and 50°C, resulting in an increase in gel strength. The decline in storage modulus between 50 and 60°C was attributed to LMM denaturation that weakened the interactions between myosin molecules and led to higher fluidity. Based on the results of Wright and Wilding (1984), Egelandsdal et al. (1986) suggested the sequence of denaturation of myosin

domains changed at high ionic strength, starting with domains of LMM. The last transition occurred at 62-63°C and was designated as the most stable region in LMM.

By comparing turbidity with viscoelasticity, Sano et al. (1990b) reported the aggregation of fish HMM (0.6 M KCl, 20 mM potassium phosphate buffer, pH 7.0) occurred at 53°C, while LMM started to aggregate at 30 and 46°C. This supported their previous suggestion that HMM participated in the development of myosin gel elasticity between 51 to 80°C. The interaction of myosin tails was responsible for the increase in G' and G" within the range of 30 to 45°C (Sano et al., 1988, 1990a). However, as HMM and LMM were mixed, the transition temperatures changed to 33 and 37°C (Sano et al., 1990b), suggesting the interaction between subfragments influences their thermal stability. Thus, the previous description of myosin denaturation might require more evidence. Circular dichroism studies on changes in helical content and fluorescent studies on hydrophobicity showed that turkey breast myosin (Arteaga and Nakai, 1992) and rabbit LMM (Morita and Yasui, 1991) started to unfold at 30°C. Fish myosin in 0.6 M NaCl, pH 6.5 unfolded at temperature as low as 25°C, and about 50% of initial helical content was lost when the temperature reached 40°C (Chan et al., 1992).

All the above observations and the results from DSC studies (Stabursvik and Martens, 1980; Wright and Wilding, 1984; Akahane et al., 1985; Rodgers et al., 1987; Bertazzon

and Tsong, 1990a, b) showed that the mechanism of myosin gelation varied with species, buffer conditions, and other unknown factors. Fish myosin has lower thermal stability, and its rod region tends to unfold at lower temperatures than those of beef, poultry, or rabbit myosin. It is also possible that the rods/LMMs of beef, poultry or rabbit unfold and aggregate at temperatures as low as 30°C. Because of the necessity of the myosin rod for gel development, the sequence of myosin denaturation and the subsequent aggregation might determine gel properties.

Factors influencing myosin gelation

Various factors have been observed to influence myosin gel strength, such as pH, salt, protein concentration, heating rate, length of myosin filaments and the presence of other myofibrillar proteins. Rabbit myosin exhibits the highest gel strength at pH 6.0 and gradually weakens as pH is increased above 6.0 (Ishioroshi et al., 1979; Samejima et al., 1984; Wicker et al., 1986). Myosin molecules were soluble and existed as monomers at high ionic strength (above 0.3 M), while the myosin molecules assembled into filaments at low ionic strength (Huxley, 1963; Kaminer and Bell, 1966). At 0.1 to 0.2 M KCl, myosin gels show higher rigidity but less elasticity than at 0.6 M KCl. Myosin in 0.3 M KCl exhibits the least rigidity, but gel rigidity increased with salt concentration above 0.3 M (Ishioroshi et al., 1979; Wicker et

al., 1986). Soluble myosin at high ionic strengths tends to produce head-to-head aggregates during heat gelation. Myosin filaments form a finer network at low ionic strength and produce greater rigidity than monomeric myosin (Ishioroshi et al., 1979; Hermansson et al., 1986; Morita et al., 1987).

Wu et al. (1991) reported the gelation of chicken breast myosin follows second order kinetics based on the rheological properties. The maximum rate constant was found at 52°C, and the maximum equilibrium shear modulus was between 48 to 50°C. Gels formed at 44-56°C were more elastic than those formed at 58-70°C. The authors suggested that low temperatures favored the aggregation process, while high temperatures weakened the intramolecular and cross-linking bonds of myosin gels.

Hermansson et al. (1986) suggested that the condition for formation of certain types of bovine myosin gels depended on their states prior to heating; variation in heating temperatures had little effect on gel structure. Sano et al. (1990a) also suggested the viscoelastic behavior during gelation related to the state of myosin. The authors observed lower G' and G" values for fish myosin filaments than monomeric myosin, which was opposite to what had been reported previously (Ishioroshi et al., 1979; Hermansson et al., 1986; Morita et al., 1987). The length of myosin filaments at low ionic strength also determined network structure and gel rigidity. By changing the speed of lowering the ionic strength (dilution vs. dialysis), Yamamoto et al. (1988)

observed that shorter filaments were formed by rapid dilution. Longer filaments were formed by dialysis. Short filaments aggregated randomly and formed coarsely aggregated gel networks with low rigidity; long filaments formed fine strand-like networks with high rigidity.

C. Thermal Effect on Actin

Filamentous actin had elastic properties and thixotropic behavior (Brotschi et al., 1978). Zaner et al. (1988) observed G-actin solutions acted as Newtonian fluids, whereas, Sato et al. (1985, 1986) reported diluted G-actin formed a viscoelastic gel upon stress. Filamentous actin had no gelling ability after heating (Yasui et al., 1979, 1980), and did not develop viscoelastic character (Sano et al., 1989a). The heat denaturation of F-actin follows first-order kinetics. ATP shows a protective effect on heat denaturation of F-actin (Ikeuchi et al., 1981), while the protective effect of ATP on the structure and function of G-actin was observed to diminish above 40°C (Lehrer and Kerwar, 1972). Ikeuchi et al. (1990) reported that heating at 35-45°C for 3 hr or at 50°C for 30 min induced the polymerization of G-actin in the presence of 0.3 mM ATP, without addition of KCl or $MgCl_2$. Electron microscopy revealed that irregular filaments were formed due to these heat treatment.

D. Thermal Gelation of Actomyosin

Even though F-actin does not show any gelling ability, it has been reported that F-actin and myosin exert a "synergistic gelling effect" in rabbit skeletal muscle. Maximum gel strength (65°C for 20 min) in 0.6 M KCl, 20mM phosphate buffer, pH 6.0 was obtained at a free myosin to F-actin molar ratio of 2.7:1, which corresponds to a weight ratio of 15:1. At this ratio, 15-20% of the total protein existed as an actomyosin complex and the remainder was free myosin (Ashgar et al., 1985). Myosin with small amounts of actomyosin was optimal at pH 6.0 in 0.6M KCl. As F-actin increased, the optimal pH decreased (Yasui et al., 1980). Ishioroshi et al. (1980) reported that F-actin did not increase myosin gel rigidity when myosin-actin mixture was incubated with ATP or pyrophosphate prior to thermal treatment. This indicated the increased rigidity was due to the interaction between myosin and actin. Dudziak et al. (1988) found that myosin to actomyosin weight ratios for postrigor turkey breast and thigh were 3.8:1 and 6.9:1, respectively. Turkey breast myosin gels were more stable and had greater rigidity than thigh myosin gels. These results coincide with myosin-to-actomyosin ratio data reported by Yasui et al. (1980). Using dynamic rheological measurements, Sano et al. (1988) reported that elasticity of fish myosin increased between 34 to 48°C. Natural actomyosin (actin-to-myosin ratio 0.34) showed higher G', G" and tangent δ than myosin. It was also found that

increasing F-actin/myosin ratio caused a decrease in elasticity of actomyosin between 46-53°C (Sano et al., 1989b). The authors suggested dissociation of myosin from actin filaments and fragmentation of actin filaments within this temperature region, resulting in breakdown of the gel matrix.

CHAPTER THREE : EFFECT OF ISOTHERMAL HEATING ON DYNAMIC RHEOLOGICAL PROPERTIES AND SECONDARY STRUCTURE OF CHICKEN BREAST MYOSIN

3.1 Abstract

Heat-induced gelation of chicken breast myosin in 0.6 M NaCl, pD or pH 6.5 was studied by monitoring changes in rheological properties using small strain dynamic testing. Secondary structural changes were analyzed by Fourier transform infrared spectroscopy (FTIR). Myosin heated for 30 min at 55 and 65°C had higher storage moduli (G') than at 75°C. No differences in loss moduli (G") were observed at any temperature. Myosin heated at 75°C showed higher loss tangent indicating more viscous character, while myosin at 55 and 65°C formed more elastic gels. The sol-to-gel transition was observed at 55°C. After 40 min cooling, G', G" and loss tangent of myosin heated at 65 and 75°C increased, while cooling had little effect on myosin heated at 55°C. Second-derivative infrared spectra of native myosin showed protein absorption bands for α-helix (1652 cm^{-1}) and ß-sheet (1636 cm^{-1} paired with 1676 cm^{-1}). Myosin at 45°C had a similar spectrum except for the appearance of weak absorption bands near 1683 (turns) and 1629 cm^{-1} (extended strands). Bands attributed to

α-helix and ß-sheet decreased with an increase in temperature above 45°C, indicating unfolding of myosin during the sol-to-gel transition. Intensity of the band at 1683 cm^{-1} increased between 45 and 55°C, showed little change at 65°C, and increased again at 75°C. The band at 1613 cm^{-1} appeared at 55°C, increased in intensity when heated at 65°C, but remained constant at 75°C. Both bands were attributed to the formation of intermolecularly hydrogen-bonded ß-structure. Band intensity at 1613 cm^{-1} and 1683 cm^{-1} did not correlate with dynamic moduli after cooling at the three heating temperatures, suggesting formation of ß-structure was not solely responsible for gel properties.

3.2 Introduction

Because of the importance of myosin in texture of comminuted meat products, myosin unfolding and aggregation during heating have been investigated to understand the mechanism of protein gelation and to manipulate protein gel functionality (Wicker et al., 1986; Dudziak et al., 1988). Heat-induced protein gelation was defined as a two-step process involving unfolding of proteins followed by aggregation into a three-dimensional network. Protein unfolding and orientation of unfolded molecules during aggregation influence the development of a gel network (Ferry,

1948; Hermansson, 1978). Clark et al. (1981) stated that network formation arose through a competition between attractive and repulsive forces. Based on these models (Ferry, 1948; Hermansson, 1978; Clark et al., 1981), Foegeding and Hamann (1992) elaborated a generalized scheme for heat-induced gelation: protein unfolding and subsequent interactions leading to the gel point (sol-to-gel transition), after which the primary matrix formed and reached equilibrium.

Thermal gelation of myosin involves unfolding of the protein and subsequent aggregation of myosin domains. Structural changes occurred in the rabbit myosin head (S-1) and hinge region in the temperature range of 37-45°C (Sutoh, et al., 1978; Swenson and Ritchie, 1980; Burke et al., 1987). Yamamoto (1990), using electron microscopy, observed that the aggregation of rabbit myosin molecules heated isothermally at 40°C occurred through the head regions to form daisy wheel-shaped oligomers with the myosin tails extending radially. This observation was supported by Sharp and Offer (1992) who found this head-head aggregation proceeded at 60°C. Both studies suggested the radially extended tails were important in cross-linking of gel network. Shortening in the myosin tail was also observed after incubation at 40°C, which might have resulted from a helix-coil transition in myosin subfragment 2 region (Yamamoto, 1990). The temperature-induced helix-coil transitions in light meromyosin (LMM) showed different results. Potekhin et al. (1979) and

Bertazzon and Tsong (1990b) assigned the denaturation peaks between 48 to 60°C to rabbit LMM in 0.5 M KCl, pH 6.5. Cross et al. (1984) attributed the low temperature transition (43°C) to LMM in 0.6 M KCl, pH 7.0. In contrast, helical content of turkey breast myosin (Arteaga and Nakai, 1992) and rabbit LMM (Morita and Yasui, 1991) as measured by circular dichroism decreased at temperatures as low as 30°C. The helical content of fish myosin started to decrease at 25°C (Chan et al., 1992). It has been accepted that myosin rod is necessary for developing elastic gel networks (Ashgar et al., 1985). Based on the above observations, the unfolding of myosin rod or LMM varied with species, heating conditions, buffer system and other unknown reasons. The sequence of myosin unfolding; therefore, might determine the gel properties.

Infrared absorption spectroscopy has been recognized as an important tool for estimating the secondary structure of polypeptides and proteins (Krimm, 1962). Fourier transform infrared spectroscopy (FTIR) improves the signal-to-noise ratio and frequency accuracy as compared to conventional dispersive techniques (Gerasimowicz et al., 1986; Susi and Byler, 1986) and yields more details for interpretation. Second derivative spectra have been used to enhance the resolution of overlapping bands and identify peaks (Susi and Byler, 1983, 1986). The spectral region between 1600 to 1700 cm^{-1} (Amide I) is most important for determining the secondary structure of proteins (Krimm, 1962). By comparing the spectra

of synthetic polypeptide and proteins with known X-ray structures, certain band frequencies were assigned to particular protein conformations (Susi and Byler, 1987; Prestrelski et al., 1991a, b). For example, the α-helix has a maxima around 1654 cm^{-1}; ß segments or extended chains exhibited several low-frequency components between 1620-1640 cm^{-1}, and a single high-frequency component near 1675 cm^{-1}. The IR bands close to 1663, 1670, 1683, 1688 and 1694 cm^{-1} were assigned to turns (Byler and Susi, 1986). A band close to 1645 cm^{-1} was assigned to irregular structures which have not been classified as standard types of secondary structure (Prestrelski et al., 1991a).

The thermal unfolding of α-helix, accompanied by an introduction or increase of ß-structure has been reported in several proteins using Raman spectroscopy (Lin and Koenig, 1976; Painter and Koenig, 1976; Clark et al., 1981; Li-Chan and Nakai, 1991) and FTIR (Byler and Purcell, 1989; Herald and Smith, 1992). Koenig and coworkers suggested that ß-structure was formed by intermolecular hydrogen bonding (Lin and Koenig, 1976; Painter and Koenig, 1976). Clark et al. (1981), using IR and laser-Raman spectroscopy to examine globular protein gels, also observed that formation of ß-sheet correlated with the aggregation process. This finding was later supported by Byler and Purcell (1989) as evidenced by the appearance of new peaks near 1614 and 1684 cm^{-1} in ß-lactoglobulin and bovine serum albumin after heat treatment. The band associated with

α-helix decreased in intensity, but was still observed after thermal denaturation, suggesting not all of the α-helices had uncoiled. Herald and Smith (1992) compared the changes in secondary structure with DSC transition temperatures and rheological properties of S-ovalbumin. The authors observed a decrease in β-sheet, α-helix and 3_{10}-helix and increases in peaks of 1614 and 1684 cm^{-1} when heated between onset and denaturation temperatures determined by DSC. Increases in intensity of bands at 1614 and 1684 cm^{-1} was found to correspond to increases in G' of S-ovalbumin gels during heating.

Since the mechanism of myosin gelation is not clear, it is necessary to understand the relation between myosin structural changes and gel development. In this study, we used small strain dynamic testing to follow the gelation of chicken breast myosin during isothermal heating and monitored changes in its secondary structure using FTIR.

3.3 Materials & Methods

Extraction of Myosin

Broiler breast muscle myosin was extracted as described by Nauss et al. (1969) at 4°C. Muscles were ground twice through a 4 mm plate with a meat grinder (Kitchen Aid, Hobart Corp., Troy, OH). The minced meat was extracted with three

volumes of modified Guba-Straub solution (0.3 M KCl, 0.1 M KH_2PO_4, 50 mM K_2HPO_4, 1 mM EDTA, 4 mM Na-pyrophosphate, pH 6.5) for 10 min with vigorous stirring but without foaming. Extraction time was limited to 15-20 min to minimize actin extraction. The extract was diluted with 3 volumes of distilled water, and the muscle residue was filtered through three layers of cheesecloth (this residue was used later for the preparation of actin). The filtrate was diluted with 6.5 volumes of 1 mM EDTA with rapid stirring and allowed to precipitate overnight. The supernatant was then removed by siphoning and precipitated protein was collected by centrifugation at 1000 x g for 45 min at 4°C. The precipitate was resuspended in a minimal, recorded volume of 3 M KCl, 25 mM PIPES buffer, pH 7.0, and subsequently diluted with distilled water to final concentrations of 0.6 M KCl, 5 mM PIPES. Magnesium chloride and sodium pyrophosphate were added to final concentration of 5 mM and 3 mM, respectively. The solution was stirred vigorously for 10 min without foaming, and centrifuged at 78,000 x g for 1 hr at 4°C (Beckman Ultracentrifuge, Model L7-65, Beckman Instruments, Inc., Palo Alto, CA). Solid $(NH_4)_2SO_4$ was added slowly to 35% saturation with constant stirring and the solution was centrifuged at 10,000 x g for 15 min at 4°C. The supernatant was brought to 48% saturation by slowly adding solid $(NH_4)_2SO_4$ with constant stirring. The myosin pellet was collected by centrifugation at 10,000 x g for 15 min at 4°C and stored at -20°C for future

use.

Prior to use, myosin was resuspended in 1 mM EDTA, 0.6 M NaCl, 50 mM Na phosphate buffer, pH 6.5, and dialyzed against two changes of the same buffer. Myosin was dialyzed a third time against the same buffer but without EDTA. The dialyzed myosin solution was centrifuged at 78,000 x g for 1 hr, 4°C. Myosin concentration was determined using an extinction coefficient of $E^{1\%}$ = 5.5 at 280 nm (Swenson and Ritchie, 1980).

The deuterated myosin was prepared by concentrating 2 mL of 2 mg/ml myosin solution in microconcentrators (Centricon-10, Amicon, Danvers, MA) at 5000 x g for 4 hr, and replacing with 0.6 M NaCl, 50 mM KD_2PO_4 buffer, pD 6.5. The deuterium exchange process was repeated twice. The microconcentrator were purged with dry nitrogen and capped prior to centrifugation.

Dynamic Rheological Measurements

Dynamic rheological testing was used to monitor gel development of myosin (10 mg/mL) at 55, 65 and 75°C for 30 min. Dynamic rheological measurements were performed using a Rheometrics Fluid Spectrometer (RFS-8400, Rheometrics, Inc., Piscataway, NJ) fitted with a 50 mm diameter parallel plate apparatus and 100 g-cm transducer. Myosin solution was loaded in the sample cup and equilibrated at the desired temperature for 1 min prior to measurement. The temperature of the sample

was verified using a thermocouple connected to the upper plate of the sample cup. The gap between upper and lower plates was controlled between 1 and 1.5 mm. Storage (G') and loss (G") moduli were recorded continuously at a frequency of 10 rad/sec (Wang and Smith, 1990) and strain of 0.03. Strain was determined in preliminary experiments by conducting strain sweeps (0.0001 to 0.5) at each isothermal temperature. Strain selected was within the linear range of all conditions. Loss tangent (tan δ = G"/G') was used to show the relative viscoelastic properties. It is 0 for a pure solid and infinite for a pure liquid.

Fourier Transform Infrared Spectroscopy

Deuterated myosin (2 mg/mL in 0.6 M NaCl, 50 mM K dideuterium phosphate, pD 6.5) in capped glass vials was purged with nitrogen gas for 10 min, heated at 45, 55, 65 and 75°C for 30 min, and cooled in ice water. Both heated and unheated myosin solutions in capped vials were purged with dry nitrogen gas for 10 min prior to testing. The sample loading was done in a glovebox under an atmosphere of nitrogen which was dried by passing through $CaSO_4$ desiccant. Myosin solutions (100 μL) were loaded into a circular demountable cell (Model P-3 N930-1117, Perkin-Elmer, Norwalk, CT) with CaF_2 windows and Teflon spacers of 75-μm path length. Infrared spectra were collected at ambient temperature using a FTIR spectrometer (Model 1800, Perkin-Elmer) equipped with an

incandescent wire source, a potassium bromide coated beam splitter, and a broad-range mercury/cadmium/telluride detector. All spectra were scanned 500 times at a resolutions of 2 cm^{-1}. Second-derivative analysis (CDS-2 Applications Software, Perkin-Elmer) was performed to enhance resolution, using the Savitzky-Golay derivative routine (Savitzky and Golay, 1964) with a 13-data point (13 cm^{-1}) window. Spectra contributed from a deuterated buffer blank and residual water vapor were subtracted before analysis. Band frequencies were assigned to secondary structural features based on published values (Byler and Susi, 1986, 1988; Prestrelski et al., 1991a, b; Susi and Byler, 1983, 1987).

Statistics

A completely randomized design containing six replications was used to study the influence of isothermal heating and cooling on dynamic rheological properties and FTIR studies of myosin. Two replicates were evaluated within each of three extractions. Tukey's test and analysis of variance (two-way ANOVA) were performed to test significance between replications and treatments (MSTAT, 1989).

3.4 Results & Discussion

Dynamic Rheological Measurements

Isothermal heating & cooling

When myosin was loaded in the sample cup heated in the circulating media, temperature gradient occurred within the protein before reaching equilibrium. The initial temperature fluctuation was not able to be controlled, and was different between three heating temperatures. Therefore, the final gel properties (after 30 min heating) were focused.

Myosin heated isothermally at 45°C did not gel as G' and G" did not change. Myosin heated at 55°C showed a sharp increase in both G' and G" during the first 5 min (Fig. 3.1a). Little change in G" was found on further heating. A slight increase then decrease in G' was observed when myosin was heated at 65°C during the first 5 min, followed by a gradual increase toward equilibrium (Fig. 3.1b). An initial transition was also observed in G"; however, prolonged heating showed little effect on G" development. Isothermal heating at 75°C caused an initial increase in G' which did not change on further heating. Little change was observed in G" throughout heating (Fig. 3.1C). Myosin at 65°C and 55°C had about 3-4 fold higher G' than myosin at 75°C after 30 min heating, while G"s were not different (Table 3.1).

Loss tangent at all three isothermal temperatures showed a two-phase transition (Fig. 3.2). Tangent δ decreased

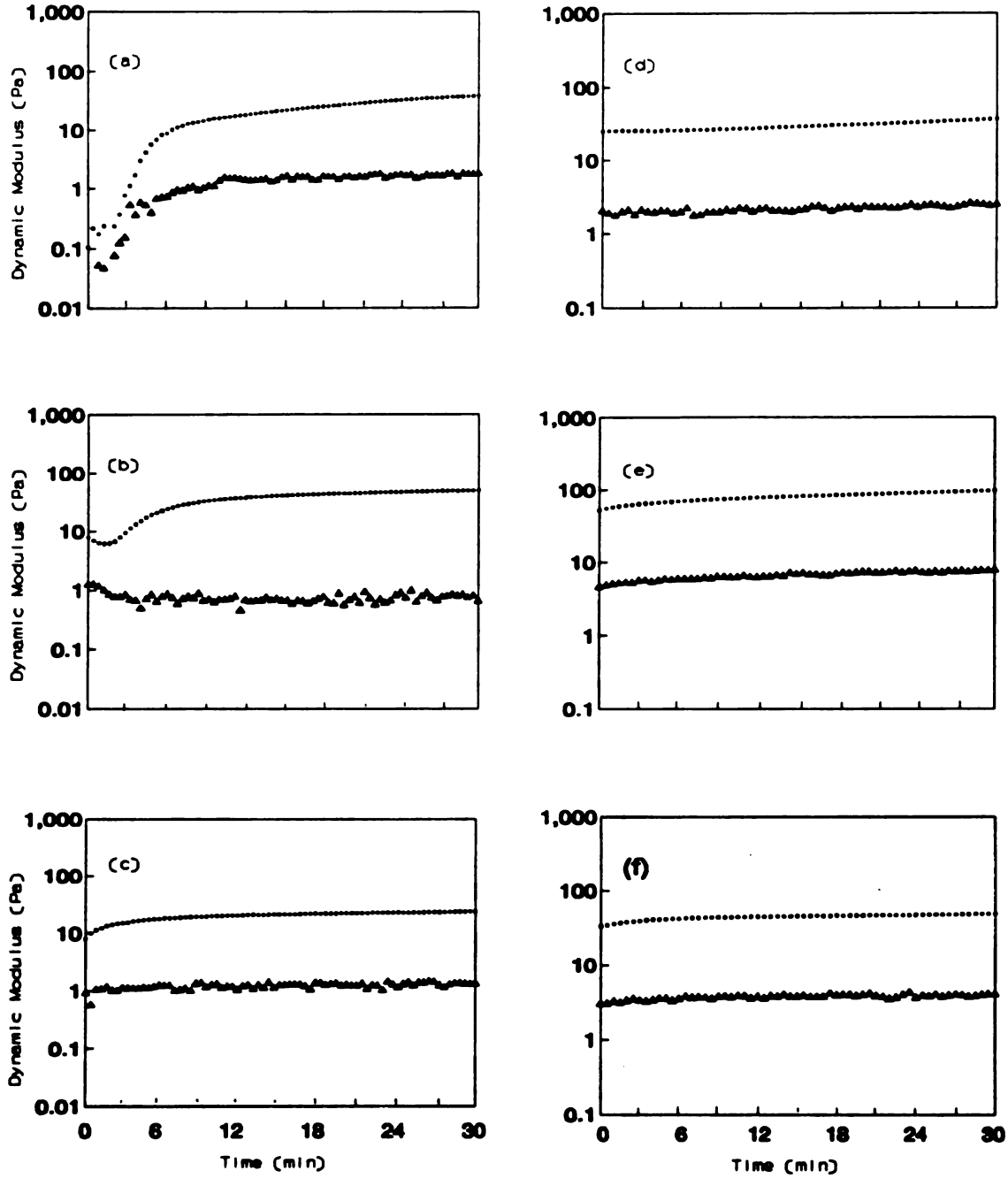

Figure 3.1. Effect of isothermal heating for 30 min and cooling on storage (dot) and loss (triangle) moduli of myosin in 0.6 M NaCl, 50 mM Na phosphate buffer, pH 6.5. (a) 55°C, (b) 65°C, (c) 75°C, and cooled after heating at respective temperatures (d) 55°C, (e) 65°C, and (f) 75°C.

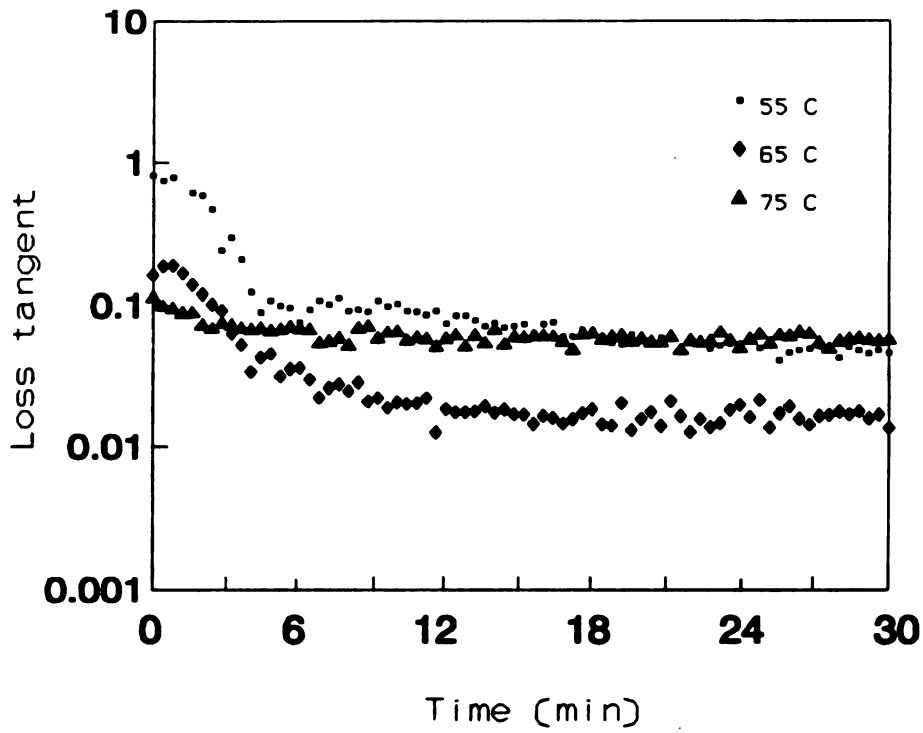

Figure 3.2. Effect of temperature on loss tangent of myosin (10 mg/mL) during isothermal heating in 0.6 M NaCl, 50 mM Na phosphate buffer, pH 6.5.

Table 3.1. Dynamic rheological properties of 10 mg/mL myosin in 0.6 M NaCl, 50 mM Na phosphate, pH 6.5 after isothermal heating and cooling[1]

Moduli	Temperature (°C) 55	65	75
HEATING[2]			
G' (Pa)	37.6^{bc}	50.2^{b}	13.7^{d}
G" (Pa)	1.47^{b}	1.42^{b}	0.69^{b}
loss tangent	0.04^{de}	0.03^{e}	0.06^{bc}
COOLING[3]			
G' (Pa)	24.7^{cd}	84.7^{a}	45.5^{bc}
G" (Pa)	1.23^{b}	5.57^{a}	3.90^{a}
loss tangent	0.05^{cd}	0.07^{b}	0.09^{a}

[1] Means within the same modulus (both heating and cooling) followed by the same letter are not different (P > 0.05).
[2] Myosin was heated at indicated temperature for 30 min.
[3] Heated myosin was cooled for 40 min to a final temperature of 27 to 30°C.

Table 3.2. Effect of temperature on loss tangent of myosin in 0.6 M NaCl, 50 mM Na phosphate, pH 6.5 during isothermal heating[1]

Loss Tangent	Temperature (°C) 55	65	75
Slope 1	-0.311^{b}	-0.124^{a}	-0.090^{a}
Slope 2	-0.014^{b}	-0.005^{a}	-0.004^{a}
Time Intersect (min)	4.3^{b}	6.0^{a}	4.1^{b}

[1] Means within rows followed by the same letter are not different (P > 0.01).

rapidly at 55°C (slope -0.311), indicating sol-to-gel transitions. After four minutes heating, tangent δ decreased at a slower rate (slope -0.014) and reached equilibrium, suggesting gel development was complete. The same trend was observed at 65 and 75°C (Table 3.2). The low tangent δ and high G' at both 55 and 65°C after 30 min heating (Table 3.1) indicated the development of gel elasticity. Myosin at 75°C had the highest loss tangent (the most viscous) after 30-min heating. The high loss tangent and low G' of myosin at 75°C suggested poorer gel quality.

Wu et al. (1991) reported that myosin gelation followed second order kinetics with a maximum rate constant at 52°C. The maximum equilibrium shear modulus was between 48 and 50°C in 0.5 M NaCl, 10 mM Na phosphate, pH 7.0. Gels formed at 44-56°C had a greater shear modulus and were more elastic than those formed at 58-70°C. In our study, high temperature heating (75°C) produced poor myosin gels; however, no significant differences in G', G" and loss tangent were observed between myosin gels formed at 55 and 65°C. One possibility for the differences was that Wu et al. (1991) reported shear modulus under equilibrium condition which required longer heating time, while we recorded the moduli after 30 min heating. The higher negative value of the second tangent δ slope at 55°C might lead to a lower loss tangent (higher elasticity) than those at 65 and 75°C during prolonged heating.

Storage moduli of myosin paralleled G" during cooling after heating at all three temperatures (Figs. 3.1d, e & f). Cooling of myosin heated at 65 and 75°C for 40 min caused a significant increase in G' , G" and tangent δ (Table 3.1). Gel elasticity was increased (higher G') but the gel had more liquid-like behavior due to cooling (higher tangent δ). On the contrary, smaller changes in moduli were observed during cooling of myosin heated at 55°C. Increases in G' and loss tangent due to cooling were also reported by Hines and Foegeding (1993) using α-lactalbumin, ß-lactoglobulin, bovine serum albumin and whey protein isolate initially heated to 80°C. According to our study, increases in moduli due to cooling occurred only for myosin heated above 55°C, suggesting cooling promoted more protein-protein interaction in certain networks formed at higher heating temperatures.

FTIR

Identification of peaks in second derivative spectra of myosin are listed in Table 3.3. The spectrum of unheated myosin showed two major peaks near 1636 cm^{-1} and 1651 cm^{-1}, as well as a minor peak around 1676 cm^{-1} (Fig. 3.3a). The bands absorbing between 1650-1657 cm^{-1} were identified as α-helix; a strong component at 1637 cm^{-1} paired with a minor peak in 1670-1680 cm^{-1} region was characterized as ß-structure (Byler and Susi, 1986; Krimm and Bandekar, 1986; Susi and Byler, 1987).

Table 3.3. Band identification of myosin second-derivative spectra (cm^{-1}) obtained by Fourier transform infrared spectroscopy[a].

Band Assignment[c]	Unheated Myosin	Isothermal Heating (°C)[b]			
		45	55	65	75
turns; hydrogen-bonded ß-sheet		1683	1683	1683	1683
ß-sheet	1676	1675			
turns			1669	1669	1672
turns				1664	1666
α-helix; loops				1658	1657
α-helix	1652	1651	1650	1650	1651
irregular				1648	1646
irregular			1640	1641	1640
ß-sheet	1636	1635	1635	1636	1636
extended strand		1629		1631	1627
hydrogen-bonded ß-sheet			1614	1613	1614

[a] Myosin concentration was 2 mg/mL in 0.6 M NaCl, 50 mM K dideuterium phosphate buffer, pD 6.5.
[b] Myosin was heated isothermally at indicated temperature for 30 min.
[c] Band assignments were made based on work of Prestrelski et al., 1991a, b; Byler and Susi, 1988, 1986; Susi and Byler, 1987, 1983.

Figure 3.3. Effect of isothermal heating for 30 min on myosin FTIR spectra. (a) unheated, (b) 45°C, (c) and (d) 55°C, (e) 65°C, and (f) 75°C. The spectra were recorded after myosin was cooled to ambient temperature.

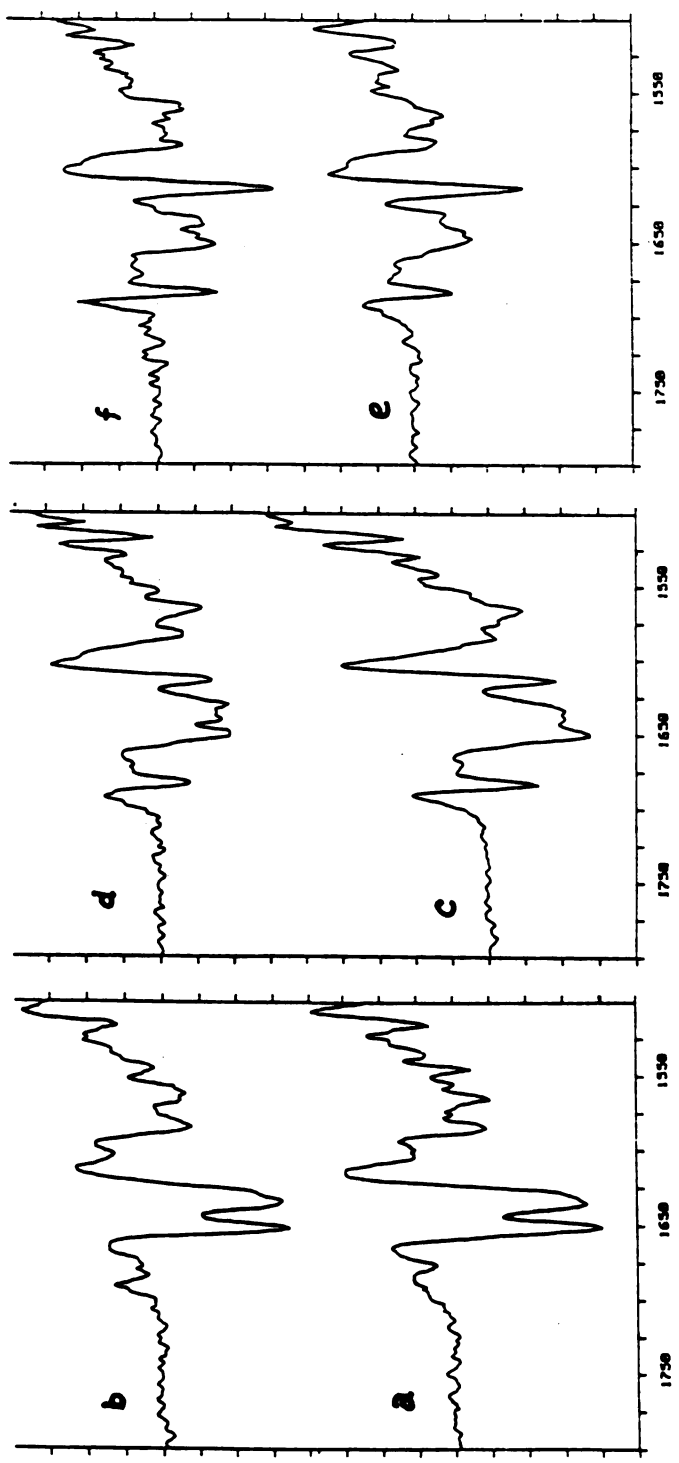
a
b
c
d
e
f
1750
1650
1550

Myosin contains two globular heads and a rod region which is a double-stranded coiled coil (Lowey et al., 1969). Based on the three dimensional structure of chicken pectoralis myosin S-1 proposed by Rayment et al. (1993a), myosin S-1 is composed of mainly α-helices and ß-strands connected by turns and loops. The band at 1651 cm^{-1} was primarily due to α-helix in the myosin S-1 and rod portions. The peak at 1636 cm^{-1} indicating ß-structure was attributed to the globular head region of myosin. Since the band frequency of loop was near 1655 cm^{-1} (Prestrelski et al., 1991a), it is possible that the absorption by loops overlapped with that of α-helix.

The spectrum of myosin heated at 45°C for 30 min was similar to that of native myosin, showing two major bands around 1635 and 1651 cm^{-1} (Fig. 3.3b). The band of 1676 cm^{-1} in native myosin was split into two components of 1683 and 1675 cm^{-1} on heating. A weak band at 1683 cm^{-1} was assigned to type II ß-turns according to Prestrelski et al. (1991a), or type III turns based on the results of Stein et al. (1991). A shoulder around 1629 cm^{-1} (extended strands) appeared. Circular dichroism (CD) studies revealed full reversibility of secondary structure of turkey breast myosin on cooling after heating at 40°C for 5-30 min and at 50°C for 5 min (Arteaga and Nakai, 1992). Morita and Yasui (1991) reported that more than 80% of the helical content of rabbit skeletal LMM could be restored by cooling after heating at 70°C and above for 20 min. It is possible that myosin heated at 45°C renatured

during cooling because the calorimetric studies reported in next Chapter showed myosin started to unfold as low as 35°C. As we evaluated myosin structure after cooling, FTIR results would not reveal the changes in secondary structure at 45°C.

When myosin was heated at 55°C, the band at 1675 cm^{-1} which was the high-frequency component of ß-structure disappeared (Fig. 3.3c and d). A weak band near 1669 cm^{-1} (turns) appeared in some of the myosin spectra at 55°C. Unresolved broad bands occurred between 1660-1620 cm^{-1} with distinguishable peaks around 1650, 1640, and 1635 cm^{-1}. Peaks which absorbed at 1651 (α-helix) and 1635 cm^{-1} (ß-sheets) decreased in intensity. These changes indicated irreversible unfolding of helices and ß-structures when heated at 55°C. The new peak observed at 1640 cm^{-1} might indicate 3_{10}-helices (1639 cm^{-1}) or more likely, the formation of irregular structures (1640-1648 cm^{-1}) (Prestrelski et al., 1991a, b). The peak at 1629 cm^{-1} first observed at 45°C and other minor bands might be masked due to the broadness of bands in frequency region of 1660-1629 cm^{-1}. The spectra within 1660-1620 cm^{-1} region was not constant at 55°C, which might be due to sol-to-gel transitions so that myosin structures were highly variable after cooling.

The band around 1669 cm^{-1} did not change when myosin was heated at 65 and 75°C, but new peaks around 1664 and 1666 cm^{-1} appeared (Fig. 3.3e and f). These frequencies have been identified as turns (Byler and Susi, 1986). A decrease in

intensity of the broad peaks in 1660-1620 cm^{-1} region was observed when compared to myosin at 55°C. A shoulder at 1658 cm^{-1} occurred in some of the spectra at 65 and 75°C, which was within the frequency range of α-helix. This shoulder might be due to loops which absorb at 1655 cm^{-1} (Prestrelski et al., 1991a). Myosin bands below 1636 cm^{-1} were assigned to the low-frequency component of extended strands (Prestrelski et al., 1991a). Bands at 1650 and 1636 cm^{-1} were present in myosin heated at 65 and 75°C, indicating the structure was not completely unfolded by heat. This observation agreed with the results of Casal et al. (1988) using ß-lactoglobulin B, as well as Byler and Purcell (1989), using ß-lactoglobulin, bovine serum albumin (BSA), and α-lactalbumin. Morita and Yasui (1991) also reported the helical content of rabbit LMM determined by CD decreased to about 10% when heated at 70°C and above for 20 min. However, most of the helix in fish myosin unfolded prior to reaching its denaturation temperature (Chan et al., 1992).

Myosin heated to 55°C showed an increase in band intensity near 1683 cm^{-1}. The intensity of this band increased when myosin was heated at 75°C. A new band near 1613 cm^{-1} appeared when myosin was heated at 55°C, increased at 65°C, and remained relatively constant at 75°C (Fig. 3.3). Similar observations were reported by other researchers. Herald and Smith (1992) reported an intense, sharp peak at 1614 cm^{-1} paired with a weaker peak at 1684 cm^{-1} for

S-ovalbumin heated at 90°C. Byler and Purcell (1989) observed new peaks near 1614 and 1684 cm^{-1} in ß-lactoglobulin and BSA after heating to 80 and 75°C, respectively. Clark et al. (1981) reported a 1620 cm^{-1} shoulder paired with a band near 1680 cm^{-1} in the IR spectrum of BSA heated at 90°C. The absorption band near 1683 cm^{-1} has been assigned to turns in native proteins (Prestrelski et al., 1991a; Stein et al., 1991). However, with the appearance of the intense band below 1620 cm^{-1} at high temperature, this observation was assigned to intermolecular hydrogen-bonded ß-sheet (Painter and Koenig, 1976; Clark et al., 1981; Byler and Purcell, 1989; Herald and Smith, 1992).

Relationship between gelation and secondary structure

Myosin formed gels when heated at 55°C and above and the bands assigned as hydrogen-bonded ß-sheet increased with temperature. No similar peaks were observed for myosin heated at 45°C or native myosin. These results suggested that hydrogen-bonded ß-structure might be correlated with the formation of a gel network. Herald and Smith (1992) reported few changes in secondary structure of S-ovalbumin before heating to the onset temperature determined by DSC. Decreases in ß-sheet, α-helix, 3_{10}-helix and increases in peaks of 1614 and 1684 cm^{-1} were observed between onset and denaturation temperatures at pD's 3, 7 and 9. The authors also reported that increases in intensity of bands at 1614 and 1684 cm^{-1}

corresponded to increases in G' of S-ovalbumin gels. Byler and Purcell (1989) observed intermolecularly hydrogen-bonded ß-strands proceeded before thermal gelation of ß-lactoglobulin and BSA. α-Lactalbumin which did not gel had no intense peak below 1620 cm^{-1}. On the contrary, Clark et al. (1981) reported gels or viscous solutions prepared using different concentration of BSA all showed similar spectra. Therefore, the authors suggested that differences in protein properties (e.g. gel vs. viscous solution) did not necessarily lead to widely different changes in secondary structures.

According to our results, myosin heated at 65°C had the highest G' after cooling. No significant differences in G' were observed between myosin heated at 55 and 75°C. The intensity of bands at 1613 and 1683 cm^{-1} were higher when myosin was heated to 65 and 75°C than those at 55°C. Even though the hydrogen-bonded ß-structure was only observed when myosin was heated above 55°C (the sol-to-gel transition temperature), the intensity of these peaks did not correlate with increased G'. Myosin heated at 75°C had the highest loss tangent and gels were not homogeneous (visible protein coagulum existed). Therefore, the intense peaks at 1613 and 1683 cm^{-1} might correspond to the formation of locally strong interactions (aggregate formation) leading to non-homogeneity, instead of an ordered gel network. The FTIR spectra showed changes in secondary structure for myosin at 55°C and above, suggesting myosin unfolding and protein protein interactions

important to the subsequent gel formation had occurred.

3.5 Conclusion

In the present study, we demonstrated the effect of isothermal heating and cooling on gel development of myosin. The sol-to-gel transition occurred at 55°C where α-helix and ß-sheet decreased due to myosin unfolding. Unfolding of myosin continued when heated to a higher temperature. Myosin gels at 65°C had the highest elasticity. Cooling of myosin caused an increase in G', G" and loss tangent at 65 and 75°C, but had no effect on myosin at 55°C. Bands assigned as hydrogen-bonded ß-sheet appeared at 55°C, and the band intensity increased at 65 and 75°C. The intensity of these bands did not correlate with increased storage modulus. It was concluded that unfolding of myosin led to the formation of hydrogen-bonded ß-sheet which was not solely responsible for gel properties.

CHAPTER FOUR : HEAT-INDUCED DENATURATION AND RHEOLOGICAL PROPERTIES OF CHICKEN BREAST MYOSIN AND F-ACTIN IN THE PRESENCE AND ABSENCE OF PYROPHOSPHATE

4.1 Abstract

The DSC endotherm of myosin had four transitions at 49, 50, 57 and 67°C with a calorimetric enthalpy (ΔH_{cal}) of 2215.8 ± 89.3 kcal/mol and van't Hoff enthalpy (ΔH_{vH}) of 69.7 ± 1.4 kcal/mol. Addition of 5 mM sodium pyrophosphate to myosin resulted in a similar heat capacity profile but reduced the ΔH_{cal} to 1727.9 ± 45.4 kcal/mol with a ΔH_{vH} of 63.3 ± 1.4 kcal/mol. Both curves were deconvoluted into 10 two-state transitions (i.e., $\Delta H_{vH} = \Delta H_{cal}$). In nondestructive dynamic testing, storage modulus (G') of myosin increased at 53.5°C, formed a transition peak, and increased again above 62°C. Addition of pyrophosphate resulted in a similar rheogram, but the transition occurred over a wider temperature range. In both cases, the fourth domain was completely unfolded prior to formation of rheologically detectable structures. The DSC endotherm of F-actin showed a single peak at 75.5 ± 0.4°C, with a ΔH_{cal} of 143.4 ± 9.6 kcal/mol, and a ΔH_{vH} of 179.2 ± 15.3 kcal/mol. The cooperative ratio (CR = $\Delta H_{vH}/\Delta H_{cal}$) of

F-actin was higher than unity, indicating intermonomer interaction. Addition of pyrophosphate to F-actin resulted in a major peak at 75.6 ± 0.5°C and a minor peak at 53.3 ± 0.1°C, even though actin with and without pyrophosphate was 90% polymerized. The transition peak at 53°C was assigned to G-actin. In nondestructive dynamic testing, the storage modulus (G') of F-actin increased at 64.1 ± 0.9°C, close to the initial unfolding temperature of 64.2°C determined by DSC; loss modulus (G") increased at 63.4 ± 1.2°C. F-actin with pyrophosphate exhibited an increase in G' and G" at 62.2 ± 0.7 and 64.0 ± 0.6°C, respectively.

4.2 Introduction

Myosin, the most abundant myofibrillar protein, is composed of two heavy chains and four light chains. Each heavy chain contains a globular head or subfragment-1 (S-1) which binds actin and ATP, and a coiled-coil α-helical rod (Harrington, 1979). Myosin has been found to be prerequisite for developing desired gel strength in model systems (Samejima et al., 1969), and its gelling ability was confined to myosin heavy chain (Ashgar et al., 1985). Actin constitutes about 20% of skeletal myofibrillar proteins, and is a globular shaped molecule referred to as monomeric G-actin. Polymerization of G-actin monomers forms F-actin (fibrous

form). In contrast to myosin, F-actin has no gelling ability (Yasui et al., 1979, 1980) and little changes in viscoelasticity were observed upon heating (Sano et al., 1989a). The currently accepted model for heat-induced protein gelation includes protein unfolding, protein-protein interactions and matrix development (Ferry, 1948; Clark et al., 1981; Foegeding and Hamann, 1992). Factors influencing protein stability or interactions may affect gel properties. Therefore, basic research related to molecular properties of myosin and F-actin during heating will provide information on the mechanism of myosin gelation and contribute to manipulation of protein functionality.

Differential scanning calorimetry (DSC) is a technique used to determine the thermodynamics of molecular systems. These thermodynamic parameters can be related to microscopic structural/conformational changes occurring in proteins on heating (Chowdhry and Cole, 1989). The calorimeter measures heat capacity (C_p) as a function of temperature. By integration of the area under the curve, the enthalpy for denaturation (ΔH_{cal}) can be estimated. From the temperature dependence of the equilibrium constant, the van't Hoff enthalpy (ΔH_{vH}) can be calculated (Tsong et al., 1970; Krishnan and Brandts, 1978; Donovan, 1984; Privalov and Potekhin 1986). It is small if the transition temperature range is broad; large if the temperature range is narrow (Donovan, 1984). For a simple two-state transition, ΔH_{cal} is

close to or equal to ΔH_{vH}. If $\Delta H_{vH} > \Delta H_{cal}$, the cooperative ratio (CR = $\Delta H_{vH}/\Delta H_{cal}$) gives the number of molecules which associate to form the cooperative unit (Donovan, 1984). Proteins with CR below unity (i.e. $\Delta H_{vH} < \Delta H_{cal}$) indicate one or more domains exist in the molecule (Tsong et al., 1970; Donovan, 1984; Privalov and Potekhin 1986; Chowdhry and Cole, 1989).

Thermal denaturation of myosin and its subfragments has been studied using DSC. Single or multiple transitions were ascribed to myosin, varying with pH, salt concentration, and species (Stabursvik and Martens, 1980; Swenson and Ritchie, 1980; Wright and Wilding, 1984; Akahane et al., 1985; Rodgers and Harrington, 1987; Rodgers et al., 1987; Bertazzon and Tsong, 1989, 1990a, b). The term "domain" has been defined as an independent, cooperative unit in a folded protein (Privalov, 1982; Shriver and Kamath, 1990). It has been reported that myosin rod in rabbit muscle undergoes a multistep endothermic process consisting of at least six quasi-independent structural domains within the temperature range from 41 to 67°C (Potekhin et al., 1979; Lopez-Lacomba, et al., 1989; Bertazzon and Tsong, 1990b). Some domains in the rod showed a CR less than unity ($\Delta H_{vH} / \Delta H_{cal} < 1$) in melting, which suggested the domains could be further resolved into subdomains (Bertazzon and Tsong, 1990b). The DSC endotherm showed a single peak at 57 and 67°C for G-actin and F-actin, respectively, at pH 8.0 (Bertazzon et al., 1990).

Based on the current gelation models (Ferry, 1984; Clark et al., 1981; Foegeding and Hamann, 1992), protein unfolding might affect subsequent protein-protein interactions and gel properties. It is important to understand how myosin and F-actin denature, and to study the contribution of the various domains in development of gel elasticity. The effect of pyrophosphate on myosin and F-actin was also investigated to provide background on its dissociation effect on actomyosin (Chapter 5). The objectives of the present study were to monitor the denaturation temperature, enthalpy and dynamic rheological properties of chicken breast muscle myosin and F-actin in the presence and absence of pyrophosphate during heating.

4.3 Materials & Methods

Extraction of Myosin

Broiler breast muscle myosin was extracted and stored in $(NH_4)_2SO_4$ at -20°C as described in Chapter 3. Prior to use, myosin was dialyzed against 0.6 M NaCl, 50 mM Na phosphate buffer, pH 6.5 with two changes of buffer. The first two dialysis buffers contained 1 mM EDTA. The dialyzed myosin solution was centrifuged at 78,000 x g for 1 hr at 4°C (Beckman Ultracentrifuge, Model L7-65, Beckman Instruments, Inc., Palo Alto, CA) to remove insoluble proteins. Myosin

concentration was determined using an extinction coefficient of $E^{1\%} = 5.5$ at 280 nm (Swenson and Ritchie, 1980).

To study the effect of pyrophosphate, myosin solutions were brought to 5 mM Na pyrophosphate and 1 mM $MgCl_2$ by addition of 1/10 volume of 50 mM Na pyrophosphate and 10 mM $MgCl_2$ stock solution. Ten milligrams per milliliter of protein were used for all measurements. The final pH of myosin was adjusted using 0.1 N HCl or NaOH, if necessary.

Purification of Actin

Preparation of Acetone Powder. Acetone powder was prepared as described by Feuer et al. (1948) at 4°C. The residue obtained after myosin extraction using modified Guba-Straub solution was diluted with 5 volumes of distilled water, stirred for 5 min and filtered through #1 filter paper (Whatman Ltd., Maidstone, England). The residue was resuspended in 5 volumes of 0.4% $NaHCO_3$ with stirring for 5 min and filtered. This step was repeated. The residue was washed twice with 5 volumes of distilled water, mixed with 5 volumes of cold acetone, stirred for 10 min, and filtered. The filtrate was discarded. The acetone extraction was repeated until the filtrate was clear. The acetone powder was dried under a hood and stored at -20°C for future use.

Isolation of Actin. Further purification of actin followed the procedures described by Spudich and Watt (1971). All procedures were performed at 4°C. Acetone powder was

mixed with 15 volumes of buffer A (5 mM Tris, 0.2 mM ATP, 0.5 mM DTT, 0.2 mM $CaCl_2$, pH 8.0; DTT was added immediately before use), stirred for 30 min, and centrifuged at 10,000 x g for 1 hr. The supernatant was filtered through one layer of cheese cloth and the volume was measured. Actin was polymerized by adding KCl and $MgCl_2$ to a final concentration of 50 mM and 2 mM, respectively, and stirred slowly for 2 hr. Tropomyosin was removed by the addition of KCl to 0.6 M with stirring for 1 hr and precipitation of F-actin by centrifugation at 80,000 x g for 3 hr (Beckman Ultracentrifuge, Model L7-65, Beckman Instruments, Inc., Palo Alto, CA). The F-actin pellet was resuspended in buffer A, and depolymerized by dialysis against the same buffer for 3 days, with two changes of buffer each day. Globular actin was centrifuged at 80,000 x g for 3 hr. Actin in supernatant was polymerized by adding KCl to a final concentration of 50 mM, $MgCl_2$ to 1 mM and ATP to 1 mM and stirred slowly for 2 hr. The F-actin solution was dialyzed overnight against 0.6 M NaCl, 50 mM sodium phosphate buffer, pH 6.5 prior to use. Concentration of actin was measured using an extinction coefficient of $E^{1\%} = 11$ at 280 nm (Duong and Reisler, 1987).

Polymerization of F-Actin. The degree of actin polymerization in 0.6 M NaCl, 50 mM Na phosphate buffer, pH 6.5 was determined by measuring the actin concentration before centrifugation ($[A]_I$) and in the supernatant ($[A]_F$) after centrifugation at 100,000 x g for 120 min (Beckman

Ultra-centrifuge, Model TL-100) (Yasui et al., 1982):

$$\%\text{Polymerization} = ([A]_I - [A]_F)/[A]_I$$

Electrophoresis

To determine the purity of extracted proteins, sodium dodecyl sulfate-polyacryamide gel electrophoresis (SDS-PAGE) (Laemmli, 1970) were performed using a Mini-Protean II electrophoresis unit (Bio-Rad Laboratories, Richmond, CA) with stacking and separating gels of 4 and 10% acrylamide, respectively. Running buffer used was 0.025 M Tris buffer, pH 8.3, containing glycine (1.4%, w/v) and SDS (0.1%, w/v). Protein samples were diluted to 1 μg/μl with SDS reducing buffer containing glycerol (10%), SDS (2%, w/v), 2-ß-mercaptoethanol (5%), and bromophenol blue in 0.0625 M Tris-HCl buffer, pH 6.8, then heated at 95°C for 4 min. Three micrograms of prepared sample and 12 μg of molecular weight standards (SDS-6H, Sigma) were loaded, and the gel was run at 200 constant volts. Molecular masses were determined by comparing the relative mobilities of protein bands to those of molecular weight standards (Weber and Osborn, 1969). Protein bands were stained with 0.25% Coomassie Brilliant Blue R250 in fixative (40% methanol, 10% acetic acid) for 30 min, and destained overnight with 40% methanol/10% acetic acid. Destained gels were stored in 7.5% acetic acid solutions at room temperature.

Dynamic Rheological Properties

Oscillatory dynamic measurements were performed using a Rheometrics Fluid Spectrometer (RFS-8400, Rheometrics, Inc., Piscataway, NJ) fitted with a 50 mm diameter parallel plate apparatus and 100 g-cm transducer. Protein solutions were loaded in the sample cup and equilibrated at 30°C for 3 min. Solutions were heated from 30 to 80°C at 1°C/min using a programmable circulating oil bath (Model MTP-6, Nelsprit Temperature Programmer, Newington, NH). The gap between upper and lower plates was between 1 and 1.5 mm. Storage (G') and loss (G") moduli were recorded continuously at a fixed frequency of 10 rad/s and strain of 0.01. The strain was selected based on the strain sweeps (0.0001 to 0.5) conducted at 30 and 80°C.

Thermal Stability

Thermal stability of myosin was measured using a differential scanning microcalorimeter (MC-2, Microcal Inc., Amherst, MA) with a scan rate of 1°C/min. Cell capacity was 1.24 mL. The effect of myosin concentration on calorimetric analysis was examined between 1 and 10 mg/mL. The final concentration chosen was 10 mg/mL for better peak resolution. Cells were cleaned after each run using 5% SDS, 0.1 M EDTA and 3% dithiothreitol in 0.02 M Tris buffer, pH 8.5 by heating to about 95°C for 1 hr. A base line obtained by running buffer vs. buffer was subtracted from the sample data files before

analysis. The heat capacity profiles (C_p vs. temperature) were defined by a calorimetric enthalpy (ΔH_{cal}), a van't Hoff enthalpy (ΔH_{vH}), a melting temperature (T_m) at which proteins are 50% denatured, and the cooperative ratio (CR) which was defined as ΔH_{vH} / ΔH_{cal} (Privalov and Potekhin, 1986; Tsong et al., 1970). For a simple two-state transition, the concentrations of intermediates between native and denatured states are very low, and ΔH_{cal} is close to or equal to ΔH_{vH}. A cooperative ratio (CR = $\Delta H_{vH}/\Delta H_{cal}$) greater than 1 indicates intermolecular interaction. Proteins with CR below unity indicate one or more significant intermediate states in the overall process (Chowdhry and Cole, 1989; Privalov and Potekhin 1986; Donovan, 1984; Tsong et al., 1970). The molecular masses used for analyses were 5.21×10^5 for myosin (Yates and Greaser, 1983), and 4.19×10^4 for actin (Elzinga et al., 1973). A conversion constant (N) of enthalpic change was used:

$$N = \frac{\text{Protein concentration (g/L)}}{\text{Molecular Weight (g/mole)}} \times 1.24 \times 10^{-3} \text{ (L)}$$

to convert the data from calories/degree to calories/degree/mole. For proteins with CR value below unity, the endotherms were fitted into a minimal number of independent transitions, assuming a two-state unfolding process (i.e. $\Delta H_{vH} = \Delta H_{cal}$). Data analysis was based on a least square fitting procedure as described by Freire and

Biltonen (1978a, b).

Statistics

Basic statistics for computing means and standard deviations and two-way analysis of variance (replication x treatment) were performed on a completely randomized design (six replicates) using MSTAT software (version C, Michigan State University).

4.4 Results & Discussion

Characterization of Myosin and F-actin

Myosin exhibited a major band of about 205 kDa on SDS gel electrophoresis that was identified as myosin heavy chain (Fig. 4.1). Two minor contaminating proteins were present, one just below myosin heavy chain, probably was C-proteins which could be removed through ion-exchange chromatography (Margossian and Lowey, 1982); the other one was about 97 kDa. Two protein bands below 29 kDa were assigned to myosin light chains. The purified actin showed a single band near 45 kDa. F-actin in the presence and absence of 5mM PPi showed 90% polymerization in 0.6 M NaCl, 50 mM Na phosphate buffer, pH 6.5 using the ultracentrifugation method.

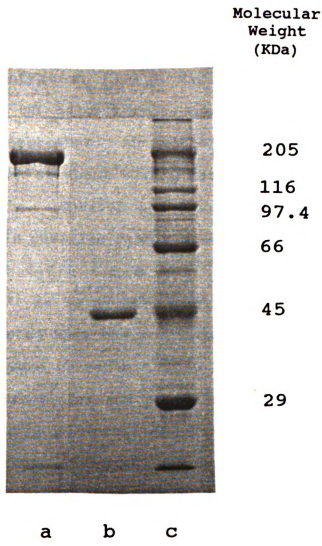

Figure 4.1. Sodium dodecyl sulfate-polyacrylamide electrophoresis gel (10%) of chicken breast myosin and actin (a: myosin; b: actin; c: molecular weight standards).

Thermal Denaturation of Myosin

The existence of contaminating proteins might change the calorimetric profile. But because of their low concentrations compared to myosin, no major effect was assumed. The effect of myosin concentration (0.6 M NaCl, 50 mM Na phosphate buffer, pH 6.5) on calorimetric analysis was examined to ensure proper measurement. An exothermic process, resulting in a negative peak at about 57.5°C was observed in solutions of 1 mg/mL myosin. Shriver and Kamath (1990) observed an exothermic peak in purified rabbit myosin S-1 at 48°C in 50 mM Tris buffer (pH 8.0), 0.6 M KCl, as well as in heavy meromyosin at 65°C in 50 mM TRIS buffer (pH 7.9), 0.1 M KCl. The authors reported that the position and magnitude of this exothermic peak were variable. They suggested the exotherm resulted from aggregation and precipitation of the unfolded protein. The endothermic profiles of myosin were the same for concentrations above 4 mg/mL; however, a higher protein content exhibited better peak resolution.

Myosin started to unfold at 36.2°C. The heat capacity profile was characterized by four endothermic peaks at 49.2 ± 0.2, 50.2 ± 0.1, 57.2 ± 0.2 and 66.8 ± 0.6°C (Fig. 4.2). The ΔH_{cal} of myosin denaturation was 2215.8 ± 89.3 kcal/mol with a ΔH_{vH} of 69.7 ± 1.4 kcal/mol. The cooperative ratio (CR = ΔH_{vH} / ΔH_{cal}) was 0.03 for myosin, suggesting the presence of multiple domains. The endotherm was deconvoluted into 10 two-state transitions (i.e. $\Delta H_{vH} = \Delta H_{cal}$). The ΔH_{vH} and ΔH_{cal} for

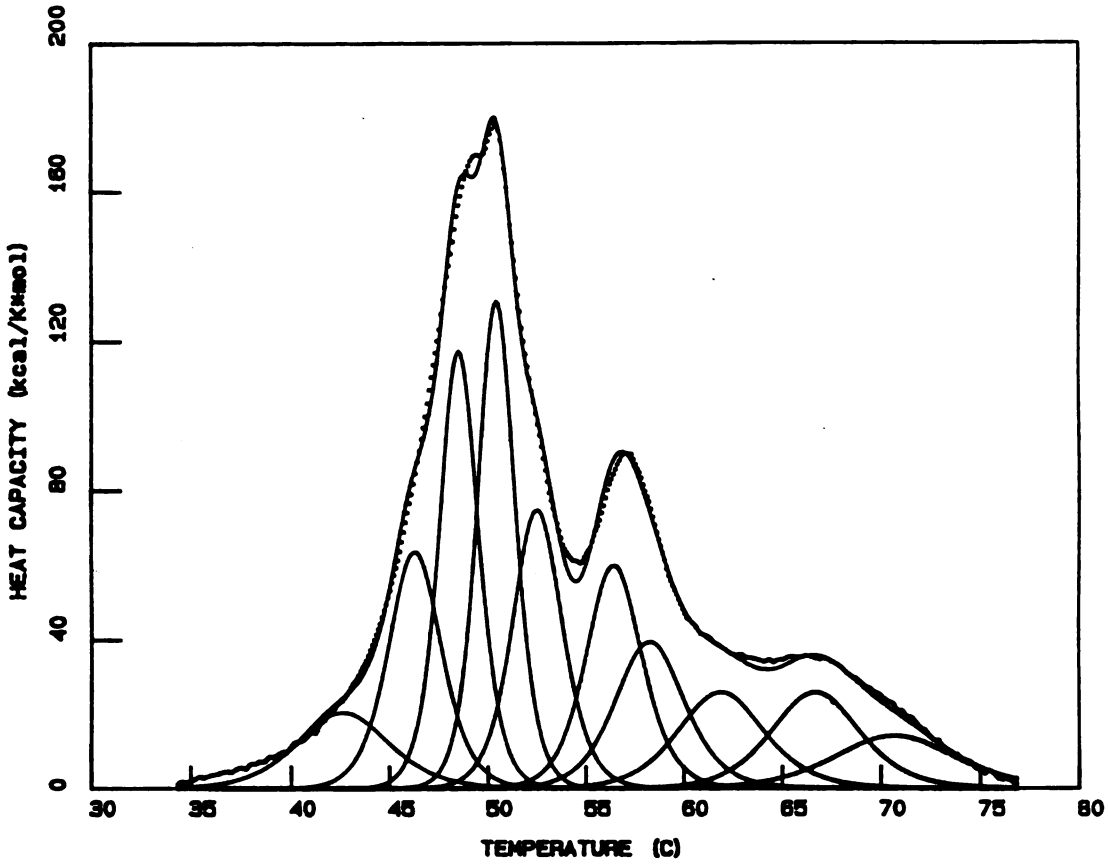

Figure 4.2. Heat capacity profile and deconvoluted peaks of myosin in 0.6 M NaCl, 50 mM Na phosphate, pH 6.5. Scan rate is 1°C/min. The dotted line is the experimental data. The theoretical endotherm and deconvoluted peaks are expressed as solid lines.

each domain were calculated (Table 4.1).

Bertazzon and Tsong (1989) reported that rabbit myosin unfolded in a multi-stage process, with a peak at 46°C and three shoulders at 43, 49, and 54°C in 0.5 M KCl, 20 mM potassium phosphate, pH 7.0. In our preparation of chicken breast myosin, the endotherm showed a shoulder at 49°C, and three major peaks at 50, 57, and 67°C. The overall endothermic profile of our chicken breast myosin was different from rabbit myosin. The temperature range of denaturation of rabbit myosin was narrower than what we observed due to the presence of a peak above 60°C in chicken myosin. The ΔH_{cal} of our chicken breast myosin was 2216 kcal/mol and was greater than that of rabbit myosin (1715 kcal/mol).

The deconvolution of endotherms by other researchers were mostly done on myosin subfragments. Rabbit myosin rod contained at least six quasi-independent domains (Potekhin et al., 1979; Lopez-Lacomba et al., 1989; Bertazzon and Tsong, 1990b). A single domain was observed in subfragment-1 (S-1) and light chains with T_m's of 46.3°C and 51.5°C, respectively, in 0.5 M KCl, pH 7.0, 20 mM K phosphate buffer, and 1 mM EDTA (Bertazzon and Tsong, 1989). Subfragment-2 (S-2) had a T_m of 48.6°C at pH 6.45, 0.5 M KCl (Bertazzon and Tsong, 1990a), and its endotherm was fitted to three two-state transitions at 47, 48.4, and 53.8°C with a ΔH_{cal} of 143, 145 and 114 kcal/mole, respectively (Bertazzon and Tsong, 1990b). The endotherm of LMM showed three main peaks at pH 6.4, and was fitted to five

Table 4.1 Temperature of myosin differential scanning calorimetry (DSC) endotherm peaks and rheological transitions when heated from 20 to 90°C at 1°C/min[ab]

Dynamic testing	DSC deconvoluted peaks	
T (C) storage modulus	T (C)	$\Delta H_{vH} = \Delta H_{cal}$[c] (kcal/mol)
	44.2 ± 0.4	148.2 ± 7.3
	47.1 ± 0.2	240.3 ± 4.8
	49.0 ± 0.2	298.0 ± 6.8
	50.7 ± 0.2	317.4 ± 17.0
53.5 ± 0.7	52.9 ± 0.3	242.4 ± 15.6
	56.4 ± 0.2	241.4 ± 10.8
59.0 ± 0.6	58.7 ± 0.5	215.7 ± 17.0
62.1 ± 0.4	62.6 ± 0.6	178.8 ± 10.4
	66.8 ± 0.4	174.5 ± 7.6
	70.8 ± 0.4	137.2 ± 17.2

[a] Values represents means of six replications ± standard deviation.
[b] Buffer system: 0.6 M NaCl, 50 mM Na phosphate buffer, pH 6.5.
[c] ΔH_{vH} = van't Hoff enthalpy; ΔH_{cal} = calorimetric enthalpy.

two-state transitions at 41.4, 48.7, 49.8, 55.9 and 57.6°C with a ΔH_{cal} of 157, 78, 114, 177 and 77 kcal/mole, repectively. The lowest stability domain was found in the hinge region at the LMM/S-2 junction (Bertazzon and Tsong, 1990b).

It was difficult to assign chicken muscle myosin domains to specific transition temperatures based on literature because of the different endotherm patterns and melting temperatures observed (Potekhin et al., 1979; Lopez-Lacomba et al., 1989; Bertazzon and Tsong, 1990b; Shriver and Kamath, 1990). However, most results showed S-1 and light chains denatured below 55°C. It might be appropriate to assign the domains above 55°C to part of myosin rod. The first domain with T_m of 44.2°C was probably from the unfolding of the hinge region. Further investigations are necessary for accurate assignment of myosin domains.

Viscoelasticity of Myosin

According to the electrophoresis study, myosin was contaminated with C-protein and one 97 kDa protein. The effect of C-protein on myosin monomer is unclear; however, Yamamoto et al. (1987) observed that C-protein reduced the diameter of myosin filaments and lowered the gel strength at low ionic strength. In the dynamic study, we assumed the contaminating proteins had little or no effect on myosin viscoelasticity.

In 0.6 M NaCl, 50 mM Na phosphate buffer, pH 6.5, the torque generated by myosin was very low at temperatures below 53°C, resulting in scattered data points for G' and G". Storage modulus of myosin increased sharply at 53.5°C, formed a transition peak at 59°C, decreased slightly between 59 and 62°C, then increased gradually until 80°C, showing development of gel elasticity (Fig. 4.3). In contrast, G" data points were scattered and did not change throughout heating. By comparing the rheological transitions of G' to the DSC deconvoluted peaks, the first four domains (T_m's of 44.2, 47.1, 49, and 50.7°C) were unfolded prior to development of gel elasticity. Rheological testing detected changes in G' during unfolding of the domain with a T_m of 53°C. The unfolding of domains with T_m's of 56.4, 58.7 and 62.6°C might be responsible for the plateau observed from 59 to 62°C in the myosin rheogram.

Effect of Pyrophosphate (5mM) on Myosin

Addition of 5 mM pyrophosphate (PPi) increased the initial unfolding temperature to 37.7°C. The first two transitions of myosin observed without PPi merged into one peak, resulting in three endothermic peaks at 48.9 ± 0.1, 56.7 ± 0.2, 65.1 ± 0.5°C. A shoulder appeared at 59.8 ± 0.1°C (Fig. 4.4). The ΔH_{cal} was decreased to 1727.9 ± 45.4 kcal/mol with a ΔH_{vH} of 63.3 ± 1.4 kcal/mol as compared to myosin alone, indicating PPi destabilized the molecule. The CR of

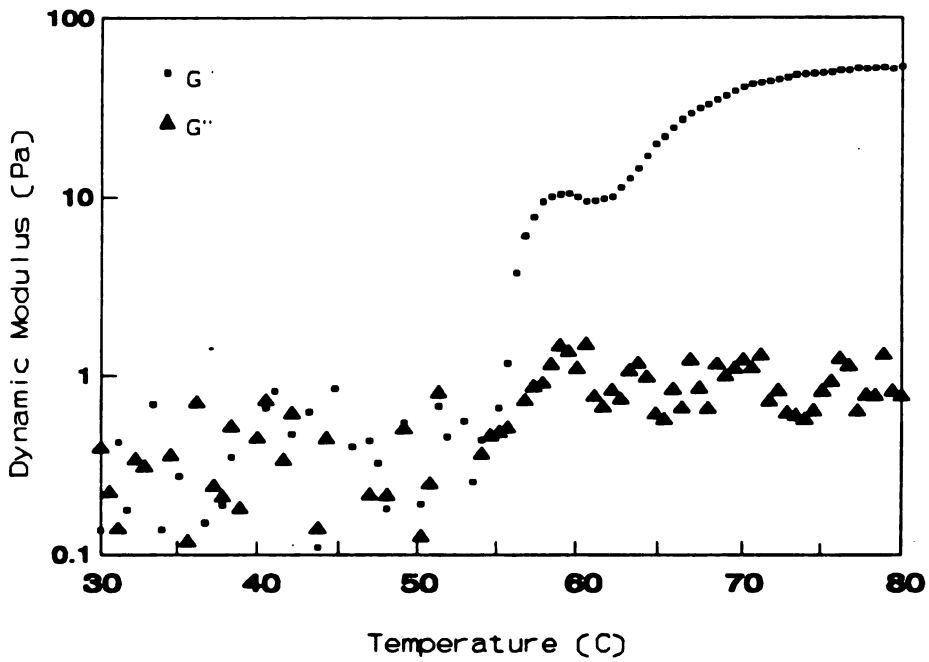

Figure 4.3. Representative rheogram on storage (G') and loss (G") moduli of myosin (10 mg/ml) heated at 1°C/min in 0.6 M NaCl, 50 mM Na phosphate buffer, pH 6.5.

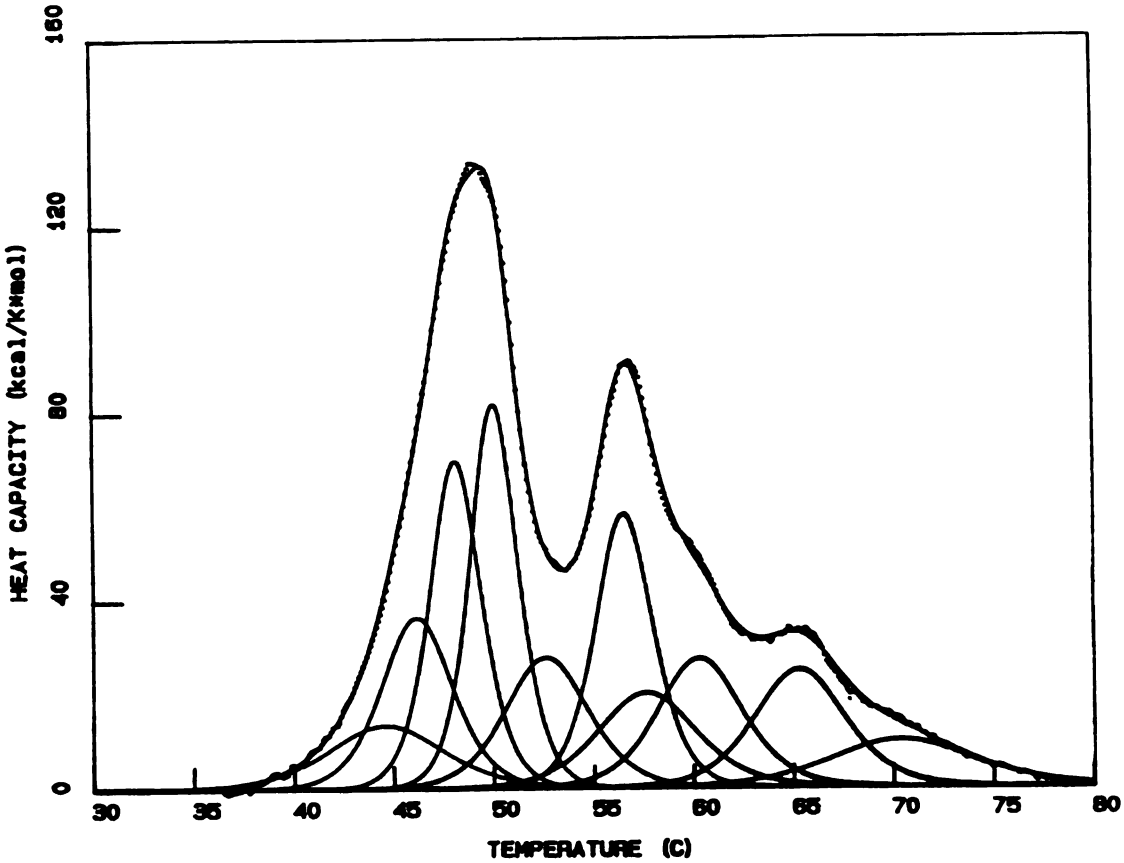

Figure 4.4. Heat capacity profile and deconvoluted peaks of myosin in the presence of 5 mM Na pyrophosphate, 1 mM $MgCl_2$, 0.6 M NaCl, 50 mM Na phosphate buffer, pH 6.5. Scan rate is 1°C/min. The dotted line is the experimental data. The theoretical endotherm and deconvoluted peaks are expressed as solid lines.

myosin with PPi was 0.04, suggesting the presence of multiple domains. The endotherm was fitted into ten deconvoluted peaks (Table 4.2). If we assume the order of domain unfolding did not change, most T_m's and enthalpies of domains decreased due to addition of PPi.

Scattered data points were observed in G' and G" below 53°C for myosin with PPi (Fig. 4.5). Storage modulus started to increase at about 53°C and reached a maximum at 61.2°C. The temperature of this peak maximum was higher than that observed in myosin alone (59°C). A slight decrease in G' occurred between 61 to 63°C, then G' increased again. Loss modulus was scattered and showed little change throughout heating. When comparing rheological transitions to DSC deconvoluted peaks, four domains unfolded prior to appearance of rheological detectable structure. This finding was similar to myosin alone. The rheological transition at 61.2°C occurred after after more than 50% of the eighth domain was unfoldeded (T_m = 60.3°C). The temperature of the second increase in G' (around 63°C) corresponded to the unfolding of the eighth and ninth domains of myosin. For myosin without PPi, fewer domains needed to unfold before this second increase in G' occurred (Table 4.1). It is possible that PPi binding increased the negative charges of myosin and thus the repulsive forces between myosin molecules, so the initial myosin interaction was inhibited or depressed. The gelation process might require more protein to unfold, for exposure of

Table 4.2 Temperature of myosin differential scanning calorimetry (DSC) endotherm peaks and rheological transitions in the presence of 5 mM pyrophosphate when heated from 20 to 90°C at 1°C/min[ab]

Dynamic testing	DSC deconvoluted peaks	
T (C) Storage modulus	T (C)	$\Delta H_{vH} = \Delta H_{cal}$[c] (kcal/mol)
	44.1 ± 0.4	100.6 ± 4.5
	46.1 ± 0.2	173.8 ± 4.8
	48.0 ± 0.2	241.0 ± 2.1
	50.0 ± 0.2	257.3 ± 5.0
53.1 ± 0.3	52.4 ± 0.3	163.7 ± 8.5
	56.3 ± 0.2	221.0 ± 7.6
	57.4 ± 0.2	159.7 ± 23.3
61.2 ± 0.7	60.3 ± 0.2	164.0 ± 9.3
62.9 ± 0.2	64.9 ± 0.2	151.7 ± 5.8
	69.6 ± 0.6	101.4 ± 9.8

[a] Values represents means of six replications ± standard deviation.
[b] Buffer system: 0.6 M NaCl, 50 mM Na phosphate buffer, pH 6.5.
[c] ΔH_{vH} = van't Hoff enthalpy; ΔH_{cal} = calorimetric enthalpy.

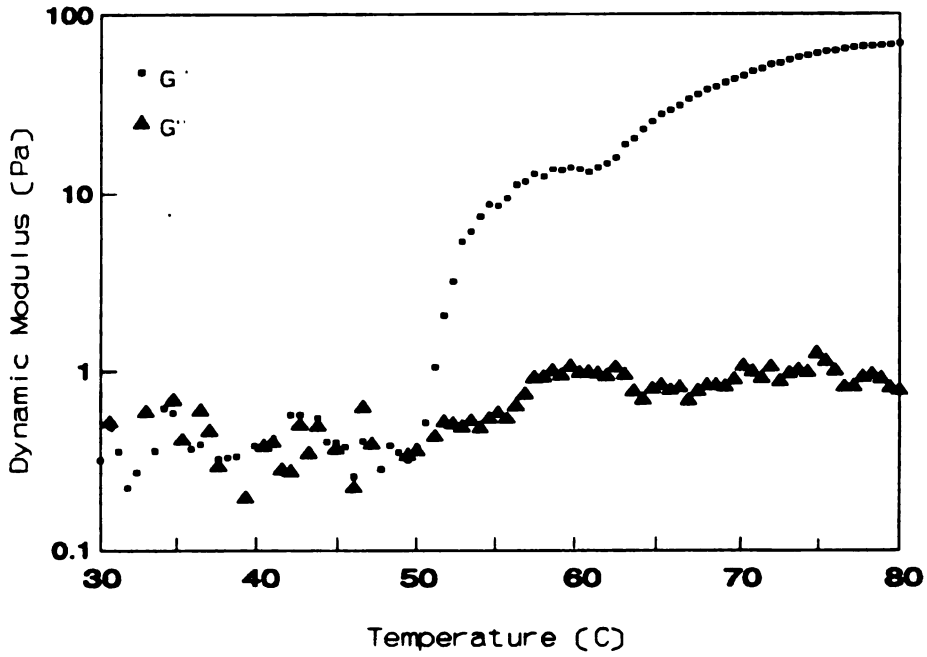

Figure 4.5. Representative rheogram on storage (G') and loss (G") moduli of myosin (10 mg/mL) heated at 1°C/min in the presence of 5 mM Na pyrophosphate, 1 mM $MgCl_2$, 0.6 M NaCl, 50 mM Na phosphate buffer, pH 6.5.

hydrophobicity and subsequent interactions overcoming the existing repulsive forces.

Lopez-Lacomba et al. (1989) observed similar endothermic profiles for rabbit myosin rod in phosphate (0.20 M) and pyrophosphate buffers (0.15 M), 0.5 M KCl, pH 6.5-9.0. They reported some stabilization in the first endothermic peak (below 50°C) and lower enthalpy for denaturation in pyrophosphate buffer which agreed with our findings. Hamai and Konno (1989) reported the binding of PPi destabilized the light chains-heavy chain binding, resulting in the formation of aggregates of light chain-deficient heavy chains. The authors suggested dissociation of light chains was due to structural changes around the light chain binding site. Based on their results, the decrease in the enthalpy of chicken breast myosin in the presence of PPi might be due to structural changes of S-1. The decreases in most T_m's and enthalpies of domains also suggested that thermal stability of S-1 influenced unfolding of other domains in myosin.

Thermal Denaturation of F-actin

Chicken breast muscle F-actin in 0.6 M NaCl, 50 mM Na phosphate buffer, pH 6.5 started to unfold at 64.2 ± 0.8°C and exhibited a single sharp peak at 75.5 ± 0.4°C with a ΔH_{cal} of 143.4 ± 9.6 kcal/mol and a ΔH_{vH} of 179.2 ± 15.3 kcal/mol (Fig. 4.6). The cooperative ratio (CR) of actin was 1.25. Bertazzon et al. (1990) reported the ΔH_{cal} of rabbit F-actin

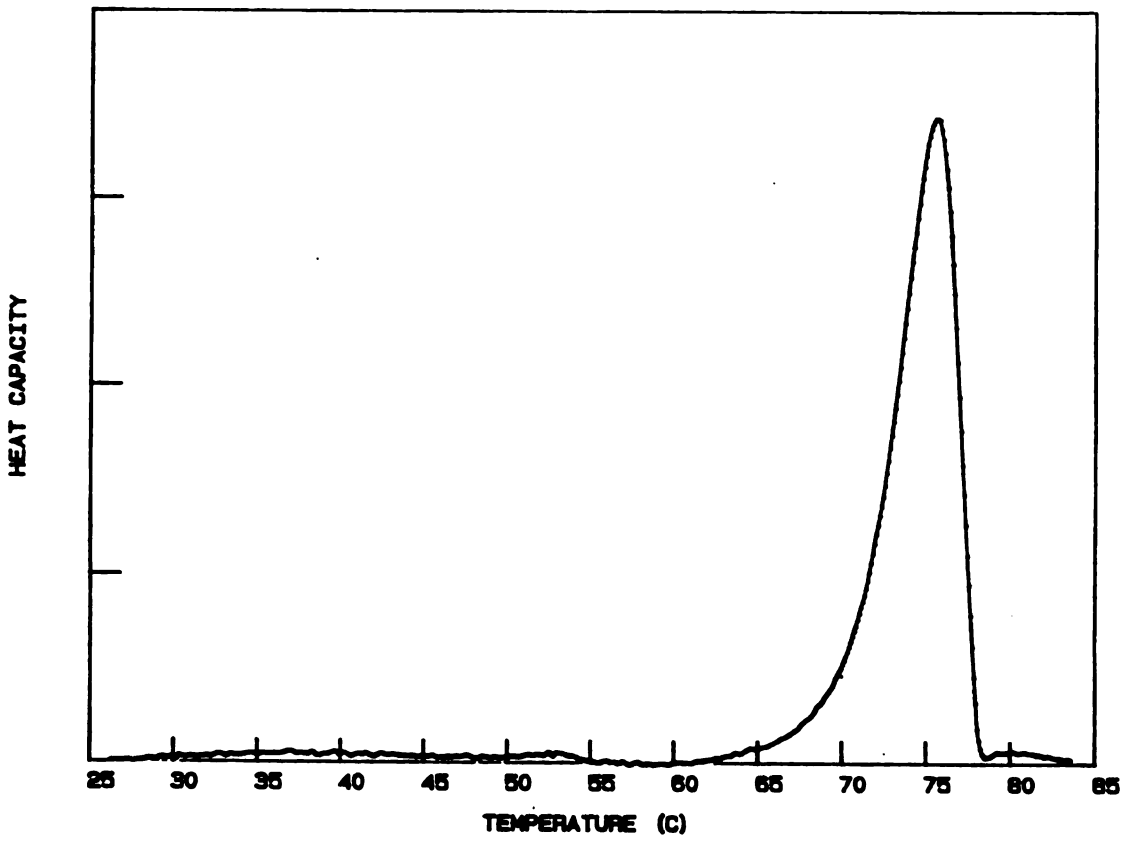

Figure 4.6. Heat capacity profile of actin in 0.6 M NaCl, 50 mM Na phosphate buffer, pH 6.5 heated at 1°C/min.

was 162 ± 10 kcal/mol, with a T_m at 67.0 ± 0.5°C and a CR of 1.4 in 2 mM HEPES, 1 mM Na-ATP, 50 mM KCl, 0.2 mM $CaCl_2$, 2 mM $MgCl_2$, and 0.5 mM mercaptoethanol at pH 8.0. Reducing the pH to 6.4 shifted T_m to 74.0 ± 0.3°C, with a ΔH_{cal} of 189 ± 10 kcal/mol and a CR of 1.51. The authors suggested that the higher CR value implied interaction among actin monomers in the filament. The higher T_m and lower ΔH_{cal} for F-actin observed in our study might be due to species differences and buffer conditions. The lower CR in our study might also result from differences in degree of actin polymerization.

Viscoelasticity of F-actin

Storage modulus (G') of F-actin started to increase at 64.1 ± 0.9°C; loss modulus (G") increased at 63.4 ± 1.2°C (Fig. 4.7). Both G' and G" reached a maximum at about 71-72°C, then decreased. Little change in viscoelasticity of F-actin occurred during heating as indicated by G' and G" below 7 Pa. This suggested F-actin did not form gels upon heating, which agreed with the results of Yasui et al. (1979; 1980) and Sano et al. (1989a). By comparing the rheogram of F-actin to its endotherm, the temperature at which G' increased (64.1°C) was close to that of the initial unfolding temperature (64.2°C). Both G' and G" decreased (71-72°C) before reaching the T_m as determined by DSC (75.5°C). These results suggested F-actin unfolding was responsible for the initial changes in rheological properties, however, an elastic gel matrix did not

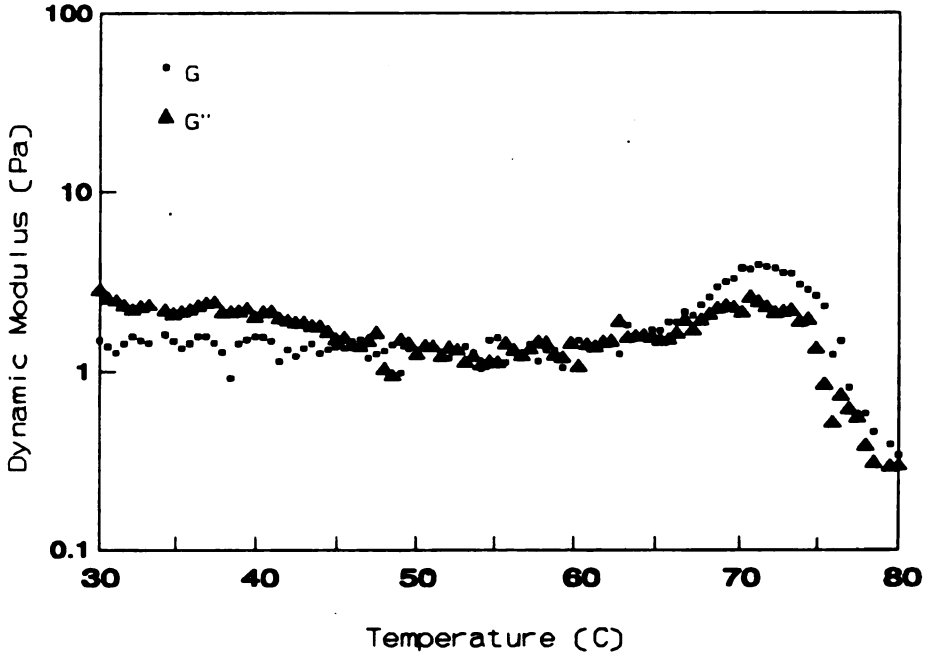

Figure 4.7. Representative rheogram on storage (G') and loss (G") moduli of actin (6 mg/ml) heated at 1°C/min in 0.6 M NaCl, 50 mM Na phosphate buffer, pH 6.5.

form.

Effect of Pyrophosphate (5 mM) on F-actin

The endotherm of F-actin with PPi exhibited one major peak at 75.4 ± 0.5°C and a minor peak at 53.3 ± 0.1°C, even though actin with and without pyrophosphate was 90% polymerized as measured by ultracentrifugation (Fig. 4.8). This minor peak with a T_m of 53°C was assigned to G-actin (Bertazzon et al., 1990). The reason for the existence of G-actin in the presence of PPi is not clear, but suggests depolymerization of F-actin by PPi. Storage modulus of F-actin with PPi increased at 62.2 ± 0.7°C, and again, was close to the initial unfolding temperature measured by DSC (61.5 ± 2.4°C); loss modulus started to increase at 64.0 ± 0.6°C (Fig. 4.9).

4.5 Conclusion

Myosin in the presence and absence of PPi showed similar endotherms which were deconvoluted into ten quasi-independent domains. Four domains were completely unfolded prior to the development of gel elasticity. Pyrophosphate increased the initial unfolding temperature of myosin and reduced both calorimetric and van't Hoff enthalpies. Endotherm of F-actin showed a single peak with CR value above unity, indicating

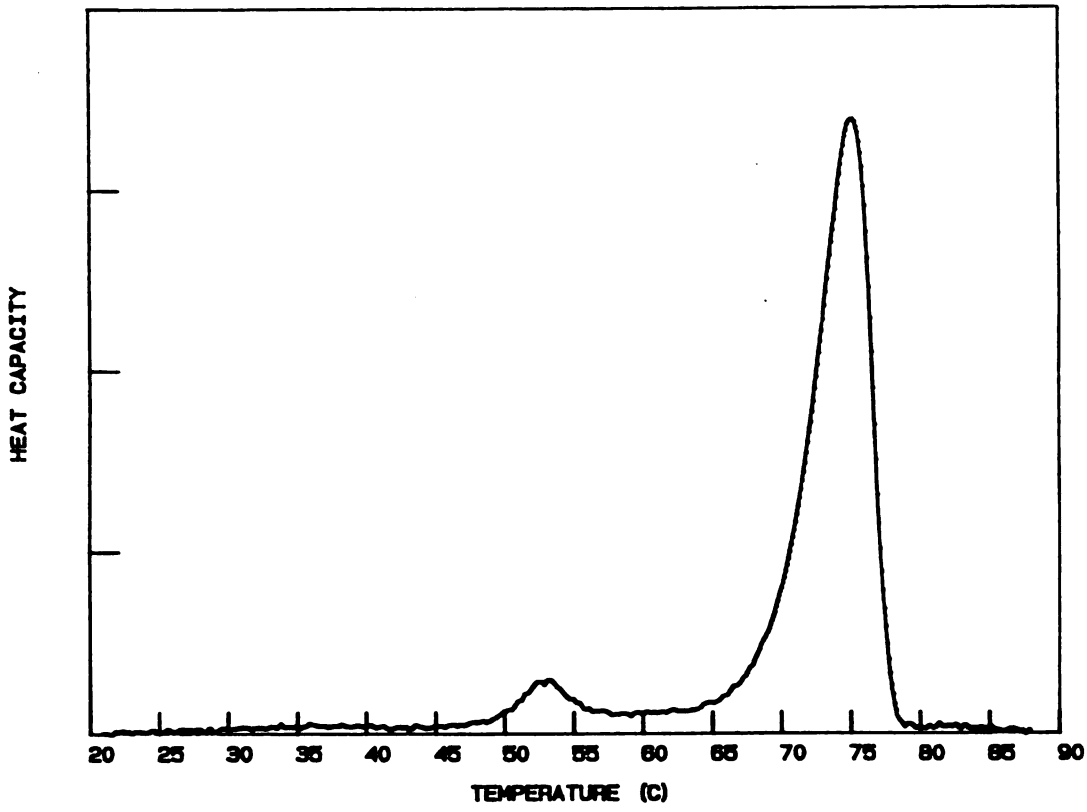

Figure 4.8. Heat capacity profile of actin in the presence of 5 mM Na pyrophosphate, 1 mM $MgCl_2$, 0.6 M NaCl, 50 mM Na phosphate buffer, pH 6.5 heated at 1°C/min.

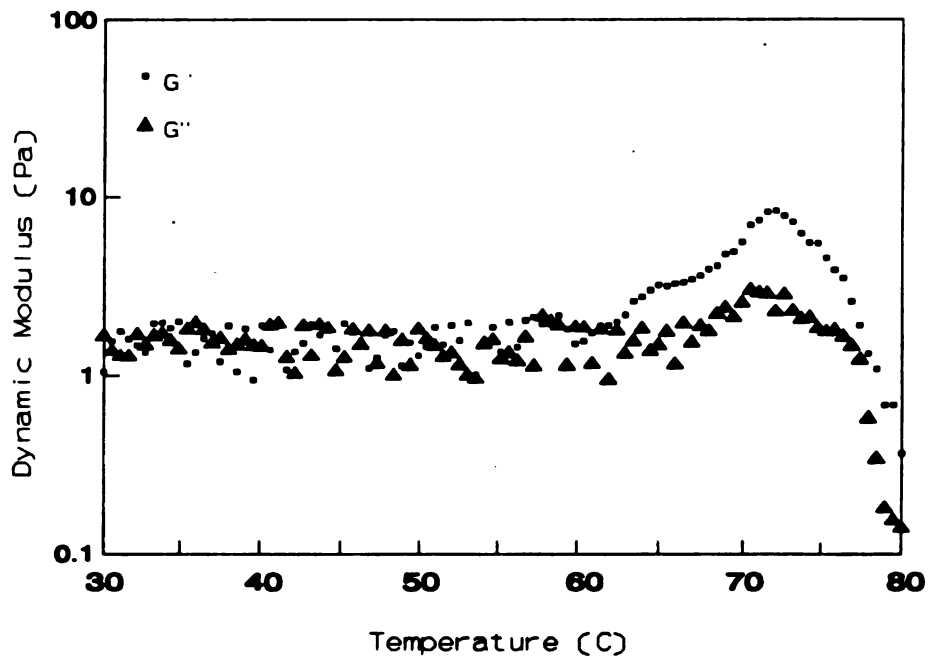

Figure 4.9. Representative rheogram on storage (G') and loss (G") moduli of actin (6 mg/mL) heated at 1°C/min in the presence of 5 mM Na pyrophosphate, 1 mM $MgCl_2$, 0.6 M NaCl, 50 mM Na phosphate buffer, pH 6.5.

intermonomer interaction. The temperature at which G' increased was close to that of the initial unfolding. Addition of pyrophosphate to F-actin resulted in partial depolymerization as evidenced by the existence of a G-actin peak at 53°C. F-actin in the presence and absence of PPi did not form elastic gels after heating. In this study, we showed the relationship between unfolding and development of visco-elasticity of two different proteins: one with multidomains (myosin), and the other, a protein with intermonomer interaction (F-actin).

CHAPTER FIVE : HEAT-INDUCED GELATION OF CHICKEN BREAST MUSCLE ACTOMYOSIN AS INFLUENCED BY WEIGHT RATIO OF ACTIN TO MYOSIN

5.1 Abstract

Heat-induced gelation of reconstituted chicken breast muscle actomyosin was studied by monitoring the thermal stability and dynamic rheological properties at different weight ratios of actin (A) to myosin (M) (A:M of 1:0, 1:1.3, 1:15, and 0:1). Analyses were performed in 0.6M NaCl, 50mM Na phosphate buffer, pH 6.5 at a heating rate of 1°C/min. Free myosin-to-actomyosin ratios were 0.2 and 2.4 for A:M of 1:1.3 and 1:15, respectively. Addition of actin delayed the initial unfolding of myosin and significantly changed the enthalpy profile. This stabilizing effect was decreased with addition of pyrophosphate. Storage (G') and loss (G") moduli of A:M 1:1.3 sol at 30°C were greater than those of myosin and A:M 1:15 sols, while A:M 1:1.3 had a higher loss tangent and lower G' at 80°C. Addition of pyrophosphate decreased G' in myosin and actomyosin solutions at 30°C, and increased viscous character after heating to 80°C. Actin affected the denaturation of structural domains of myosin and possibly

altered the gelation mechanism.

5.2 Introduction

Myosin is an asymmetric molecule, consisting of two globular heads (S-1) attached to a long coiled-coil rod portion. Investigations of muscle proteins by Ashgar et al. (1985) suggested that the gelling potential of myosin was confined to the myosin rod, while S-1 exhibited poor gelling ability upon heating. Addition of F-actomyosin affected the gelation of myosin rod by increasing cross-link formation. Maximum gel strength in 0.6 M KCl, pH 6.0 was obtained at a free myosin to F-actin molar ratio of 2.7:1, which corresponded to a weight ratio of 15:1. At this ratio, 15-20% of the total protein existed as an actomyosin complex and the remainder was free myosin (Asghar et al., 1985). Dudziak et al. (1988) reported that postrigor turkey breast myosin formed gels of greater rigidity than thigh myosin. They found that myosin to actomyosin weight ratios for breast and thigh were 3.8:1 and 6.9:1, respectively. Sano et al. (1989b) found that increases in the fish F-actin : myosin ratio changed the rheogram of storage modulus of the actomyosin in temperature range 46-53°C.

Inorganic pyrophosphate (PPi) has been used as a nonhydrolyzable adenosine triphosphate (ATP) analog, to investigate muscle contraction and the nucleotide binding site

in myosin. During muscle contraction, myosin cross-bridges extending from the thick filament cyclically interact with the thin actin filaments as ATP is hydrolyzed (Huxley, 1969). Addition of PPi was found to change both muscle fiber tension and fiber stiffness. These changes were due to cross-bridge detachment (Thomas and Cooke, 1980; Chen and Reisler, 1984; Brenner et al., 1986) or changes in cross-bridge structure upon binding (Goody et al., 1976; Padron and Huxley, 1984). It was also found that this ligand-induced dissociation of actin and myosin was enhanced by high ionic strength and by low temperatures (Konrad and Goody, 1982; Biosca, et al., 1986; Pate and Cooke, 1988). Pyrophosphate binds strongly to myosin with a binding constant of 2.07×10^6 M^{-1}, and may cause local structural changes in S-1 (Nauss et al., 1969). Dissociation of actomyosin by addition of PPi prior to heating caused a decrease in gel strength (Ishioroshi et al., 1980; O'Neil et al., 1993). Kijowski and Mast (1988) reported enhanced thermal stability of myosin in the presence of PPi using differential scanning calorimetry (DSC).

In previous work, the dynamic rheological properties of chicken breast salt-soluble proteins (SSP), which exhibited a myosin-to-actin weight ratio of 1.3 : 1, were pH-dependent in 0.6 M NaCl during heating at 1°C/min (Wang et al, 1990). The causes of the observed viscoelastic transitions during heating were not known. Secondly, F-actin/myosin ratios influenced gel strength as well as rheological transitions, and the

effect of actin on the gelation of myosin is not clear. Therefore, the purpose of this paper was to understand the role of F-actin on myosin unfolding and gel development in both bound (actomyosin) and free forms (free F-actin). The objectives of the present study were to (a) determine the denaturation temperature, enthalpy changes and rheological properties as a function of actin-to-myosin weight ratios during heating, and (b) study the effect of pyrophosphate on both actomyosin unfolding and viscoelastic properties.

5.3 Materials & Methods

Extraction of Myosin and Actin

Broiler breast muscle myosin and actin were extracted and stored as described in Chapter 4. Prior to use, myosin was dialyzed against 0.6 M NaCl, 50 mM Na phosphate buffer, pH 6.5 with two buffer changes, and centrifuged at 78,000 x g for 1 hr (Beckman Ultracentrifuge, Model L7-65, Beckman Instruments, Inc., Palo Alto, CA). Actin was polymerized by adding KCl to a final concentration of 50 mM, $MgCl_2$ to 1 mM and ATP to 1 mM with slow stirring for 2 hr, and dialyzed against 0.6 M NaCl, 50 mM Na phosphate buffer, pH 6.5 overnight. Protein concentration was determined using an extinction coefficient of $E^{1\%} = 5.5$ at 280 nm for myosin (Swenson and Ritchie, 1980), and 11 for actin (Duong and Reisler, 1987).

Characterization of Actin : Myosin (A:M) Weight ratio

Purified actin and myosin were mixed to prepare solutions of different actin (A) to myosin (M) weight ratios (1:0, 1:1.3, 1:15 and 0:1). The volume ($Volume_I$) and concentration ($[Myosin]_I$) of myosin added in each actomyosin solution were recorded for later estimation of free-to-bound myosin ratio. Free myosin, actomyosin and F-actin in 0.6 M NaCl, 50 mM phosphate buffer, pH 6.5 in each solution were quantified using ultracentrifugation (Yasui et al., 1982) by centrifuging at 100,000 x g for 2 hr (Beckman ultracentrifuge, Model TL-100). Protein absorbance in supernatant ($Abs_{supernatant}$) was measured at 280 nm after centrifugation, and subtracted from the absorbance of unpolymerized G-actin. The volume of supernatant was recorded ($Volume_F$). The degree of F-actin polymerization was based on the results in Chapter 4. Absorbance attributed to actin (Abs_{actin}) was estimated by multiplying the original concentration of actin by (1 - %polymerization) x $E^{1\%}$. The difference was the absorbance due to myosin (Abs_{myosin}):

$$Abs_{supernatant} - Abs_{actin} = Abs_{myosin}$$

Myosin concentration after centrifugation ($[Myosin]_F$) was determined from absorbance using $E^{1\%}$ of 5.5. The free-to-bound myosin ratio was calculated as follows:

Free myosin-to-bound myosin ratio =

$$\frac{[\text{Myosin}]_I \times \text{Volume}_I \text{ (mLs)} - [\text{Myosin}]_F \times \text{Volume}_F \text{ (mLs)}}{[\text{Myosin}]_I \times \text{Volume}_I}$$

To evaluate the effect of pyrophosphate, the protein solution was brought to 5 mM Na pyrophosphate and 1 mM $MgCl_2$ by addition of 1/10 volume of 50 mM Na pyrophosphate and 10 mM $MgCl_2$ stock solution. Final pH of myosin was adjusted using 0.1 N HCl or NaCl if necessary.

Dynamic Rheological Properties

Oscillatory dynamic measurements were performed using a Rheometrics Fluid Spectrometer (RFS-8400, Rheometrics, Inc., Piscataway, NJ) fitted with a 50 mm diameter parallel plate apparatus and 100 g-cm transducer. Storage (G') and loss (G") moduli were recorded continuously at a fixed frequency of 10 rad/s and strain of 0.01 while heating from 30 to 80°C at 1°C/min as described in Chapter 4. Protein concentration was 10 mg/ml for myosin and actomyosin solutions, and 6 mg/ml for F-actin.

Thermal Stability

Thermal stability of actin and actomyosin solutions of different ratios were measured using a differential scanning microcalorimeter (MC-2, Microcal Inc., Amherst, MA) with a scan rate of 1°C/min as described in Chapter 4.

Concentrations of 4-7 mg/mL and 5 mg/mL were used for actin and actomyosin, respectively. Heat capacity profiles (C_p vs. temperature) were defined by endothermic peak temperatures and changes in heat capacity (ΔC_p) (Tsong et al., 1970; Privalov and Potekhin, 1986). All data acquisition and analysis software were provided by the manufacturer.

Statistics

Because of the heterogeneous variance existing within each treatment combination, all statistics were performed using log-transformed data (Gill, 1987). Two factor completely randomized design with six replicates (actomyosin ratio and pyrophosphate) was performed under 30 and 80°C using MSTAT software (version C, Michigan State University). Bonferroni t statistics were used to test the significant difference of comparisons among means.

5.4 Results & Discussion

Characterization of Actin-to-Myosin Weight Ratio

Free myosin-to-bound myosin (actomyosin) ratio (%) was 0.2 ± 0.02 for A:M 1:1.3 (w/w), and 2.4 ± 0.4 for A:M 1:15 (w/w) after correction for unpolymerized actin.

Thermal denaturation

An actomyosin weight ratio of 1:15 increased the initial unfolding temperature by 2°C as compared to myosin alone; increasing F-actin to A:M 1:1.3 stabilized myosin by an additional 4°C (Table 5.1). The enthalpy profile of myosin was also significantly altered in the presence of F-actin (Fig. 5.1). The broad peak at 50°C of myosin was shifted toward a higher temperature with addition of F-actin. Increases in heat capacity were also observed at 57 and 66.5°C.

In the presence of pyrophosphate (PPi), F-actin had little effect on myosin denaturation as indicated by similar endothermic profiles (Fig. 5.2). The initial unfolding temperature of myosin, A:M 1:15, and A:M 1:1.3 were not different (Table 5.1). However, the broad peak at 49°C slightly increased to 50.5°C at ratio 1:1.3. A more significant change in heat capacity occurred around 66°C. The peak height at 66°C increased with addition of F-actin similar to the protein without PPi (Fig. 5.2).

Actin binds the S-1 region of myosin head (Mornet et al., 1979), and interacts with myosin light chains (Sutoh, 1982, 1983). Presumably, the stability of myosin S-1 and light chains should be increased due to actin binding. Pyrophosphate was reported to dissociate the actomyosin complex (Greene and Eisenberg, 1980). When F-actin binds to myosin, we observed the stabilization of myosin initial

Table 5.1. Enthalpic transitions of actomyosin at different actin-to-myosin weight ratio in 0.6 M NaCl, 50 mM Na phosphate buffer, pH 6.5, heated from 20 to 90°C at 1°C/min[12]

T(C)	Initial	Peak 1	Peak 2	Shoulder	Peak 3
without pyrophosphate					
Myosin	36.2 (0.4)	49.2 (0.2)	50.2 (0.1)	57.2 (0.2)	66.8 (0.6)
AM 1:15	38.5 (0.9)		49.8 (0.2)	56.7 (0.3)	66.5 (0.2)
AM 1:1.3	42.2 (0.3)		50.2 (0.2)	56.1 (0.1)	66.5 (0.1)
with 5 mM pyrophosphate					
Myosin	37.7 (0.3)	48.9 (0.1)	56.7 (0.2)	59.8 (0.1)	65.1 (0.5)
AM 1:15	38.3 (0.4)	49.5 (0.2)	56.7 (0.1)	59.9 (0.1)	64.5 (0.3)
AM 1:1.3	38.6 (0.7)	50.5 (0.2)	56.8 (0.2)	59.7 (0.1)	66.1 (1.4)

[1] Protein concentration: myosin, 10 mg/ml; Actomyosin, 5 mg/ml.
[2] Number in the bracket is the standard deviation of means

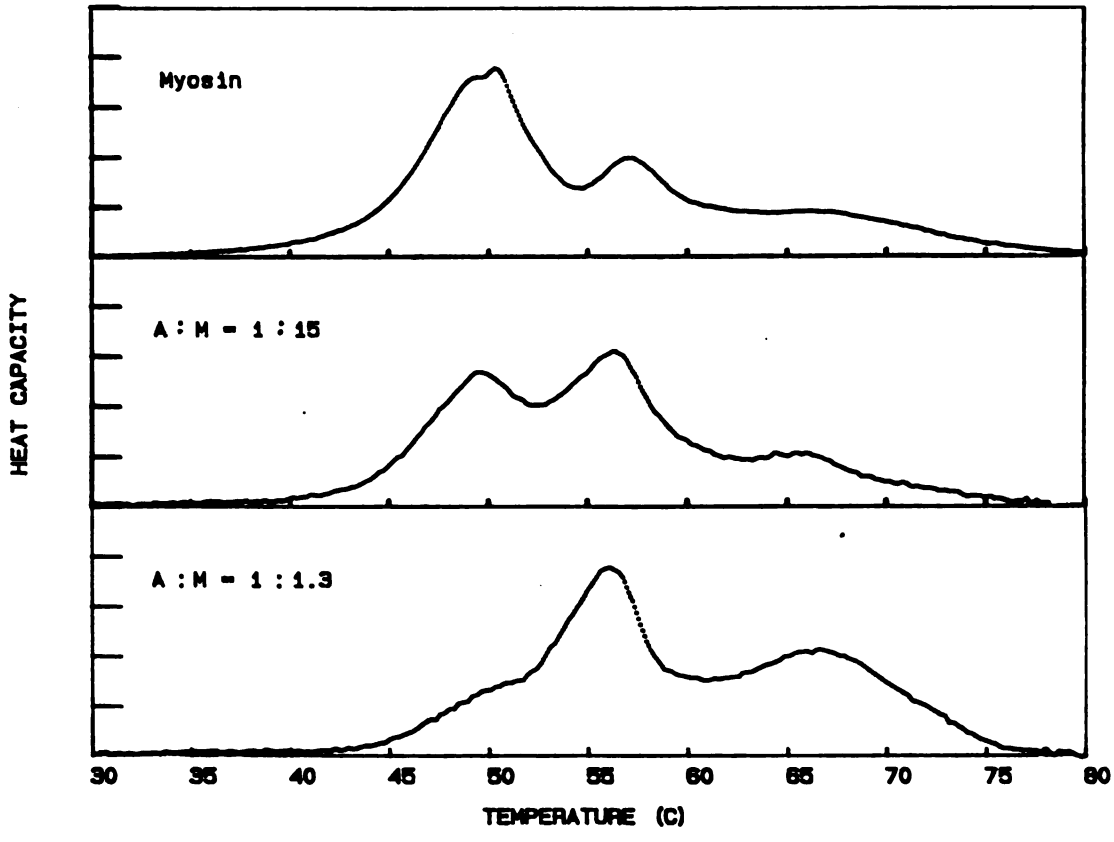

Figure 5.1. Effect of actin (A)-to-myosin (M) weight ratio on myosin denaturation in 0.6 M NaCl, 50 mM Na phosphate buffer, pH 6.5 heated at 1°C/min.

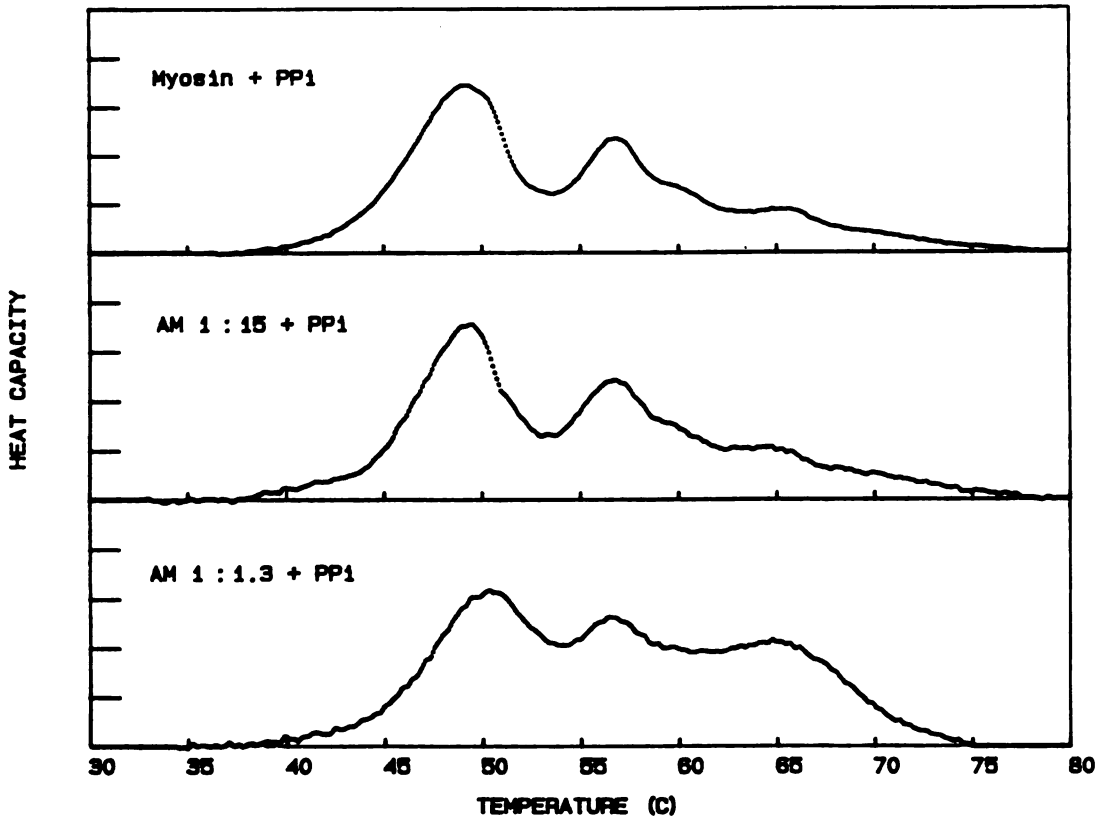

Figure 5.2. Effect of actin (A)-to-myosin (M) weight ratio on myosin denaturation in the presence of 5 mM Na pyrophosphate (PPi), 1 mM $MgCl_2$, 0.6 M NaCl, 50 mM Na phosphate buffer, pH 6.5 heated at 1°C/min.

unfolding temperature, a decrease in heat capacity of the broad peak at 50°C, and an increased peak height at 57°C. Those effects did not occur in the presence of PPi when F-actin was dissociated from myosin. Thus, at least part of the broad peak at 50°C in myosin could be due to the unfolding of S-1 and light chains. This stabilized peak of actomyosin appeared to become superimposed on the peak at 57°C.

Our calorimetric study showed the initial unfolding was influenced by actin-myosin binding. If the segment with the lowest stability was assigned to myosin hinge region in the junction of HMM and LMM (Burke et al., 1973), then this result suggested that binding of actin to myosin, not only affects thermal unfolding of S-1 and light chains, but also other regions of the myosin molecule.

The increase in peak height at 66 to 67°C occurred both with and without pyrophosphate; thus, this peak was not due to shift of the 50°C peak which occurred only in the absence of pyrophosphate. The peak at 66 to 67°C was more likely due to denaturation of increased amount of F-actin in both conditions. Additionally, based on our previous study (Chapter 4), F-actin tended to partly dissociate to G-actin in the presence of pyrophosphate, and started to unfold at 49°C with a T_m of 53.3°C. The higher heat capacity around 53°C region in A:M 1:1.3 ratio compared to the other two ratios might be due to unfolding of G-actin (Fig. 5.2).

Viscoelastic properties

Initial transitions in G' and G" were observed at 49 and 50°C, respectively, due to addition of F-actin to myosin at a ratio 1:15 (w/w). Storage modulus increased to a maximum at 59°C, decreased rapidly from 59 to 63.6°C, then increased again (Fig. 5.3). Loss modulus followed a similar pattern except G" decreased when heated above 63°C. An initial transition at 52°C for both G' and G" was observed at a ratio of 1:15 in the presence of PPi (Fig. 5.4). Both G' and G" increased to a maximum at 57 and 56.5°C, respectively, then decreased. Storage modulus began to increase at 63°C, while G" did not change after 62°C. The transitions occurred within a narrower temperature range for actomyosin with PPi (52 to 63°C) than actomyosin alone (49 to 64°C). In the presence of PPi, a larger decrease in both G' and G" after reaching peak maximum was also observed than those of actomyosin 1:15 alone except it occurred over a wider temperature range (from 56 to 63°C) when F-actin was dissociated from myosin.

Addition of F-actin to an A:M 1:1.3 ratio increased the G' and G" below 50°C (Fig. 5.5) in comparison to myosin and A:M 1:15. A large decrease in G' and G" occurred from about 57 to 65°C which was larger than that observed in A:M 1:15 solutions. Further heating caused a slight decrease in both G' and G". In the presence of PPi, the difference between G' and G" in A:M 1:1.3 solution below 50°C decreased as compared to solutions without PPi (Fig. 5.6), even though both moduli

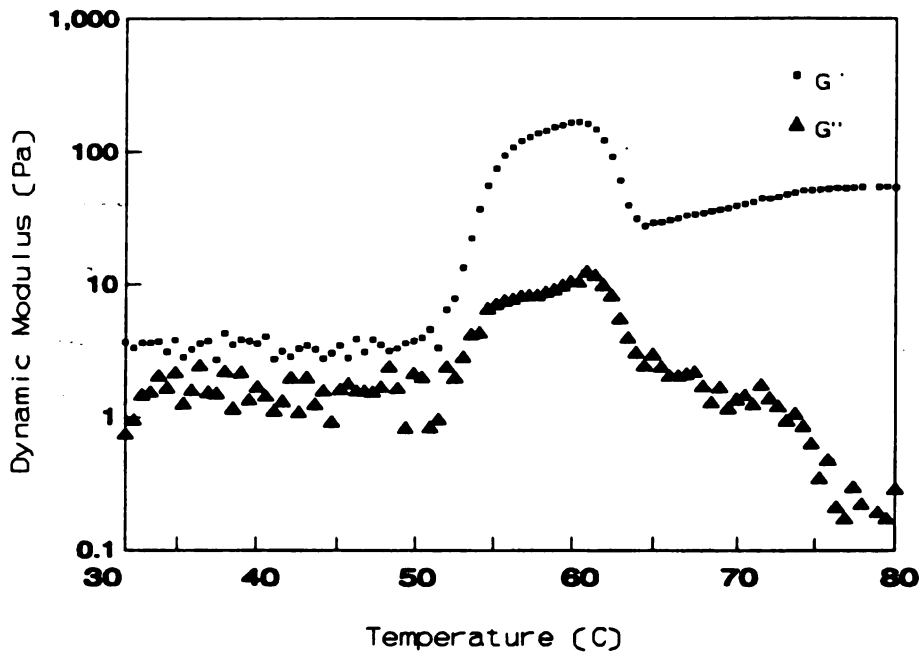

Figure 5.3. Representative rheogram on storage (G') and loss (G") moduli of 10 mg/mL actomyosin at actin-to-myosin weight ratio of 1:15, heated at 1°C/min in 0.6 M NaCl, 50 mM Na phosphate buffer, pH 6.5.

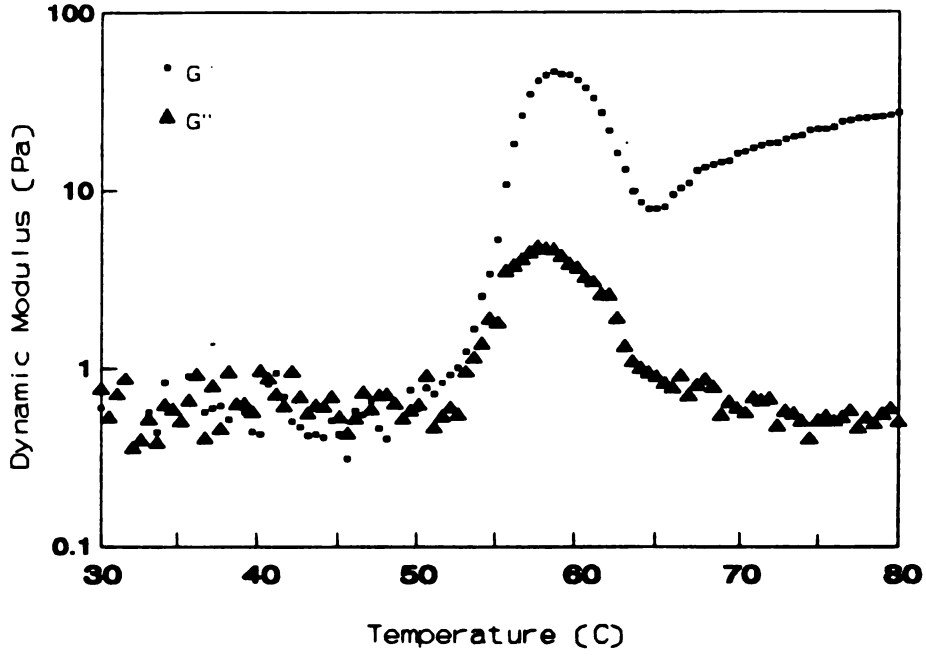

Figure 5.4. Representative rheogram on storage (G') and loss (G") moduli of 10 mg/mL actomyosin at actin-to-myosin weight ratio of 1:15, heated at 1°C/min in the presence of 5 mM Na pyrophosphate, 1 mM $MgCl_2$, 0.6 M NaCl, 50 mM Na phosphate buffer, pH 6.5.

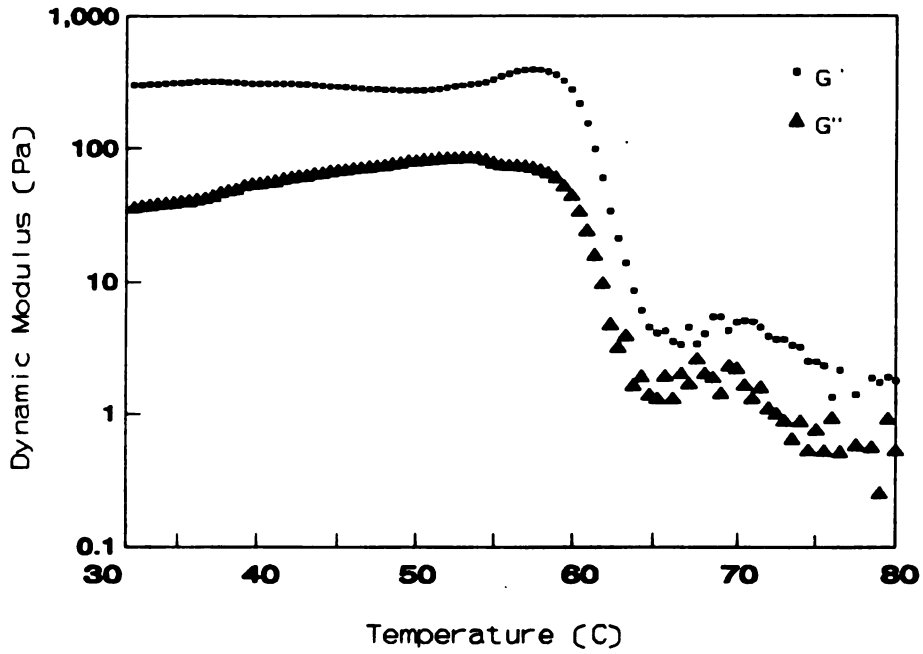

Figure 5.5. Representative rheogram on storage (G') and loss (G") moduli of 10 mg/mL actomyosin at actin-to-myosin weight ratio of 1:1.3, heated at 1°C/min in 0.6 M NaCl, 50 mM Na phosphate buffer, pH 6.5.

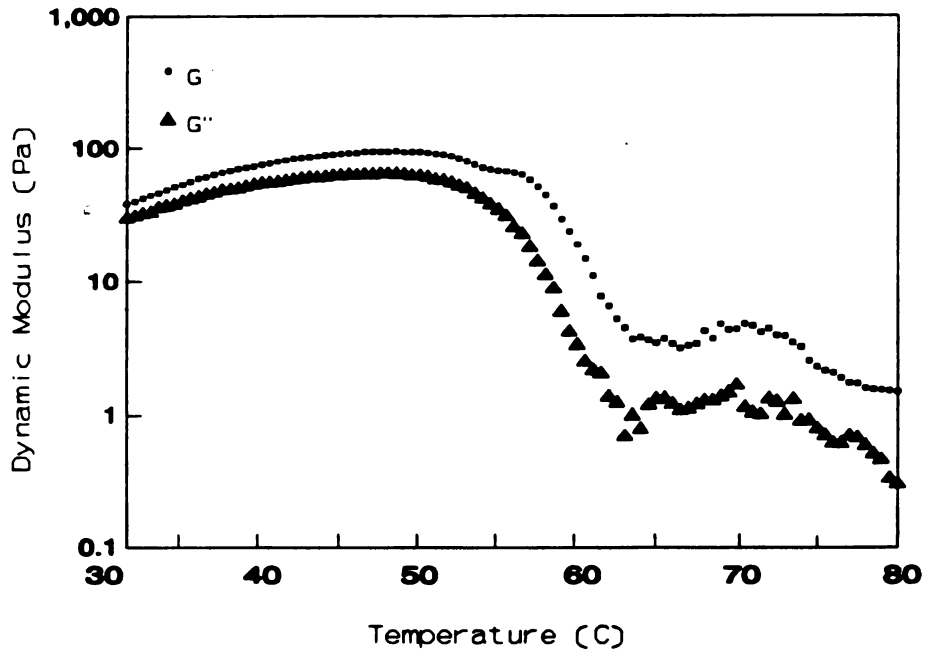

Figure 5.6. Representative rheogram on storage (G') and loss (G") moduli of 10 mg/mL actomyosin at actin-to-myosin weight ratio of 1:1.3, heated at 1°C/min in the presence of 5 mM Na pyrophosphate, 1 mM $MgCl_2$, 0.6 M NaCl, 50 mM Na phosphate buffer, pH 6.5.

were still higher than myosin and A:M 1:15. Storage modulus increased to a maximum at 55°C, decreased until 62°C, then gradually decreased again. Loss modulus started to decrease at 50°C, earlier than those without PPi (around 57°C), then gradually declined when heated above 59°C. Similar to what was observed in A:M 1:15 with PPi, a decrease in both moduli occurred earlier and over a wider temperature range in comparison to those without PPi.

Sano et al. (1989b) have reported a similar effect of F-actin on fish muscle myosin in the temperature range of 46-53°C, and proposed that the altered transitions resulted from the dissociation of myosin molecules from actin filaments, fragmentation of the actin filament, and subsequent breakdown of gel matrices. According to our results, the presence of F-actin caused a sharp decrease in G' and G" in temperature range of 50-65°C regardless of whether actin was free or bound to myosin. It suggested this moduli decrease was more likely due to F-actin itself rather than the dissociation of actomyosin or network breakdown.

Effect of Pyrophosphate and A:M Ratio on Viscoelastic Properties

Because of the existence of a large heterogeneous variance, statistics were performed using log-transformed data (Gill, 1987). The heterogeneous variance was stabilized even though it could not be totally removed after data

transformation. It was found that two main factors, A:M ratio and pyrophosphate effect, significantly interacted; therefore, the comparison for one factor was tested within each level of the other factor. Ten comparisons were made at 30 and 80°C, and the percentage confidence of mean differences were shown in Table 5.2. Even though moderate heterogeneous variance still existed, the confidences of difference were strong in most contrasts ($\alpha<0.01$). Consequently, differences were significant when heterogeneous variance was removed.

Effect of actomyosin weight ratios

At 30°C, significant differences in G' of gels were observed between myosin and AM 1:15, while G" and phase angle were similar (Figs. 5.7, 5.8 & 5.9). Heating to 80°C increased gel elasticity of myosin and A:M 1:15 as indicated by a high G' and low phase angle. Ishioroshi et al. (1980) reported that a 15:1 free myosin to F-actin weight ratio generated the highest gel strength in 0.6M KCl, pH 6.0. However, we observed no difference in either G' or phase angle between gels prepared with myosin alone or AM 1:15. Different heating conditions and buffer environments might have a distinct effect on gel properties. Secondly, the chicken breast AM 1:15 prepared in our lab contained 29% actomyosin which was greater than the 15-20% actomyosin reported by Ishioroshi et al. (1980).

Actomyosin 1:1.3 had more elastic character at 30°C than

Table 5.2 Percent confidence of mean differences in comparisons[12]

Comparisons	log G'	log G"	log(phase angle)
30°C			
AM ratio effect			
M vs AM15	***	***	N
M vs AM13	***	***	***
AM15 vs AM13	***	***	***
MP vs AP15	N	N	N
MP vs AP13	***	***	N
AP15 vs AP13	***	***	N
Pyrophosphate effect			
M vs MP	N	N	N
AM15 vs AP15	***	***	N
AM13 vs AP13	***	***	***
A vs AP	N	N	N
80°C			
AM ratio effect			
M vs AM15	N	*	N
M vs AM13	***	N	***
AM15 vs AM13	***	N	***
MP vs AP15	***	N	N
MP vs AP13	***	***	***
AP15 vs AP13	***	*	***
Pyrophosphate effect			
M vs MP	N	N	**
AM15 vs AP15	***	N	***
AM13 vs AP13	***	N	***
A vs AP	***	**	***

[1] Abbreviations : M=myosin; A=actin; AM15=actin-to-myosin ratio 1:15 (w/w); AM13=actin-to-myosin ratio 1:1.3 (w/w); P=with pyrophosphate;

[2] *** = 99.99% confidence, ** = 99.98% confidence, * = 99.9% confidence that mean results are different; N=nonsignificant difference.

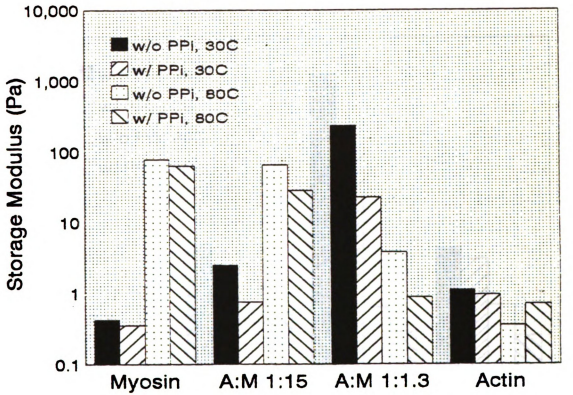

Figure 5.7. Effect of actin-to-myosin weight ratios and pyrophosphate on storage modulus at 30 and 80°C. Protein concentration is 10 mg/mL except actin is 6 mg/mL. Buffer condition is 0.6 M NaCl, 50 mM Na phosphate, pH 6.5.

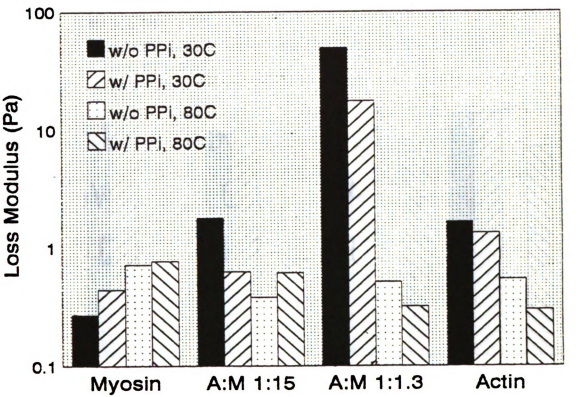

Figure 5.8. Effect of actin-to-myosin weight ratios and pyrophosphate on loss modulus at 30 and 80°C. Protein concentration is 10 mg/mL except actin is 6 mg/mL. Buffer condition is 0.6 M NaCl, 50 mM Na phosphate, pH 6.5.

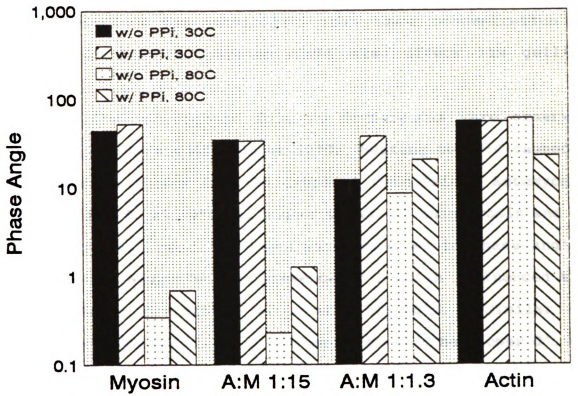

Figure 5.9. Effect of actin-to-myosin weight ratios and pyrophosphate on phase angle at 30 and 80°C. Protein concentration is 10 mg/mL except actin is 6 mg/mL. Buffer condition is 0.6 M NaCl, 50 mM Na phosphate, pH 6.5.

myosin and AM 1:15 due to the addition of F-actin (83% existed as actomyosin). However, AM 1:1.3 did not form as good a gel network at 80°C as indicated by a higher phase angle when compared to those for myosin and AM 1:15. This suggested a negative effect of F-actin on myosin gelation; however, we cannot exclude the possibility that lower concentration of myosin in AM 1:1.3 system might also affect its gelling ability.

In the presence of PPi, no differences were observed between myosin and AM 1:15 at 30°C. Heating to 80°C caused a decrease in G' for AM 1:15 compared to myosin. Actomyosin 1:1.3 with PPi at 30°C had higher G' and G" than myosin and AM 1:15; however, no differences were observed in phase angle. The results suggested the presence of F-actin influenced the viscoelastic properties of myosin at 30°C. Similar to proteins without PPi, AM 1:1.3 heated to 80°C had lower G', G" and phase angle in comparison to myosin and AM 1:15 in the presence of PPi. This again confirmed the negative effect of F-actin on myosin gelation in both the free or bound states.

Effect of pyrophosphate

Addition of PPi to myosin did not change G' and G" at 80°C in comparison to myosin alone, except for an increase in viscous character (higher phase angle). For AM 1:15, PPi caused a decrease in G' and G" at 30°C due to actomyosin dissociation. When heated to 80°C, G' of AM 1:15 decreased

but with higher phase angle. Both AM 1:1.3 with PPi at 30 and 80°C showed lower G' and higher phase angle than those without PPi. These observations indicated that PPi-induced dissociation of actomyosin decreased the elastic character of actomyosin gel. Even with a small amount of free F-actin in myosin (A:M 1:15), a significant increase in viscous character was observed. This increased viscous character was attributed to the rheological character of free F-actin as well as the effect of PPi on myosin alone. In contrast to myosin and actomyosin, addition of PPi to F-actin caused a decrease in phase angle, indicating more elastic character.

5.5 Conclusion

Interaction between actin and myosin not only stabilized S-1 and light chain, but also some domains in the myosin rod. Delay of S-1 and light chain unfolding seemed to interfere with denaturation of myosin rod. This stabilization effect was diminished in the presence of pyrophosphate due to dissociation of actomyosin. It was possible that the stabilized myosin domains altered the gelation mechanism and gel properties. However, the negative effect of F-actin, regardless of whether it was free or bound to myosin, seemed to alter the rheological properties of myosin. Free F-actin decreased gel elasticity more than bound F-actin.

CHAPTER SIX : CONCLUSION

In the first study, we demonstrated the effect of isothermal heating and cooling on myosin gel development and its secondary structure. The effects of temperature and pyrophosphate on thermal stabilities of myosin and actin molecules were examined in the second study, and the gelation progress was monitored. The third study showed the effect of actin-to-myosin weight ratio on protein unfolding and gelation of actomyosin. Pyrophosphate was used to dissociate the actomyosin complex, and thus influence gel properties.

The secondary structure of cooled myosin after heating at 45°C for 30 min did not change significantly from that of native myosin. The DSC study of myosin showed that conformational changes of myosin occurred at temperatures as low as 36°C. It was therefore concluded that unfolding below 45°C was reversible. Moreover, the rheological properties could not be measured at 45°C because the torque generated by myosin solution was below instrument sensitivity, suggesting no elastic character was developed after 30 min heating. The sol-to-gel transition occurred at 55°C as evidenced by the rapid development of gel elasticity within the first 4 min of heating. FTIR spectra showed that α-helix and β-sheet

decreased due to myosin unfolding, and hydrogen bonded ß-structure appeared which might correspond to protein aggregation. Increases in storage modulus (G') were also observed for myosin at 65 and 75°C. Similar to the spectra of myosin at 55°C, α-helices and ß-sheet continued to unfold and intense peaks for hydrogen-bonded ß-structure were observed. Due to visible protein aggregates present in myosin at 75°C, the hydrogen-bonded ß-structure might be one of the structural changes occuring during gelation, but not solely responsible for it.

In scanning experiments, myosin unfolded at 36°C and had four transitions with a cooperative ratio below unity. F-actin unfolded at about 65°C and showed a single peak. A similar heat capacity profile was observed for myosin with pyrophosphate (PPi); however, PPi induced partial dissociation of F-actin. Addition of PPi only slightly changed the rheogram of F-actin, suggesting this dissociation had no effect on viscoelastic properties of F-actin. By comparing the melting temperatures of deconvoluted peaks with G' transitions, the temperature of the second increase in G' (around 63°C) was increased upon addition of PPi. This G' transition corresponded to the unfolding of the seventh and eighth domains of myosin. For myosin without PPi, fewer domains needed to unfold before this second increase in G' occurred. It is possible that PPi binding increased the negative charges of myosin and thus the repulsive forces

between myosin molecules, so the initial myosin aggregation was inhibited or depressed. The gelation process might require more protein to unfold, for exposure of hydrophobicity and subsequent interactions overcoming the existing repulsive forces.

Binding between F-actin and myosin at different weight ratio changed both the myosin unfolding profile and gelation rheogram. The endothermic peaks of myosin below 55°C were shifted toward higher temperatures due to the binding of F-actin to myosin and subsequent structural changes. Addition of PPi dissociated the actomyosin complex as evidenced by the similar heat capacity profile as myosin alone. Higher G' and G" were observed at 30°C due to actomyosin interaction. In the presence of PPi, both moduli decreased due to actomyosin dissociation. Increased quantities of F-actin decreased myosin gel elasticity at 80°C. This effect was enhanced (increase in phase angle) when F-actin was dissociated from myosin. On the contrary, phase angle of F-actin at 80°C was decreased upon addition of PPi, suggesting increase in elastic character.

CHAPTER SEVEN : RECOMMENDATIONS AND FUTURE RESEARCH

Functionalities of muscle proteins are important in developing different meat products. The heat-induced gelation process is essential to produce meat products with desired properties. Poultry rolls and restructured meat products require that proteins bind meat pieces together and hold water. Palatability of sausages is determined by a spreadable texture as well as fat and water holding within the gel network. And frankfurter may need a firm, elastic gel network to increase yield and prevent fat loss (Whitting, 1988).

Before the mechanism of protein gelation was understood, quality control and new product development are often achieved through trial and error. In the mid 80's, consumers were warned to reduce sodium consumption for health reasons. Reduced salt use in meat products became a goal of processors. However, salt is a key ingredient for extracting myofibrillar proteins for binding. Formulations with reduced salt require other ingredient substitutions or processing schedules to improve meat binding. Another example is low-fat/lean meat products due to consumers concern regarding cardiovascular disease. Palatability is a problem with low-fat products; fat contributes juiciness. To improve product quality, fat

replacement using hydrocolloids or high-sheared protein became popular recently. Any of the above changes required research to achieve the desired product properties. Understanding the mechanism of protein gelation as well as protein structural changes and their role during gelation will allow us to utilize these ingredients more successfully and predict product properties resulting from formulation changes. Therefore, basic research related to muscle gelation is essential and is the main purpose of the present studies.

In our first study, we demonstrated the effect of isothermal heating on gel properties of chicken breast myosin. Myosin heated at 55°C for 30 min developed a gel network; however, its elasticity decreased when cooled to ambient temperature. Myosin at 65°C had the highest gel elasticity, suggesting this temperature is desired for a firm, elastic gel. Heating at high temperature is often required for food safety reasons. According to our results, myosin aggregated rapidly at 75°C, probably without enough time for proteins to unfold and orient themselves prior to cross-linking. Protein aggregates occurred and a poor gel was formed, even though the elastic character of myosin gel increased at both 65 and 75°C after cooling. Therefore, investigations into the effect of multiple-stage heating (slower heating rate or lower temperature on initial stage, followed by high temperature heating) is suggested.

Even though the small strain dynamic testing is a

nondestructive testing, the internal heat generated by oscillation will cause an increase in the temperatures of myosin and structural changes (Ferry, 1980b). The input strain might also have effect on rearrangement and cross-linking of unfolded myosin molecules and subsequent gel formation (Clark, 1992). Since the effect of strain field on protein gelation has not been investigated, we suggest monitoring myosin gelation as a function of strain, possibly to alter the arrangement of unfolded myosin, and improve protein-protein interaction. Moreover, Hori (1985) proposed a nondestructive hot-wire method to monitor the physical properties resulting from the structural changes of a test fluid. The heat transfer coefficient of the test fluid around the hot wire was related to its physical properties, especially viscosity (Miyawaki et al., 1990). This technique was applied to on-line monitoring and control of a cheese-making process--determination of the optimum time for curd cutting (Hori, 1985). It might be possible to use the hot-wire method to monitor myosin gelation without the effect of generated internal heat and strain field.

In the second and third studies, we observed the influence of actin-to-myosin ratio and pyrophosphate (PPi) on chicken breast myosin gelation. The results showed that the increased amount of actomyosin in myosin would decrease gel elastic character. Addition of PPi to dissociate actomyosin further increased the viscous character in final gels.

Different muscle sources (cardiac muscle, smooth muscle) have been reported to have different gelling ability and actin-to-myosin ratios. Differences in gel properties might be due to the presence of different myosin isoform, and/or the different ratios of actin-to-myosin in the muscle. The results of our two studies demonstrated the effect of F-actin on chicken myosin gelation. We cannot conclusively suggest that the actin-to-myosin ratio is the reason causing this discrepancy. However, it is one step toward understanding and possibly improving the gelation properties of other muscle system. Therefore, we proposed to investigate the gelation of different myosin isoforms and the effect of actin-to-myosin ratio in different muscle source, to fully understand the effect of actomyosin or F-actin on myosin gelation.

In the third study, we also found that increasing F-actin stabilized some myosin domains, i.e. domains unfolded at a higher temperature at which protein-protein interactions might also occur. This might be one of reasons that actomyosin had lower gel elasticity, and probably be the cause of low gelling ability of post-rigor deboned chicken meat. By changing myosin domain unfolding, or protein-protein interaction of meat system through varying environmental conditions, it might be possible to improve actomyosin gelation. So, we suggest to further investigate factors influencing the mechanism of myosin/actomyosin gelation by changing pH or using stabilizing and/or destabilizing salts. Some of the myosin domains are

sensitive to pH and salt, so by changing either or both factors, the unfolding and interaction between these domains are possible to be modulated. And the protein gel properties might be improved or controlled. Moreover, incorporate other food ingredients into the myosin and actomyosin system to monitor their effect on protein unfolding and aggregation. And apply these ingredients to real meat systems to evaluate the validity of gelation mechanism.

BIBLIOGRAPHY

Adelstein, R.S. and Eisenberg, E. 1980. Regulation and kinetics of the actin-myosin-ATP interaction. Ann. Rev. Biochem. 49: 921-956.

Akahane, T., Chihara, S., Niki, T.P., Sano, T., Tsuchiya, T., Noguchi, S.F., Ookami, H., and Matsumoto, J.J. 1985. Differential scanning calorimetric studies on thermal behaviors of myofibrillar proteins. Bull. Japan. Soc. Sci. Fish 51: 1841-1846.

Arata, T., Mukohata, Y., and Tonomura, T. 1977. Structure and function of the two heads of the myosin molecule. VI. ATP hydrolysis, shortening and tension development of myofibrils. J. Biochem. Tokyo 82: 801-812.

Arntfield, S.D. and Murray, E.D. 1981. The influence of processing parameters on food protein functionality. I. Differential scanning calorimetry as an indicator of protein denaturation. Can. Inst. Food Sci. Technol. J. 14: 289-294.

Arrondo, J.L.R.. Young, N.M., and Mantsch, H.H. 1988. The solution structure of concanavalin A probed by FT-IR spectroscopy. Biochim. Biophys. Acta 952: 261-268.

Arteaga, G.E. and Nakai, S. 1992. Thermal denaturation of turkey breast myosin under different conditions: effect of temperature and pH, and reversibility of the denaturation. Meat Sci. 31: 191-200.

Ashgar, A., Samejima, K., and Yasui, T. 1985. Functionality of muscle proteins in gelation mechanisms of structured meat proteins. CRC Crit. Rev. Food Sci. Nutr. 22: 27-106.

Balint, M., Szilagyi, L., Fekete, G., Blazso, M., and Biro, N.A. 1968. Studies on proteins and protein complexes of muscle by means of proteolysis. V. Fragmentation of light meromyosin by trypsin. J. Mol. Biol. 37: 317-330.

Balint, M., Wolf, I., Tarcsafalvi, A., Gergely, J., and Streter, F.A. 1978. Location of SH-1 and SH-2 in the heavy chain segment of heavy meromyosin. Arch. Biochem. Biophys. 190: 793-799.

Bandekar, J. and Krimm, S. 1988a. Normal mode spectrum of the parallel-chain ß-sheet. Biopolymers 27: 909-921.

Bandekar, J. and Krimm, S. 1988b. Vibrational spectroscopy of $_{L}$-valyl-glycyl-glycine, a parallel-chain ß-structure. Biopolymers 27: 885-908.

Barnes, H.A., Hutton, J.F., and Walters, K. (Ed.). 1989. *An Introduction to Rheology*. Elsevier Sci. Publ. Co. Inc., NY.

Bertazzon, A. and Tsong, T.Y. 1989. High-resolution differential scanning calorimetric study of myosin, functional domains and supramolecular structures. Biochemistry 28: 9784-9790.

Bertazzon, A., Tian, G.H., Lamblin, A., and Tsong, T.Y. 1990. Enthalpic and entropic contributions to actin stability: calorimetry, circular dichroism, and fluorescence study and effects of calcium. Biochemistry 29: 291-298.

Bertazzon, A. and Tsong, T.Y. 1990a. Effect of Ions and pH on the thermal stability of thin and thick filaments of skeletal muscle: high-sensitivity differential scanning calorimetric study. Biochemistry 29: 6447-6452.

Bertazzon, A. and Tsong, T.Y. 1990b. Study of effects of pH on the stability of domains in myosin rod by high-resolution differential scanning calorimetry. Biochemistry 29: 6453-6459.

Biosca, B., Greene, L.E., and Eisenberg, E. 1986. Binding of ADP and ATP analogs to cross-linked and non-cross-linked acto.S-1. J. Biol. Chem. 261: 9793-9800.

Boger, D.V. and Rama Murthy, A.V. 1969. Normal stress measurement and evaporation effects on the Weissenberg rheogniometer. Trans. Soc. Rheol. 13: 405-408.

Braiman, M.S. and Rothschild, K.J. 1988. Fourier transform infrared techniques for probing membrane protein structure. Ann Rev. Biophys. Biophys. Chem. 17: 541-570.

Brenner, B., Yu, L.C., Greene, L.E., Eisenberg, E., and Schoenberg, M. 1986. Ca^{2+}-sensitive cross-bridge dissociation in the presence of magnesium pyrophosphate in skinned rabbit psoas fibers. Biophys. J. 50: 1101-1108.

Briskey, E.J. and Fukazawa, T. 1971. Myofibrillar proteins of skeletal muscle. Adv. Food Res. 19: 279-360.

Brotschi, E.A., Hartwig, J.H., and Stossel, T.P. 1978. The gelation of actin by actin-binding protein. J. Biol. Chem. 253: 8988-8993.

Bruhn, C.M., Cotter, A., Diaz-Knauf, D., Sutherlin, J., West, E., Wightman, N., Williamson, E., and Yaffee, M. 1992. Consumer attitudes and market potential for foods using fat substitutes. Food Technol. 46: 81-86.

Burke, M., Himmelfarb, S., and Harrington, W.F. 1973. Studies on the "hinge" region of myosin. Biochemistry 12: 701-710.

Burke, M and Reisler, E. 1977. Effect of nucleotide binding on the proximity of the essential sulfhydryl groups of myosin. Chemical probing of movement of residues during conformational transitions. Biochemistry 16: 5559-5563.

Burke, M., Zaager, S., and Bliss, J. 1987. Substructure of skeletal myosin subfragment 1 revealed by thermal denaturation. Biochemistry 26: 1492-1496.

Burros, B.C. 1986. Thermal analysis and food chemistry. American Laborary 18: 20-27.

Byler, D.M. and Purcell, J.M. 1989. FTIR examination of thermal denaturation and gel formation in whey proteins. SPIE 1145: 415-417.

Byler, D.M. and Susi, H. 1986. Examination of the secondary structure of proteins by deconvolved FTIR spectra. Biopolymers 25: 469-487.

Byler, D.M. and Susi, H. 1986. Application of computerized infrared and Raman spectroscopy to conformation studies of casein and other food proteins. J. Ind. Microbiol. 3: 73-88.

Cantor, C.R. and Timasheff, S.N. 1982. Optical Spectroscopy of proteins. Ch. 2. In *The Proteins*, 3rd ed., Vol. 5, H. Neurath and R.L. Hill, (Ed.), pp. 279-306. Academic Press, New York.

Carlsson, L., Nystrom, L.E., Lindberg, V., Kannan, K.K., Cid-Dresdner, H., and Lovgren, S. 1976. Crystallisation of a non-muscle actin. J. Mol. Biol. 105: 353-366.

Casal, H.L., Kohler, U., and Mantsch, H.H. 1988. Structural and conformational changes of ß-lactoglobulin B: an infrared spectroscopic study of the effect of pH and temperature. Biochim. Biophys. Acta. 957: 11-20.

Chalovich, J.M. and Eisenberg, E. 1982. Inhibition of actomyosin ATPase activity by troponin-tropomyosin without blocking the binding of myosin to actin. J. Biol. Chem. 257: 2432-2437.

Chan, J.K., Gill, T.A., and Paulson, A.T. 1992. The dynamics of thermal denaturation of fish myosins. Food Res. Int. 25: 117-123.

Chen, T. and Reisler, E. 1984. Tryptic digestion of rabbit skeletal myofibrils: an enzymatic probe of myosin cross-bridges. Biochemistry 23: 2400-2407.

Chowdhry, B.Z. and Cole, S.C. 1989. Differential scanning calorimetry: applications in biotechnology. TIBTECH 7: 11-18.

Clark, A.H. 1992. Gels and gelling. Ch.5. In *Physical Chemistry of Foods*, H.G. Schwartzberg and R.W. Hartel (Eds.), p. 263-305. Marcel Dekker, Inc., NY.

Clark, A.H. and Lee-Tuffnell, C.D. 1986. Gelation of globular proteins. Ch. 5. In *Functional Properties of Food Macromolecules*, J.R. Mitchell and D.A. Ledward (Ed.), p. 240. Elsevier Applied Science Publishers LTD, Landon and New York.

Clark, A.H. and Ross-Murphy, S.B. 1987. Structural and mechanical properties of biopolymer gels. Adv. Polymer Sci. 83: 57-192.

Clark, A.H., Saunderson, D.H.P., and Suggett, A. 1981. Infrared and laser-Raman spectroscopic studies of thermally-induced globular protein gels. Int. J. Peptide Protein Res. 17: 353-364.

Creighton, T.E. (Ed.). 1993. Physical interactions that determine the properties of proteins. Ch.4. In *Proteins: Structures and Molecular Properties*, 2rd ed., pp. 157-160. W.H. Freeman and Company, NY.

Cross, R.A., Bardsley, R.G., Ledward, D.A., Small, J.V., and Sobieszek, A. 1984. Conformational stability of the myosin rod. Eur. J. Biochem. 145: 305-310.

Davies, J.R., Bardsley, R.G., Ledward, D.A., and Poulter, R.G. 1988. Myosin thermal stability in fish muscle. J. Sci. Food Agric. 39: 61-68.

Dong, A., Huang, P., and Caughey, W.S. 1990. Protein secondary structures in water from second-derivative amide I infrared spectra. Biochemistry 29: 3303-3308.

Donovan, J.W. 1984. Scanning calorimetry of complex biological structures. TIBS 9: 340-344.

Dousseau, F. and Pezolet, M. 1990. Determination of the secondary structure content of proteins in aqueous solutions from their amide I and amide II infrared bands. Comparison between classical and partial least-squares methods. Biochemistry 29: 8771-8779.

Dudziak, J.A., Foegeding, E.A., and Knopp, J.A. 1988. Gelation and thermal transitions in post-rigor turkey myosin/ actomyosin suspensions. J. Food Sci. 53: 1278-1281.

Duong, A.M. and Reisler, E. 1987. The binding of myosin sub-fragment 1 to actin can be measured by proteolytic rates method. J. Biol. Chem. 262: 4124-4128.

Egbert, W.R., Huffman, D.L., Chen, C., and Dylewski, D.P. 1991. Development of low fat ground beef. Food Tech. 45: 64-73.

Egelandsdal, B., Fretheim, K., and Samejima, K. 1986. Dynamic rheological measurements on heat-induced myosin gels: effect of ionic strength, protein concentration and addition of adenosine triphosphate or pyrophosphate. J. Sci. Food Agric. 37: 915-926.

Eisenberg, E. and Moos, C. 1968. Adenosine triphosphate activity of acto-heavy meromyosin, a kinetic analysis of activation. Biochemistry 7: 1486-1489.

Eisenberg, E. and Greene, L.E. 1980. The relation of muscle biochemistry and muscle physiology. Ann. Rev. Physiol. 42: 293-309.

Elzinga, M., Collins, J.H., Kuehl, W.M., and Adelstein, R.S. 1973. Complete amino acid sequence of actin of rabbit skeletal muscle. Proc. Natl. Acad. Sci. 70: 2687-2691.

Ferry, J.D. 1948. Protein gels. Adv. Prot. Chem. 4: 1-78.

Ferry, J.D. 1980a. The nature of viscoelastic behavior. Ch. 1. In "Viscoelastic Properties of Polymers," 3rd ed., J. D. Ferry (Ed.), p. 1-14. John Wiley and Sons, Inc., NY.

Ferry, J.D. (Ed.). 1980b. Applications to practical problems. Ch.19. In *Viscoelastic Properties of Polymers*, 3rd ed., pp. 570-576. John Wiley and Sons, Inc., NY.

Feuer, G.Y., Molnar, F., Pettko, E., and Straub, F.B. 1948. Acta Physiol. Acad. Sci. Hung. 1: 150. [In Methods in Enzymol. (1982) 85: 166-167].

Flory, P.J. 1941. J. Amer. Chem. Soc. 63: 3083, 3091, 3096. Cited in Schwartzberg, H.G. and Hartel, R.W. (1992), *Physical Chemistry of Foods*, p. 272-279, Marcel Dekker, Inc., NY.

Foegeding, E.A. and Hamann, D.D. 1992. Physicochemical aspects of muscle tissue behavior. Ch.8. In *Physical Chemistry of Foods*, H.G. Schwartzberg and R.W. Hartel (Eds.), p. 423-441. Marcel Dekker, Inc., NY.

Foegeding, E.A. and Ramsey, S.R. 1986. Effect of gums on low-fat meat batters. J. Food Sci. 51: 33-36, 46.

Frank, G. and Weeds, A.G. 1974. The amino-acid sequence of the alkali light chains of rabbit skeletal-muscle myosin. Eur. J. Biochem. 44: 317-334.

Freire, E. and Biltonen, R.L. 1978a. Statistical mechanical deconvolution of thermal transitions in macromolecules. I. Theory and application to homogeneous systems. Biopolymers 17: 463-479.

Freire, E. and Biltonen, R.L. 1978b. Statistical mechanical deconvolution of thermal transitions in macromolecules. II. General treatment of cooperative phenomena. Biopolymers 17: 481-496.

Fukazawa, T., Hashimoto, Y., and Yasui, T. 1961. Effect of some proteins on the binding quality of an experimental sausages. J. Food Sci. 26: 541-549.

Gazith, J., Himmelfarb, S., and Harrington, W.F. 1970. Studies on the subunit structure of myosin. J. Biol. Chem. 245: 15-22.

Gerasimowicz, W.V., Byler, D.M., and Susi, H. 1986. Resolution enhanced FT-IR spectra of soil constituents: humic acid. Appl. Spectrosc. 40: 504-507.

Gershman, L.C., Stracher, A., and Dreizen, P. 1969. Subunit structure of myosin. III. A proposed model for rabbit skeletal myosin. J. Biol. Chem. 244: 2726-2736.

Gill, J.L. (Ed.). 1987. Completely randomized designs and analysis of variance. Ch. 2. In *Design and Analysis of Experiments : in the Animal and Medical Sciences*, 4th ed., vol.1, pp. 223-224. Iowa State University Press, Ames, Iowa.

Goody, R.S., Holmes, K.C., Mannherz, H.G., Leigh, J.B., and Rosebaum, G. 1976. Cross-bridge conformation as revealed by x-ray diffraction studies of insect flight muscle with

ATP analogues. Biophys. J. 15: 687-705.

Gorga, J.C., Dong, A., Manning, M.C., Woody, R.W., Caughey, W.S., and Strominger, J.L. 1989. Comparison of the secondary structures of human class I and class II major histocompatibility complex antigens by Fourier transform infrared and circular dichroism spectroscopy. Proc. Natl. Acad. Sci. USA. 86: 2321-2325.

Gottlieb, M. and Macosko, C.W. 1982. The effect of instrument compliance on dynamic rheological measurements. Rheol. Acta 21: 90-94.

Greene, L.E. and Eisenberg, E. 1980. Dissociation of the actin-subfragment 1 complex by adenyl-5'-yl imido-diphosphate, ADP, and PPi. J. Biol. Chem. 255: 543-548.

Hamai, M. and Konno, K. 1989. Thermal stability as a probe of S-1 structure. J. Biochem. 106: 803-807.

Hanson, E.J. and Lowy, J. 1963. The structure of F-actin and of actin filaments isolated from muscle. J. Mol. Biol. 6: 46-60.

Harrington, W.F. 1971. A mechanochemical mechanism for muscle contraction. Proc. Natl. Acad. Sci. USA. 68: 685-689.

Harrington, W.F. 1979a. Contractile proteins of the myofibril. In *The Proteins*, H. Neurath and R.L. Hill (Ed.), Vol. 4, p. 245-409. Academic Press, New York.

Harrington, W.F. 1979b. On the origin of the contractile force in skeletal muscle. Proc. Natl. Acad. Sci. USA. 76: 5066-5070.

Harrington, W.F. and Himmelfarb, S. 1972. Effect of adenosine di- and triphosphates on the stability of synthetic myosin filaments. Biochemistry 11: 2045-2052.

Hayashida, M., Maita, T., and Matsuda, G. 1991. The primary structure of skeletal muscle myosin heavy chain: I. Sequence of the amino-terminal 23 kDa fragment. J. Biochem. 110: 54-59.

Herald, T.J. and Smith, D.M. 1992. Heat-induced changes in the secondary structure of hen egg S-ovalbumin. J. Agric. Food Chem. 40: 1737-1740.

Hermans, J.R. 1965. Investigation of the elastic properties of the particle network in gelled solutions of hydro-colloids. I. Carboxymethyl cellulose. J. Polymer Sci. Part A 3: 1859-1868.

Hermansson, A.-M. 1978. Physico-chemical aspects of soy proteins structure formation. J. Texture Studies 9: 33-58.

Hermansson, A.-M., Harbitz, O., and Langton, M. 1986. Formation of two types of gels from bovine myosin. J. Sci. Food Agric. 37: 69-84.

Hines, M.E. and Foegeding, E.A. 1993. Interactions of α-lactalbumin and bovine serum albumin with ß-lactoglobulin in thermally induced gelation. J. Agric. Food Chem. 41: 341-346.

Holmes, K.C., Popp, D., Gebhard, W., and Kabsch, W. 1990. Atomic model of the actin filament. Nature 347: 44-49.

Hori, T. 1985. Objective measurements of the process of curd formation during rennet treatment of milks by the hot wire method. J. Food SCi. 50: 911-917.

Huxley, A.F. and Niedergerke, R. 1954. Structural changes in muscle during contraction. Interference microscopy of living muscle fibers. Nature 173: 971-973.

Huxley, A.F. and Simmons, R.M. 1971. Proposed mechanism of force generation in striated muscle. Nature 233: 533-539.

Huxley, H.E. 1963. Electron microscope studies on the structure of natural and synthetic protein filaments from striated muscle. J. Mol. Biol. 7: 281-308.

Huxley, H.E. 1969. The mechanism of muscular contraction. Science 164: 1356-1366.

Huxley, H.E. and Hanson, J. 1954. Changes in the cross-striations of muscle during contraction and stretch and their structural interpretation. Nature 173: 973-976.

Hvidt, S., Chang, T., and Yu, H. 1984. Rigidity of myosin and myosin rod by electric birefringence. Biopolymers. 23: 1283-1294.

Hvidt, S., Nestler, F.H.M., Greaser, M.L., and Ferry, J.D. 1982. Flexibility of myosin rod determined from dilute solution viscoelastic measurements. Biochemistry 21: 4064-4073.

Ikeuchi, Y., Ito, T., and Fukazawa, T. 1981. A kinetic analysis of thermal denaturation of F-actin. Int. J. Biochem. 13: 1065-1069.

Ikeuchi, Y., Iwamura, K., and Suzuki, A. 1990. Heat

denaturation of rabbit skeletal G-actin in tne presence of ATP. J. Sci. Food Agric. 50: 287-296.

Inoue, A., Kikuchi, K., and Tonomura, Y. 1977. Structure and function of the two heads of the myosin molecule. V. Enzymatic properties of heads B and A. J. Biochem. Tokyo 82: 783-800.

Inoue, A., Takenaka, H., Arata, T., and Tonomura, Y. 1979. Functional implications of the two-headed structure of myosin. Adv. Biophys. 13: 1-194.

Ishioroshi, M., Samejima, K., and Yasui, T. 1979. Heat-induced gelation of myosin: factors of pH and salt concentration. J. Food Sci. 44: 1280-1283.

Ishioroshi, M., Samejima, K., Arie, Y., and Yasui, T. 1980. Effect of blocking the myosin-actin interaction in heat-induced gelation of myosin in the presence of actin. Agric. Biol. Chem. 44: 2185-2194.

Jackson, W.M. and Brandts, J.F. 1970. Thermodynamics of protein denaturation. A calorimetric study of the reversible denaturation of chymotrypsinogen and conclusions regarding the accuracy of the two-state approximation. Biochemistry 9: 2294-2301.

Josephs, R. and Harrington, W.F. 1968. On the stability of myosin filaments. Biochemistry 7: 2834-2847.

Judge, M.D., Aberle, E.D., Forrest, J.C., Hedrick, H.B., and Merkel, R.A. (Ed.). 1989a. Nutritive value of meat. Ch. 13. In *Principles of Meat Science*, 2nd ed., pp. 289-298. Kendall/Hunt Pub. Co., Dubuque, Iowa.

Judge, M.D., Aberle, E.D., Forrest, J.C., Hedrick, H.B., and Merkel, R.A. (Ed.). 1989b. Structure and composition of muscle and associated tissues. Ch. 2. In *Principles of Meat Science*, 2nd ed., pp. 19-55. Kendall/Hunt Pub. Co., Dubuque, Iowa.

Judge, M.D., Aberle, E.D., Forrest, J.C., Hedrick, H.B., and Merkel, R.A. (Ed.). 1989c. Conversion of muscle to meat and development of meat quality. Ch. 5. In *Principles of Meat Science*, 2nd ed., pp. 97-123. Kendall/Hunt Pub. Co., Dubuque, Iowa.

Kabsch, W., Mannherz, H.G., Suck, D., Pai, E.F., and Holmes, K.C. 1990. Atomic structure of the actin : DNase I complex. Nature 347: 37-44.

Kabsch, W. and Vandekerckhove, J. 1992. Structure and function

of actin. Annu. Rev. Biophys. Biomol. Struct. 21: 49-76.

Kamath, U. and Shriver, J.W. 1989. Characterization of thermotropic state changes in myosin subfragment-1 and heavy meromyosin by UV difference spectroscopy. J. Biol. Chem. 264: 5586-5593.

Kaminer, B. and Bell, A.L. 1966. Myosin filamentogenesis: effects of pH and ionic concentration. J. Mol. Biol. 20: 391-401.

Karn, J., Brenner, S., and Barnett, L. 1983. Protein structural domains in the Caenorhabditis Elegans Unc-54 myosin heavy chain gene are not separated by introns. Proc. Natl. Acad. Sci. USA. 80: 4253-4257.

Kijowski, J.M. and Mast, M.G. 1988. Thermal properties of proteins in chicken broiler tissues. J. Food Sci. 53: 363-366.

King, L. and Lehrer, S.S. 1989. Thermal unfolding of myosin rod and light meromyosin: circular dichroism and tryptophan fluorescence studies. Biochemistry 28: 3498-3502.

Komine, Y., Maita, T., and Matsuda, G. 1991. The primary structure of skeletal muscle myosin heavy chain: II. Sequence of the 50 kDa fragment of subfragment-1. J. Biochem. 110: 60-67.

Konrad, M. and Goody, R.S. 1982. Kinetic and thermodynamic properties of the ternary complex between F-actin, myosin subfragment 1 and adenosine 5'-[β, γ-imido] triphosphate. Eur. J. Biochem. 128: 547-555.

Krimm, S. 1962. Infrared spectra and chain conformation of proteins. J. Mol Biol. 4: 528-540.

Krimm, S. and Bandekar, J. 1986. Vibrational spectroscopy and conformation of peptides, polypeptides and proteins. Adv. Protein Chem. 38: 181-364.

Krishnan, K.S. and Brandts, J.F. 1978. Scanning calorimetry. Meth. Enzymol. 49: 3-14.

Laemmli, U.K. 1970. Cleavage of structural proteins during the assembly of the head of bacteriophage T_4. Nature 227: 680-685.

Lehrer, S.S. and Kerwar, G. 1972. Intrinsic fluorescence of actin. Biochemistry 11: 1211-1217.

Li-Chan, E. and Nakai, S. 1991. Raman spectroscopic study of thermally and/or dithiothreitol induced gelation of lysozyme. J. Agric. Food Chem. 39: 1238-1245.

Lin, V.J.C. and Koenig, J.L. 1976. Roman studies of bovine serum albumin. Biopolymers 15: 203-218.

Lopez-Lacomba, J.L., Guzman, M., Cortijo, M., Mateo, P.L., Aguirre, R., Harvey, S.C., and Cheung, H.C. 1989. Differential scanning calorimetric study of the thermal unfolding of myosin rod, light meromyosin, and sub-fragment 2. Biopolymers 28: 2143-2159.

Lowey, S., Slayter, H.S., Weeds, A., and Baker, H. 1969. Substructure of the myosin molecule. I. Subfragments of myosin by enzymatic degradation. J. Mol. Biol. 42: 1-29.

Lu, R.C. 1980. Identification of a region susceptible to proteolysis in myosin subfragment-2. Proc. Natl. Acad. Sci. USA 77: 2010-2013.

Lu, R.C. and Wong, A. 1985. The amino acid sequence and stability predictions of the hinge region in myosin subfragment 2. J. Biol. Chem. 260: 3456-3461.

Lymn, R.W. and Taylor, E.W. 1971. Mechanism of adenosine triphosphate hydrolysis by actomyosin. Biochemistry 10: 4617-4624.

Mahmood, R. and Yount, R.G. 1984. Photochemical probes of the active site of myosin. J. Biol. Chem. 259: 12956-12959.

Maita, T., Miyanishi, T., Matsuzono, K., Tanioka, Y., and Matsuda, G. 1991a. The primary structure of skeletal muscle myosin heavy chain: III. Sequence of the 22 kDa fragment and the alignment of the 23 kDa, 50 kDa, and 22 kDa fragments. J. Biochem. 110: 68-74.

Maita, T., Yajima, E., Nagata, S., Miyanishi, T., Nakayama, S., and Matsuda, G. 1991b. The primary structure of skeletal muscle myosin heavy chain: IV. Sequence of the rod, and the complete 1,938-residue sequence of the heavy chain. J. Biochem. 110: 75-87.

Margossian, S.S. and Lowey, S. 1982. Preparation of myosin and its subfragments from rabbit skeletal muscle. Methods Enzymol. 85: 56-71.

McLachlan, A.D. 1984. Structural implications of the myosin amino acid sequence. Ann. Rev. Biophys. Bioeng. 13: 167-189.

McLachlan, A.D. and Karn, J. 1982. Periodic charge distributions in the myosin rod amino acid sequence match cross-bridge spacings in muscle. Nature 299: 226-231.

McLachlan, A.D. and Stewart, M. 1975. Tropomyosin coiled-coil interactions: evidence for an unstaggered structure. J. Mol. Biol. 98: 293-304.

McMindes, M.K. 1991. Application of isolated soy protein in low-fat meat products. Food Tech. 45: 61-64.

Mendelson, R.A., Morales, M.F., and Botts, J. 1973. Segmental flexibility of the S-1 moiety of myosin. Biochemistry 12: 2250-2255.

Miyawaki, O., Sato, Y., Yano, T., Ito, K., and Saeki, Y. 1990. Fundamental aspects of viscosity monitoring by the hot wire technique. J. Food Sci. 55: 854-857.

Morita, J.-I. and Yasui, T. 1991. Involvement of hydrophobic residues in heat-induced gelation of myosin tail subfragments from rabbit skeletal muscle. Agric. Biol. Chem. 55: 597-599.

Morita, J.-I., Choe, I., Yamamoyo, K. Samejima, K., and Yasui, T. 1987. Heat-induced gelation of myosin from leg and breast muscles of chicken. Agric. Biol. Chem. 51:2895-2900.

Morita, J.-I. and Ogata, T. 1991. Role of light chains in heat-induced gelation of skeletal muscle myosin. J. Food Sci. 56: 855-856.

Mornet, D., Bertrand, R., Pantel, P., Audemard, E., and Kassab, R. 1981a. Structure of the actin-myosin interface. Nature (London) 292: 301-306.

Mornet, D., Bertrand, R., Pantel, P., Audemard, E., and Kassab, R. 1981b. Proteolytic approach to structure and function of actin recognition site in myosin heads. Biochemistry 20: 2110-2120.

Mornet, D., Pantel, P., Audemard, E., and Kassab, R. 1979. The limited tryptic cleavage of chymotryptic S-1: an approach to the characterization of the actin site in myosin heads. Biochem. Biophys. Res. Commun. 89: 925-932.

Mornet, D. and Ue, K. 1984. Proteolysis and structure of skeletal muscle actin. Proc. Natl. Acad. Sci. USA Biol. 81: 3680-3684.

Morris, E.R. and Ross-Murphy, S.B. 1981. Chain flexibility of

polysaccharides and glycoproteins from viscosity measurements. Tech. Life Sci. B310: 1-46. Cited in Blanshard, J.M.V. and Mitchell, J.R. (1988), *Food Structure-Its Creation and Evaluation*, p. 392, Butterworths Inc., Boston.

Muhlrad, A. and Chaussepied, N. 1990. Effect of nucleotides, actin and temperature on thermolysin digestion of myosin subfragment-1. Eur. J. Biochem. 192: 663-668.

Muhlrad, A. and Hozumi, T. 1982. Tryptic digestion as a probe of myosin S-1 conformation. Proc. Natl. Acad. Sci. USA 79: 958-962.

Muhlrad, A., Kasprzak, A.A., Ue, K., Ajtai, K., and Burghardt, T.P. 1986. Characterization of the isolated 20 kDa and 50 kDa fragments of the myosin head. Biochim. Biophys. Acta 869: 128-140.

Muhlrad, A. and Morales, M.F. 1984. Isolation and partial renaturation of proteolytic fragments of the myosin head. Proc. Natl. Acad. Sci. USA 81: 1003-1007.

Murayama, T. 1978. Introduction to dynamic mechanical behavior. Ch.1. In *Dynamic Mechanical Analysis of Polymeric Material*, T. Murayama (Ed.), p. 1-22. Elsevier Sci. Pub. Co. Inc., NY.

Nakai, S. 1983. Structure-function relationships of food proteins with an emphasis on the importance of protein hydrophobicity. J. Agric. Food Chem. 31: 676-683.

Nakai, S. and Li-Chan, E. (Ed.). 1988. Hydrophobic interaction. Ch.1. In *Hydrophobic Interactions in Food Systems*, pp. 4-9. CRC Press, Inc. Florida.

Nakamaye, K.L., Wells, J.A., Bridenbaugh, R.L., Okamato, Y., and Yount, R.G. 1985. 2-[(4-Azido-2-nitrophenyl) amino] ethyl triphosphate, a novel chromophoric and photo-affinity analogue of ATP. Synthesis, characterization, and interaction with myosin subfragment 1. Biochemistry 24: 5226-5235.

Nauss, K.M., Kitagawa, S., and Gergely, J. 1969. Pyrophosphate binding to and adenosine triphosphatase activity of myosin and its proteolytic fragments. J. Biol. Chem. 244: 755-765.

O'Neill, E., Morrissey, P.A., and Mulvihill, D.M. 1993. Heat-induced gelation of actomyosin. Meat Sci. 33: 61-74.

Padron, R. and Huxley, H.E. 1984. The effect of the ATP analog

MgAMPPNP on the structure of crossbridges in vertebrate skeletal muscles: x-ray diffraction and mechanical studies. J. Muscle Res. Cell Motil. 5: 613-655.

Painter, P.C. and Koenig, J.L. 1976. Raman spectroscopic study of the proteins of egg white. Biopolymers 15: 2155-2166.

Park, J.W. and Lanier, T.C. 1989. Scanning calorimetric behavior of tilapia myosin and actin due to processing of muscle and protein purification. J. Food Sci. 54: 49-51.

Parry, D.A.D. 1981. Structure of rabbit skeletal myosin: analysis of the amino acid sequences of two fragments from the rod region. J. Mol. Biol. 153: 459-464.

Pate, E. and Cooke, R. 1988. Energetics of the actomyosin bond in the filament array of muscle fibers. Biophys. J. 53: 561-573.

Patel, M., Kilara, A., Huffman, L., Hewitt, S., and Houlihan, A. 1990. Studies on whey protein concentrates. 1. Compositional and thermal properties. J. Dairy Sci. 73: 1439-1449.

Payne, K. and Veis, A. 1988. Fourier transform IR spectroscopy of collagen and gelatin solutions: deconvolution of the amide I band for conformational studies. Biopoly. 27: 1749-1760.

Pollard, T.D. and Cooper, J.A. 1986. Actin and actin-binding proteins. A critical evaluation of mechanisms and functions. Ann. Rev. Biochem. 55: 987-1035.

Potekhin, S.A., Trapkov, V.A., and Privalov, P.L. 1979. Stepwise pattern of the thermal denaturing of helical fragments of myosin. Biofizika 24: 46-50.

Prestrelski, S.J., Byler, D.M., and Liebman, M.N. 1991a. Comparison of various molecular forms of bovine trypsin: correlation of infrared spectra with X-ray crystal structures. Biochemistry 30: 133-143.

Prestrelski, S.J., Byler, D.M., and Thompson, M.P. 1991b. Infrared spectroscopic discrimination between α- and 3_{10}-helices in globular proteins: reexamination of amide I infrared bands of α-lactalbumin and their assignment to secondary structures. Int. J. Peptide Protein Res. 37: 508-512.

Privalov, P.L. 1982. Stability of proteins: proteins which do not present a single cooperative system. Adv. Protein Chem. 35: 1-104.

Privalov, P.L. and Potekhin, S.A. 1986. Scanning microcalorimetry in studying temperature-induced changes in proteins. Methods Enzymol. 131: 4-51.

Rayment, I., Rypniewski, W.R., Schmidt-Base, K., Smith, R., Tomchick, D.R., Benning, M.M., Winkelmann, D.A., Wesenberg, G., and Holden, H.M. 1993a. Three-dimensional structure of myosin subfragment-1: a molecular motor. Science 261: 50-58.

Rayment, I., Holden, H.M., Whittaker, M., Yohn, C.B., Lorenz, M., Holmes, K.C., and Milligan R.A. 1993b. Structure of the actin-myosin complex and its implications for muscle contraction. Science 261: 58-65.

Redowicz, M.J., Szilagyi, L., and Strzelecka-Golaszewska, H. 1987. Conformational transitions in the myosin head induced by temperature, nucleotide and actin. Eur. J. Biochem. 165: 353-362.

Reisler, E., Burke, M., and Harrington, W.F. 1974. Cooperative role of two sulfhydryl groups in myosin adenosine triphosphatase. Biochemistry 13: 2014-2022.

Rodgers, M.E. and Harrington, W.F., 1987. Hinging of rabbit myosin rod. Biochemistry 26: 8697-8703.

Rodgers, M.E., Karr, T., Biedermann, K., Ueno, H., and Harrington, W.F. 1987. Thermal stability of myosin rod from various species. Biochemistry 26: 8703-8708.

Rosser, R.W., Nestler, H.M., Schrag, J.L., Ferry, J.D., and Greaser, M. 1978. Infinite dilution viscoelastic properties of myosin. Macromolecules 11: 1239-1242.

Samejima, K., Hashimoto, Y., Yasui, T., and Fukazawa, T. 1969. Heat gelling properties of myosin, actin, actomyosin and myosin-subunits in a saline model system. J. Food Sci. 34: 242-245.

Samejima, K., Takahashi, K., Yasui, T. 1976. Heat-induced denaturation of myosin total rod. Agric. Biol. Chem. 40: 2455-2464.

Samejima, K., Ishioroshi, M., and Yasui, T. 1981. Relative roles of the head and tail portions of the molecule in heat-induced gelation of myosin. J. Food Sci. 46: 1412-1418.

Samejima, K., Yamauchi, H., Asghar, A., and Yasui, T. 1984. Role of myosin heavy chains from rabbit skeletal muscle in the heat-induced gelation mechanism. Agric. Biol.

Chem. 48: 2225-2232.

Sano, T., Nogushi, S.F., Tsuchiya, T., and Matsumoto, J.J. 1988. Dynamic viscoelastic behavior of natural actomyosin and myosin during thermal gelation. J. Food Sci. 52: 924-928.

Sano, T., Nogushi, S.F., Matsumoto, J.J., and Tsuchiya, T. 1989a. Dynamic viscoelastic behavior of F-actin on heating. J. Food Sci. 54: 231-232.

Sano, T., Nogushi, S.F., Matsumoto, J.J., and Tsuchiya, T. 1989b. Role of F-actin in thermal gelation of fish actomyosin. J. Food Sci. 54: 800-804.

Sano, T., Nogushi, S.F., Matsumoto, J.J., and Tsuchiya, T. 1990a. Effect of ionic strength on dynamic viscoelastic behavior of myosin during thermal gelation. J. Food Sci. 55: 51-54.

Sano, T., Nogushi, S.F., Matsumoto, J.J., and Tsuchiya, T. 1990b. Thermal gelation characteristics of myosin subfragments. J. Food Sci. 55: 55-58.

Sato, M., Leimbach, G., Schwarz, W.H., and Pollard, T.D. 1985. Mechanical properties of actin. J. Biol. Chem. 260: 8585-8592.

Sato, M., Schwarz, W.H., and Pollard, T.D. 1986. *Acanthamoeba* profilin affects the mechanical properties nonfilamentous actin. J. Biol. Chem. 261: 10701-10706.

Savitzky, A., and Golay, J.E. 1964. Smoothing and differentiation of data by simplified least square procedure. Anal. Chem. 36: 1628-1639.

Schaub, M.C., Watterson, J.G., and Waser, P.G. 1975. Conformational differences in myosin. IV. Radioactive labelling of specific thiol groups as influenced by ligand binding. Hoppe-Seyler's Z. Physiol. Chem. 356: 325-339.

Setton, A. and Muhlrad, A. 1984. Effect of mild heat treatment on the ATPase activity and proteolytic sensitivity of myosin subfragment-1. Arch. Biochem. Biophys. 235: 411-417.

Sharp, A. and Offer, G. 1992. The mechanism of formation of gels from myosin molecules. J. Sci. Food Agric. 58: 63-73.

Shriver, J.W. and Kamath, U. 1990. Differential scanning

calorimetry of the unfolding of myosin subfragment 1, subfragment 2, and heavy meromyosin. Biochemistry 29: 2556-2564.

Shriver, J.W. and Sykes, B.D. 1981. Phosphorus-31 nuclear magnetic resonance evidence for two conformations of myosin subfragment-1·nucleotide complexes. Biochemistry 20: 2004-2012.

Shriver, J.W. and Sykes, B.D. 1982. Energetics of the equilibrium between two nucleotide-free myosin subfragment 1 states using fluorine-19 nuclear magnetic resonance. Biochemistry 21: 3022-3028.

Skolnick, J. 1987. Possible role of helix-coil transitions in the microscopic mechanism of muscle contraction. Biophys. J. 51: 227-243.

Smith, E.L., Hill, R.L., Lehman, I.R., Lefkowitz, R.J., Handler, P., and White, A. (Ed.). 1983. Muscle. Ch. 8, In *Principles of Biochemistry: Mammalian Biochemistry*, 7th ed., p 277. McGraw-Hill, Inc., Singapore.

Spudich, J.A. and Watt, S. 1971. The regulation of rabbit skeletal muscle contraction. I. Biochemical studies of the interaction of the tropomyosin-troponin complex with actin and the proteolytic fragments of myosin. J. Biol. Chem. 246: 4866-4871.

Squire, J.M. (Ed.). 1986. Ch. 4, In *Muscle: Design, Diversity, and Disease*, pp. 77-93, 135. Benjamin/Cummings Publishing Co., Inc., Menlo Park, CA.

Stabursvik, E. and Martens, H. 1980. Thermal denaturation of proteins in post rigor muscle tissue as studied by differential scanning calorimetry. J. Sci. Food Agric. 31: 1034-1042.

Stauffer, D., Coniglio, A., and Adam, M. 1982. Gelation and critical phenomena. Adv. Polymer Sci. 44: 103-158.

Steffe, J.F. (Ed.). 1992. Viscoelasticity. Ch. 4, In *Rheological Methods in Food Process Engineering*, pp. 168-185. Freeman Press, East Lansing, MI.

Stein, P.E., Leslie, A.G.W., Finch, J.T., and Carrell, R.W. 1991. Crystal structure of uncleaved ovalbumin at 1.95A resolution. J. Mol. Biol. 221: 941-959.

Stockmayer, W.H. 1943. Theory of molecular size distribution and gel formation in branched-chain polymers. J. Chem. Phys. 11: 45-55.

Stockmayer, W.H. 1944. Theory of molecular size distribution and gel formation in branched polymers. II General cross linking. J. Chem. Phys. 12: 125-131.

Suck, D., Kabsch, W., and Mannherz, H.G. 1981. Three-dimensional structure of the complex of skeletal muscle actin and bovine pancreatic DNAase I at 6-Å resolution. Proc. Natl. Acad. Sci. 78: 4319-4323.

Surewicz, W.K. and Mantsch, H.H. 1988. New insight into protein secondary structure from resolution-enhanced infrared spectra. Biochim. Biophys. Acta 952: 115-130.

Surewicz, W.K., Moscarello, M.A. and Mantsch, H.H. 1987a. Fourier transform infrared spectroscopic investigation of the interaction between myelin basic protein and dimyristoyl-phosphatidylglycerol bilayers. Biochemistry 26: 3881-3886.

Surewicz, W.K., Moscarello, M.A. and Mantsch, H.H. 1987b. Secondary structure of the hydrophobic myelin protein in a lipid environment as determined by Fourier-transform infrared spectrometry. J. Biol. Chem. 262: 8598-8602.

Susi, H., Timasheff, S.N., and Stevens, L. 1967. Infrared spectra and protein conformations in aqueous solutions. I. The amide I band in H_2O and D_2O solutions. J. Biol. Chem. 242: 5460-5466.

Susi, H. and Byler, D.M. 1983. Protein structure by Fourier transform infrared spectroscopy: second derivative spectra. Biochem. Biophys. Research Comm. 115: 391-397.

Susi, H. and Byler, D.M. 1986. Resolution-enhanced Fourier transform infrared spectroscopy of enzymes. Methods Enzymol. 130: 290-311.

Susi, H. and Byler, D.M. 1987. Fourier transform infrared study of proteins with parallel ß-chains. Arch. Biochem. Biophys. 258: 465-469.

Sutoh, K. 1982a. Identification of myosin-binding sites on the actin sequence. Biochemistry 21: 3654-3661.

Sutoh, K. 1982b. An actin binding site on the 20K fragment of myosin subfragment 1. Biochemistry 21: 4800-4804.

Sutoh, K. 1983. Mapping of actin-binding sites on the heavy chain of myosin subfragment 1. Biochemistry 22: 1579-1585.

Sutoh, K., Sutoh, K., Karr, T., and Harrington, W.F. 1978.

Isolation and physico-chemical properties of a high molecular weight subfragment-2 of myosin. J. Mol. Biol. 126: 1-22.

Swenson, C.A. and Ritchie, P.A. 1980. Conformational transitions in the subfragment-2 region of myosin. Biochem 19: 5371-5375.

Tait, J.F. and Frieden, C. 1982. Polymerization-induced changes in the fluorescence of actin labeled with iodoacetamido-tetramethylrhodamine. Arch. Bioch. Bioph. 216: 133-141.

Takashi, R., Muhlrad, A., and Botts, J. 1982. Spatial relationship between a fast-reacting thiol and a reactive lysine residue of myosin subfragment 1. Biochemistry 21: 5661-5668.

Tanford, C. (Ed.). 1980. *The Hydrophobic Effect: Formation of Micells and Biological Membranes*, 2nd ed. John Wiley & Sons, NY.

Tanner, R.I. (Ed.). 1985. *Engineering Rheology*. Oxford Univ. Press, NY.

Thomas, D.D. 1978. Large scale rotational motions of proteins detected by electron paramagnetic resonance and fluorescence. Biophys. J. 24: 439-462.

Thomas, D.D. and Cooke, R. 1980. Orientation of spin-labeled myosin heads in glycerinated muscle fibers. Biophys. J. 32: 891-906.

Timasheff, S.N., Susi, H., and Stevens, L. 1967. Infrared spectra and protein conformations in aqueous solutions. II. Survey of globular proteins. J. Biol. Chem. 242: 5467-5473.

Tong, S.W. and Elzinga, M. 1983. The sequence of the NH_2-terminal 204-residue fragment of the heavy chain of rabbit skeletal muscle myosin. J. Biol. Chem. 258: 13100-13110.

Tsong, T.Y., Hearn, R.P., Wrathall, D.P., and Sturtevant, J.M. 1970. A calorimetric study of thermally induced conformational transitions of ribonuclease A and certain of its derivatives. Biochemistry 9: 2666-2677.

Tsong, T.Y., Karr, T., and Harrington, W,F, 1979. Rapid helix-coil transitions in the S-2 region of myosin. Proc. Natl. Acad. Sci. USA. 76: 1109-1113.

Vibert, P.J. and Craig, R. 1982. Three-dimensional reconstruction of thin filaments decorated with a Ca^{2+}-regulated myosin. J. Mol. Biol. 157: 299-319.

Voutsinas, L.P., Nakai, S., and Harwalkar, V.R. 1983. Relationships between protein hydrophobicity and thermal functional properties of food proteins. Can. Inst. Food Sci. Technol. J. 16: 183-190.

Wagner, P.D. and Giniger, E. 1981. Hydrolysis of ATP and reversible binding to F-actin by myosin heavy chains free of all light chains. Nature 292: 560-562.

Wagner, P.D. and Weeds, A.G. 1977. Studies on the role of myosin alkali light chains. J. Mol. Biol. 109: 455-473.

Wagner, P.D. and Yount, R.G. 1975. Stoichiometry of labeling of myosin's proteolytic fragments by a purine disulfide analog of adenosine triphosphate. Biochemistry 14: 1900-1907.

Wang, S.F. 1990. Effect of pH and NaCl on the thermal-physical behavior of chicken breast salt-soluble proteins. M. S. Thesis. Michigan State University, East Lansing, MI 48824.

Watanabe, B. 1989. Amino-acid sequence of the hinge region in chicken myosin subfragment-2. Biol. Chem. Hoppe-Seyler 370: 55-61.

Weber, K. and Osborn, M. 1969. The reliability of molecular weight determinations by dodecyl sulfate-polyacrylamide gel electrophoresis. J. Biol. Chem. 244: 4406-4412.

Weeds, A.G. and Pope, B. 1977. Studies on the chymotryptic digestion of myosin. Effects of divalent cations on proteolytic susceptibility. J. Mol. Biol. 111: 129-157.

Wells, J.A. and Yount, R.G. 1979. Active site trapping of nucleotide crosslinking to sulfhydryl groups in myosin subfragment 1. Proc. Natl. Acad. Sci. USA 76: 4966-4970.

Wells, J.A., Sheldon, M, and Yount, R.G. 1980. Magnesium nucleotide is stoichiometrically trapped at the active site of myosin and its proteolytic fragments by thiol crosslinking reagents. J. Biol. Chem. 255: 1598-1602.

Whitting, R.C. 1988. Ingredients and processing factors that control muscle protein functionality. Food Technol. 42: 104-114, 210.

Whorlow, R.W. 1980. *Rheological Techniques*. Halsted Press,

NY.

Wicker, L., Lanier, T.C., Hamann, D.D., and Akahane, T. 1986. Thermal transitions in myosin-ANS fluorescence and gel rigidity. J. Food Sci. 51: 1540-1543.

Wicker, L. Lanier, T.C., Knopp, J.A. and Hamann, D.D. 1989. Influence of various salts on heat-induced ANS fluorescence and gel rigidity development of Tilapia (*Serotherodon aureus*) myosin. J. Agric. Food Chem. 37: 18-22.

Wicker, L and Knopp, J. A. 1988. The binding of 8-anilino-1-naphthalene sulfonate (ANS) to fish myosin and the effect of salts on the thermal transitions of fish myosin-ANS complex. Arch. Biochem. Biophys. 266: 452-461.

Wright, D.J. and Wilding, P. 1984. Differential scanning calorimetric study of muscle and its proteins: myosin and its subfragments. J. Sci. Food Agric. 35: 357-372.

Wu, J.Q., Hamann, D.D., and Foegeding, E.A. 1991. Myosin gelation kinetic study based on rheological measurements. J. Agric. Food Chem. 39: 229-236.

Xiong, Y.L., Brekke, C.J., and Leung, H.K. 1987. Thermal denaturation of muscle proteins from different species and muscle types as studied by differential scanning calorimetry. Can. Inst. Food Sci. Technol. J. 20: 357-362.

Yamada, T., Shimizu, H., Nakanishi, M., and Tsuboi, M. 1981. Environment of the tryptophan residues in a myosin head: a hydrogen-deuterium exchange study. Biochemistry 20: 1162-1168.

Yamamoto, K., Samejima, K., and Yasui, T. 1987. The structure of myosin filaments and the properties of heat-induced gel in the presence and absence of C-protein. Agric. Biol. Chem. 51: 197-203.

Yamamoto, K. and Sekine, T. 1979a. Interaction of myosin subfragment-1 with actin. I. Effect of actin binding on the susceptibility of subfragment-1 to trypsin. J. Biochem. Tokyo 86: 1855-1862.

Yamamoto, K. and Sekine, T. 1979b. Interaction of myosin subfragment-1 with actin. II. Location of actin binding site in a fragment of subfragment-1 heavy chain. J. Biochem. Tokyo 86: 1863-1868.

Yamamoto, K. and Sekine, T. 1979c. Interaction of myosin

subfragment-1 with actin. III. Effect of cleavage of the subfragment-1 heavy chain on its interaction with actin. J. Biochem. Tokyo 86: 1869-1881.

Yamamoto, K. 1990. Electron microscopy of thermal aggregation of myosin. J. Biochem. 108: 896-898.

Yamamoto, K., Samejima, K. and Yasui, T. 1988. Heat-induced gelation of myosin filaments. Agric. Biol. Chem. 52: 1803-1811.

Yasui, T., Ishioroshi, M., Nakano, H., and Samejima, K. 1979. Changes in shear modulus, ultrastructure and spin-spin relaxation times of water associated with heat-induced gelation of myosin. J. Food Sci. 44: 1201-1204.

Yasui, T., Ishioroshi, M., and Samejima, K. 1980. Heat-induced gelation of myosin in the presence of actin. J. Food Biochem. 4:. 61-78.

Yasui, T., Ishioroshi, M., and Samejima, K. 1982. Effect of actomyosin on heat-induced gelation of myosin. Agric. Biol. Chem. 46: 1049-1059.

Yates, L.D. and Greaser, M.L. 1983. Quantitative determination of myosin and actin in rabbit skeletal muscle. J. Mol. Biol. 168: 123-141.

Young, M., Blanchard, M.H., and Brown, D. 1968. Selective nonenzymic cleavage of the myosin rod: isolation of the coiled-coil α-rope section from the C-terminus of the molecule. Proc. Natl. Acad. Sci. USA 61: 1087-1094.

Zaner, K.S., King, R.G., Newman, J., Schick, K.L., Furukawa, R., and Ware, B.R. 1988. Rheology of G-actin solutions. J. Biol Chem. 263: 7186-7189.

Ziegler, G.R. and Acton, J.C. 1984. Mechanisms of gel formation by proteins of muscle tissue. Food Technol. 38: 77-82.